



Proceedings of
10th Annual Symposium on Research and Industrial Training
of
Department of Electronics

11th December 2023



Department of Electronics
Faculty of Applied Sciences
Wayamba University of Sri Lanka
Kuliyapitiya, 60200
Sri Lanka

Editorial Board

Editor-in- chief

Dr. Y.A.A. Kumarayapa

Co-editors

Eng. S.R.L. Gunawardhana

Ms. M.N.T. Meghathirana

Ms. K.K.W.K.G De Silva

Board Members

Dr. Y.A.A. Kumarayapa

Snr. Prof. K.P. Vidanapathirana

Snr. Prof. (Mrs.) G.A.K.S. Perera

Prof. L.D.R.D. Perera

Prof. (Mrs.) J.M.J.W. Jayasinghe

Prof. M.A.A. Karunarathna

Dr. W.A.S. Wijesinghe

Mr. K.K.C.S. Kiriella

Eng. S.R.L. Gunawardhana

Mr. P.G.T.R. Payagala

Review Panel

Snr. Prof. K.P. Vidanapathirana

Snr. Prof. (Mrs.) G.A.K.S. Perera

Prof. L.D.R.D. Perera

Prof. (Mrs.) J.M.J.W. Jayasinghe

Prof. M.A.A. Karunarathna

Dr. Y.A.A. Kumarayapa

Dr. W.A.S. Wijesinghe

Mr. K.K.C.S. Kiriella

Eng. S.R.L. Gunawardhana

Mr. P.G.T.R. Payagala

©Department of Electronics, Faculty of Applied Sciences,
Wayamba University of Sri Lanka, 2023

ISSN 2362 0560

Designing and Printing at Department of Electronics,
Faculty of Applied Sciences, Wayamba University of Sri Lanka , Kuliypitiya

Message from the Dean

It is a great pleasure to pen this message to mark the 10th Annual Symposium on Research and Industrial Training of the Department of Electronics, ASRITE-2023.

ASRITE is organized by the Department of Electronics at the Faculty of Applied Sciences, and was started ten years ago to provide a platform for the final year undergraduates of the faculty, who have followed Electronics as a major subject for their degree programs, to present their Research Project and Industrial Project outcomes. Today, undergraduates in the B.Sc. (Joint Major) Degree program and in the B.Sc. (Special) Degree program in Applied Electronics have the opportunity to share their research findings and strengthen and consolidate their soft skills at ASRITE. It is earnestly expected that the undergraduates would take the maximum advantage of this opportunity provided through ASRITE.

It is unique to ASRITE that, prior to the presentations, the students demonstrate their project work to a panel of reviewers enabling clarifications and verifications of research work be made in advance, so that more accurate evaluations and feedback could be given. It is noteworthy that students have developed technically advanced systems and solutions by using their knowledge and skills in Electronics, Computer Science and other related disciplines. Some of the systems developed have the potential to go beyond prototyping, and with further improvements, would surely find practical applications.

I am thankful to the Head of the Department of Electronics, all the academic staff of the Department, the Project Supervisors, the Department Research Project Coordinator and the Industrial Training Coordinator for the assistance extended in supervising and guiding the students and for leading them up to presentations. The Coordinator of ASRITE-2023, editors of proceedings, and symposium panel members also deserve our appreciation. My thanks should also go to the administrative staff, non-academic staff and the academic support staff of the University for their service to make this event a reality. It is highly commendable that the Department has been able to stage the event physically amidst various constraints.

I am confident that the work presented at the Symposium would be thought-provoking and would contribute to technical advancements.

I wish the Symposium every success and congratulate the presenters on their skills and achievements.

Prof. L.D.R.D. Perera
Dean / Faculty of Applied Sciences
11.12.2023

Foreword

I am very happy to write this prelude to the proceedings of the 10th Annual Symposium on Research and Industrial Training (ASRITE) 2023 organized by the Department of Electronics at the Faculty of Applied Sciences, Wayamba University of Sri Lanka. This annual event has become a significant platform for researchers, academicians, and industry professionals to share their knowledge, experiences, and latest advancements in the field of electronics.

I would like to express my sincere gratitude to the Vice-Chancellor of Wayamba University of Sri Lanka, Snr. Prof. Udith K. Jayasinghe, and the Dean of the Faculty of Applied Sciences, Prof. L.D.R.D. Perera, for their valuable guidance and solid support for organizing ASRITE 2023.

My deepest appreciation goes to the Research Coordinator of the Department of Electronics, Prof. (Mrs.) J.M.J.W. Jayasinghe, and the Industrial Training Coordinator, Mr. K.K.C.S. Kiriella, for their tireless efforts in coordinating the various aspects of ASRITE 2023.

Special thanks are due to the Coordinator of ASRITE 2023, Mr. K.K.C.S. Kiriella who almost completed the research work demonstration and final presentation Symposium works with the support of e-Society junior undergraduate supporters as well with the support of non-academic staff members. Then, the thanks also go to Mr. S.R.L. Gunawardhana, and some academic support staff for their exceptional work in managing the publication of the proceeding of the event.

I extend my heartfelt gratitude to all the department members and administrative staff of the faculty for their unwavering support and contributions in making ASRITE 2023 a resounding success. Their collaborative efforts and enthusiasm are truly commendable.

Finally, I would like to acknowledge the active participation of final year undergraduate researchers, their supervisors, academicians, and industry collaborators for presenting their valuable work at the symposium. Their contributions enriched the discussions and fostered a stimulating learning environment.

We believe that the knowledge and insights shared at ASRITE 2023 will contribute significantly to the advancement of the field of electronics and inspire future generations of researchers and innovators.

Dr. Y.A. Ajith Kumarayapa
Head
Department of Electronics
Faculty of Applied Sciences
Wayamba University of Sri Lanka

CONTENTS

Individual Research Papers

1. **DEVELOPMENT OF A LOW-COST, PORTABLE FLUORIDE ION DETECTOR FOR A WATER QUALITY MONITORING SYSTEM** **1**
A.H.M.N.H. Abeyratne , L.D.R.D. Perera
2. **SOLAR POWERED AUTOMATIC WATERING AND LIQUID FERTILIZER SUPPLYING SYSTEM FOR INDOOR POTTED PLANTS** **8**
R.A.J.R. Perera , G.A.K.S. Perera
3. **WEATHER FORECASTING BASED AUTOMATED SWITCHING SYSTEM FOR HYBRID PV SYSTEMS** **15**
U.I.K. Perera , Y.A.A. Kumarayapa
4. **COMBINED POWER SYSTEM USING A LI-POLYMER BATTERY, SUPERCAPACITOR BANK AND SOLAR CELLS FOR A DRONE** **23**
T.K.C.Samarasinghe , K.P. Vidanapathirana
5. **DRYING NATURAL RUBBER (LATEX) SHEETS BY USING A SOLAR PANEL** **30**
W.M.S.M. Weerasinghe , G.A.K.S. Perera
6. **REDUCING HOUSEHOLD ELECTRICITY CONSUMPTION WITH A SMART MONITORING SYSTEM** **37**
U.T. Nanayakkarawasam , W.A.S. Wijesinghe
7. **ANALYZE INDOOR ENVIRONMENT QUALITY USING IOT BASED MONITORING SYSTEM** **43**
J.K.A.T.R. Jayasuriya , J.M.J.W. Jayasinghe
8. **RESEARCH ON ENHANCING THE PERFORMANCE OF VLC-BASED IMAGE TRANSMISSION AT LOW BIT RATE** **51**
K.B.M.N. Neranjan , Y.A.A. Kumarayapa
9. **SMART ELEPHANT CHASING AND WARNING SYSTEM** **60**
A.A.P.P. Navoda , K.P. Vidanapathirana

10. DESIGN AND ANALYSIS OF A FILTER NETWORK FOR IMPROVED TV SIGNAL QUALITY	69
D.H.L. Zoysa , J.M.J.W. Jayasinghe , T. Premathilake	
11. INVESTIGATION OF ENERGY EFFICIENT LIGHTING SOLUTION FOR DC POWERED SYSTEM	77
P.F.D.C. Fonseka , K.K.C.S.Kiriella	
Industrial Training Research Papers	
12. IMAGE PROCESSING BASED MONKEY REPELLENT SYSTEM	85
M. K. Gunarathna , M. A. A. Karunarathna	
13. A BATTERY ANALYZER FOR A VEHICLE ELECTRICAL SYSTEM DIAGNOSTIC TOOL	91
J.K.A.T.R. Jayasuriya , L.D.R.D. Perera	
14. IOT BASED HEAT DETECTOR FOR DISTRIBUTION TRANSFORMER	98
U.T. Nanayakkarawasam , Y.A.A. Kumarayapa	
15. IOT BASED BATTERY MANAGEMENT SYSTEM	105
A.A.P.P. Navoda , W.A.S. Wijesinghe , M.P.T.R. Wijebandara	
16. SMART MANHOLE MONITORING SYSTEM	112
K.B.M.N. Neranjan1, K.P. Vidanapathirana, T. Herath	

DEVELOPMENT OF A LOW-COST, PORTABLE FLUORIDE ION DETECTOR FOR A WATER QUALITY MONITORING SYSTEM

A.H.M.N.H. Abeyratne*, L.D.R.D. Perera

Department of Electronics, Wayamba University of Sri Lanka, Kuliypitiya, Sri Lanka

*navanjanahimansi@gmail.com

ABSTRACT

Consumption of groundwater contaminated with fluoride is suspected to cause chronic kidney disease of unknown etiology (CKDu). Monitoring water quality and detection of fluoride ion in drinking water will help mitigate the occurrence of CKD in Sri Lanka. This paper presents the design of a photometry-based device that can detect very low concentrations of Fluoride ions (F^-) instantly. The designed system consists of an Arduino Uno board, a photodiode sensor and an LED source. The color sensor module GY 31 TCS3200 was used as the photodetector. For testing purposes, water samples with known fluoride concentration were prepared using a solution of NaF. Rhodamine dye which produces observable changes in color on interaction with F^- ion was used to facilitate Fluoride ion detection. A linear relationship between the device output and the Fluoride concentration was observed, and with the help of this relationship Fluoride ion concentrations in the range from 1ppm to 6ppm could be detected. The designed system is low cost, portable and can be integrated into a water quality monitoring system.

Keywords: Fluoride, Optical sensing, Chronic Kidney Disease (CKDu)

1.0 INTRODUCTION

Rural people in the dry zone of Sri Lanka are facing a major health crisis -the chronic kidney disease of unknown etiology (CKDu). Due to unsustainable activities and population expansion, many people depend on depleted groundwater supplies which have naturally high fluoride content that frequently exceeds permissible limits. There may be a connection between high Fluoride levels and CKDu, according to research concerning people without access to clean water sources [1].

Among those contaminants in water sources, Fluoride is one of most prevalent elements in the crust of the Earth. It is also one of the very few compounds that can negatively impact human health when ingested through water [2]. According to the World Health Organization (WHO) the maximum contamination limit for Fluoride is 1.5 mg/L in drinking water to prevent health risks. In 1985 the first Hydro-Geochemical Atlas of Sri Lanka published that there are high concentration of Fluoride distributed in groundwater in the dry zone of Sri Lanka [3]. According to recent researches, drinking water with higher levels of Mg^{2+} and F^- may have a direct relationship with CKDu as complexes containing these elements formed in hard water can cause renal injury [3]. Well-water in Sri Lanka had a fluoride concentration ranging from 0 to 7 mg/L. The district of Anuradhapura had the highest fluoride concentration at 7.0 mg/L while Monaragala had the second-highest level at 6.8 mg/L [4]. Regular Testing of individual well-water quality is essential for maintaining safe and reliable water supply. Awareness of water quality allows for appropriate interventions to prevent potential contamination and avoid health risks. Although there are laboratory instruments that can measure the water quality, those

are not practical everywhere in these affected areas due to high cost, complexity and the larger size of the instrument. These costly monitoring systems are beyond the reach of both the government and the people in these affected zones.

The traditional water quality monitoring techniques have several drawbacks. Most communities are unable to afford expensive, heavy tools, which make early identification and preventative care more difficult. This study offers a novel solution: a portable, inexpensive fluoride testing tool with a photodiode sensor and an LED for real-time reading. The designed system, which is based on widely available technology, will facilitate monitoring water quality by providing affordability, portability, and ease of use. Frequent monitoring will enable the communities and health care personnel to monitor the quality of water, detect possible contamination early, and take appropriate actions.

In the designed photometric system, rhodamine dye was used to facilitate detection of Fluoride ion content. Rhodamine is a fluorescent dye that has been widely employed in the fabrication of sensors for detection of numerous ions, including Fluoride. It is one of the dyes used for detection of F^- . Other common anions present in water give minimum or negative results with Rhodamine, and it has proved its selectivity for Fluoride. The interaction of rhodamine-based sensors with fluoride ions trigger particular chemical reactions that result in observable changes in fluorescence or color. These changes can be used to detect fluoride ions with the unaided eye [5]. The simplest rhodamine has an excitation wavelength of 517 nm and an emission spectrum of fluorescence at 496 nm. As member of the xanthene dye class, rhodamine dyes typically possess great brightness, good photo stability, high molar absorptivity in the visible range, and capacity to control dye substitution. It has been possible to create a number of fluorinated Rhodamine derivatives, some of which have been described as highly discriminating colorimetric fluoride probes for imaging intracellular fluoride in living cells [6]. In Rhodamine based sensors, Fluoride ions and Rhodamine interact through specific chemical reactions, such as fluoride-induced Spiro lactam ring opening, which results in observable changes in fluorescence. Long excitation and emission wavelengths, low background interference, minimal or non-toxicity, greater sensitivity and selectivity, good chemical and photochemical stability are all necessary for a perfect fluorescent probe for bio sensing fluoride [6].

The design of a photometric device that can detect very low levels of Fluoride ion concentration in water is reported here. The designed system consists of an Arduino Uno board, a photo-detector and an LED light source. With the designed system, F^- ions in the range of 1 ppm to 6 ppm could be detected.

2.0 EXPERIMENTAL

2.1 Monitoring Intensity of Transmitted Light

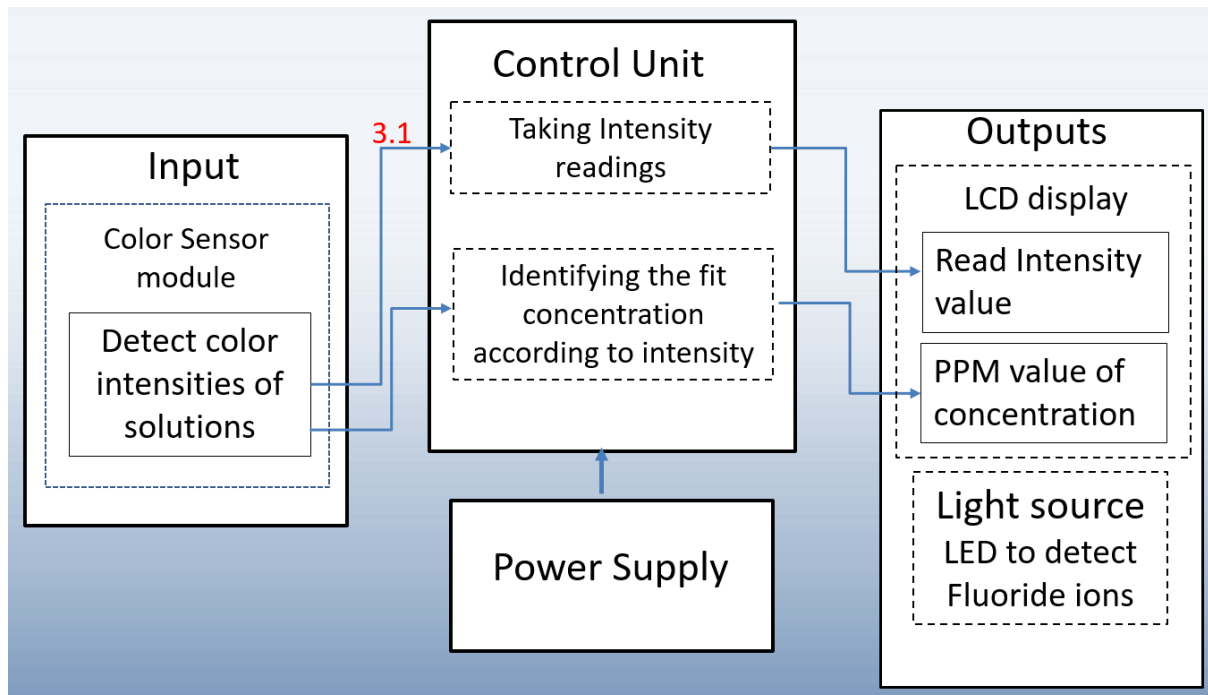


Figure 2.1: Block diagram of the designed system

The accurate detection of the intensity of transmitted light is the most important process of this project. The GY-31 TCS3200 color sensor module was used to monitor the intensity of the transmitted light coming through the solution. Color sensor module was connected to the Arduino board as shown in the figure, and was mounted in the sample holder so as to receive the maximum of transmitted light.

A pre-prepared Rhodamine solution with a concentration of 20 ppm was used. A very low concentration of Rhodamine was sufficient to obtain accurate measurements.

2.1.1 Sensor Designing

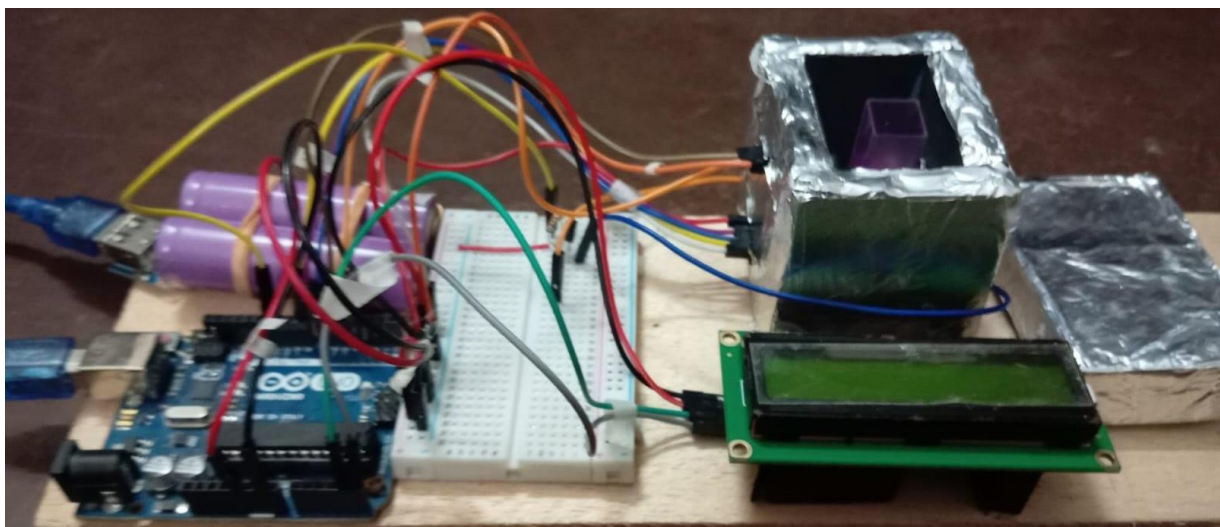


Figure 2.2: Implemented Fluoride ion detector

The sample chamber was designed to obtain reliable measurements by preventing external light from falling onto the light detector. A black color material was used for the basic structure as it has light absorbing properties. Then the outside of the holder was covered with aluminum foil to further enhance its light-blocking capabilities. A lid, which is also important to prevent external light and to be kept in place even when the instrument is off to prevent dirt and moisture from entering the sample compartment, was designed with the same materials. The sample chamber was shaped and cut to fit the cuvette, ensuring a secure and stable fit for the sample, and to place the sensor and the light source for its maximum output.

The prototype was put through testing in a lab setting. When the LED is on, the color sensor detects the light intensity and modifies its resistance that causes changes in output of circuits.

2.1.2 Preparation of F⁻ solutions

A 100 ml of 10 ppm Sodium Fluoride (NaF) solution was prepared by mixing NaF with 100 ml of distilled water. A series of solution samples with F⁻ concentration from 1 ppm to 6 ppm were prepared by diluting the above NaF solution. 3 ml of this diluted solution was filled into cuvettes, and 6 microlitres of Rhodamine was added to each cuvette. An analytical scale was used to determine the mass of NaF and a magnetic stirrer was used to mix NaF solutions.

3.0 RESULTS AND DISCUSSION

The results obtained in design and implementation of the system shown in Figure 2.2, are discussed in this section.

3.1 Sample testing

The NaF solution samples were tested using a spectrophotometer before testing with the implemented system.

3.1.1 Spectrophotometer testing

Each sample was tested with the spectrophotometer [7]. When the F⁻ concentration was increased, the absorbance also increased as shown in Figure 3.1. With spectrophotometer data presented in Table 3.1, the maximum absorption was observed at a wavelength of 540 nm.

Table 3.1 : The values of absorbance observed with spectrophotometer

238	535	0.236	0.247	0.221	0.215	0.268	0.203	0.208
239	536	0.237	0.249	0.222	0.217	0.268	0.204	0.209
240	537	0.238	0.25	0.223	0.218	0.269	0.204	0.209
241	538	0.239	0.25	0.224	0.218	0.269	0.205	0.21
242	539	0.241	0.251	0.225	0.219	0.27	0.206	0.21
243	540	0.241	0.251	0.225	0.219	0.27	0.206	0.21
244	541	0.24	0.25	0.224	0.219	0.269	0.205	0.209
245	542	0.241	0.25	0.225	0.219	0.27	0.205	0.21
246	543	0.241	0.249	0.224	0.218	0.269	0.204	0.209
247	544	0.24	0.248	0.223	0.218	0.268	0.204	0.208
248	545	0.239	0.247	0.223	0.217	0.267	0.203	0.207

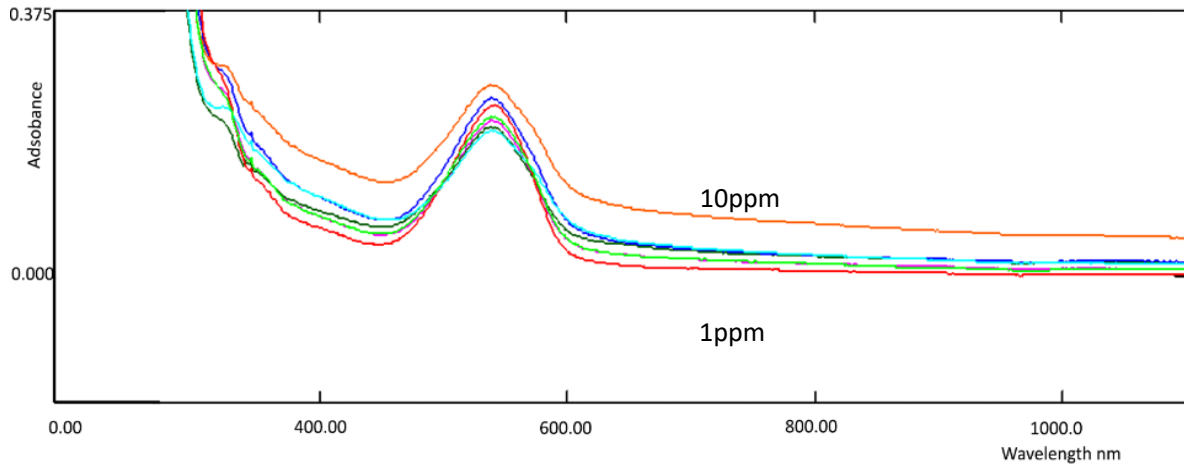


Figure 3.1: plot of absorbance Vs wavelength for NaF samples with different concentrations

3.1.2 Testing the samples with designed system

The pattern of output voltage changing was determined using NaF solution samples with known concentrations. Table 3.2 shows the observed output voltage of the device for different NaF concentrations.

Table 3.2: Output voltage of the implemented system

F ⁻ concentration (ppm)	Output Voltage (mV)
1	2840
2	2220
3	2001
4	1900
5	1800
6	1724

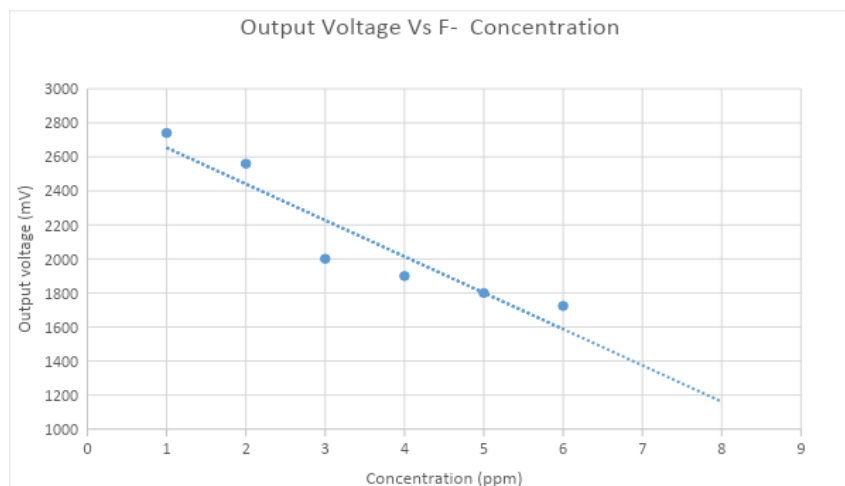


Figure 3.2: Plot of output voltage Vs F⁻ concentration

A linear relationship was observed between the output voltage of the device and the F^- concentration (Figure 4) and the formula $y = -213.17 x + 2866.9$ was derived from the above graph. Here, y is the output voltage of the device in mV and x is the F^- concentration in ppm.

3.1.3 Implementing the system to measure fluoride concentration of unknown water samples

The system code involving the above formula was implemented to determine unknown Fluoride ion concentrations in water samples. Table 3.3 shows theoretically evaluated and experimentally observed voltage outputs for water samples with F^- concentrations in the range 0.5 - 5.5 ppm, showing the accuracy of the system.

Table 3.3: Detector output voltages obtained practically and theoretically

F^- ion concentration (ppm)	Experimentally observed output voltage (mV)	Theoretically derived output voltage (mV)	Error of the system %
0.5	2740	2760.3	0.735
1.5	2540	2547.1	0.121
2.5	2322	2333.9	0.471
3.5	2121	2120.8	-0.009
4.5	1908	1907.6	-0.020
5.5	1699	1694.4	-0.271

As further developments, this system could be fully automated to get continuous observations after locating it at a specific water source without any manual operations, including filling the cuvette with water samples and adding dye in specific volumes. Also, if light of specific wavelength that could detect only fluoride is used, the dye will be unnecessary. Apart from that, the power source can be replaced with solar panels to use rechargeable batteries in remote locations.

4.0 CONCLUSION

An Arduino based photometric system was developed to detect F^- ions dissolved in water. The detection mechanism was a combination of Rhodamine dye based and optical sensing. The system produced a linear output for the F^- ion concentration range analyzed and it was possible to accurately detect F^- ions in the 1 ppm to 6 ppm concentration range. The system is cost-effective, field deployable and user friendly, and hence it can be integrated into a water quality monitoring system to mitigate CKDu.

ACKNOWLEDGEMENTS

The authors would like to express their sincere gratitude and appreciation for the staff at the Department of Electronics and Department of Nano Science Technology of the Wayamba University of Sri Lanka for the support received throughout this research project.

REFERENCES

- [1] H. A. S. Herath, K. Kubota, T. Kawakami, S. Nagasawa, A. Motoyama, S. K. Weragoda, S. K. Yatigammana, "Potential risk of drinking water to human health in Sri Lanka," *Insights*, vol. 18, p. 241–250, 2017.
- [2] S. Imbulana and K. Oguma, "Groundwater as a potential cause of Chronic Kidney Disease of unknown etiology (CKDu) in Sri Lanka: a review," *Journal of Water and Health*, vol. 19, p. 393–410, 2021.
- [3] S. Indika, Y. Wei, T. Cooray, T. Ritigala, K. B. S. N. Jinadasa, S. K. Weragoda and R. Weerasooriya, "Groundwater-based drinking water supply in Sri Lanka: Status and perspectives," *Water*, vol. 14, p. 1428, 2022.
- [4] D. N. D. Liyanage, S. Diyabalanage, S. P. Dunuweera, S. Rajapakse, R. M. G. Rajapakse and R. Chandrajith, "Significance of Mg-hardness and fluoride in drinking water on chronic kidney disease of unknown etiology in Monaragala, Sri Lanka," *Environmental Research*, vol. 203, p. 111779, 2022.
- [5] G. Sivaraman and D. Chellappa, "Rhodamine based sensor for naked-eye detection and live cell imaging of fluoride ions," *Journal of Materials Chemistry B*, vol. 1, p. 5768–5772, 2013.
- [6] Y. Jiao, B. Zhu, J. Chen and X. Duan, "Fluorescent sensing of fluoride in cellular system," *Theranostics*, vol. 5, p. 173, 2015.
- [7] K.A.S. Dilshan and Y.A.A. Kumarayapa, "Low-cost liquid density sensor solution to automate the phosphoric acid recovery process of active carbon," *Proceed. ASRITE*, p.32-38, 2021.

SOLAR POWERED AUTOMATIC WATERING AND LIQUID FERTILIZER SUPPLYING SYSTEM FOR INDOOR POTTED PLANTS

R.A.J.R. Perera*, G.A.K.S. Perera

Department of Electronics, Wayamba University of Sri Lanka, Kuliyaipitiya, Sri Lanka

*jinaliperera98@gmail.com

ABSTRACT

Identifying and providing requirements of indoor potted plants on time, especially water and fertilizer, is crucial for their healthy growth. Several previous studies have addressed the issue of supplying water but do not facilitate fertilizer supply. The system discussed here was designed to supply both water and liquid fertilizer for indoor potted plants. The Arduino UNO board of the system uses feedback from the soil moisture sensor to generate signals that trigger the activation of the water and the fertilizer pumps via the relay module. The system is powered by rechargeable batteries which can be charged using solar energy. It provides numerous benefits for both users and the environment. It saves both the time and the effort of the users by automating plant care, promotes resource conservation by reducing water and fertilizer use, and is also cost-effective by reducing the dependence on conventional electricity sources. In addition, this is quite simple, user friendly and cost effective. The designed system can be improved to make it more versatile for the use of indoor planting.

Keywords: Indoor potted plants, Solar energy, Watering and liquid fertilizer supplying system

1.0 INTRODUCTION

Plants play an essential role in the ecosystem by producing oxygen and absorbing carbon dioxide. Thus, increasing the abundance of plants in our surroundings can have a significant positive impact on air quality, health, and well-being. However, with rapid urbanization and industrialization, people are spending more time in artificial environments. So indoor planting is an ideal way to bring nature indoors and reap the associated benefits. Indoor plants include all kinds of foliage plants and flowering plants that can be grown in many indoor spaces [1]. Due to limited space in urban areas and numerous other scientific benefits, including improving air quality, reducing stress levels, improving overall well-being, happiness, and productivity of workers, and boosting cognitive functions of the brain, indoor plants are becoming popular in incorporating them into homes and workplaces. They can also serve as a natural decoration and add aesthetic value to indoor spaces [2,3]. To reap the maximum benefits from indoor plants, their healthy growth should be ensured providing their requirements as necessary. Water and fertilizer are two important requirements among them [1]. But with the busy schedules of people, there is a possibility to forget to water the plants and supply fertilizer on time. If watering and fertilizer supply can be automated, that will make life easier for plant owners. At the same time, it is highly essential to pay attention on implementing an automated system at low cost and through energy saving approaches. This addresses the value of using renewable energy such as solar and wind.

Many recent studies have focused on automated systems for watering plants. The primary function of these systems is to check the soil moisture level and activate a water pump if the

moisture level is less than a threshold value. When moisture meets the threshold, it automatically sets off the pump. These systems include mainly a moisture sensor, a relay, a motor, and a power supply. Some of these systems have used Liquid Crystal Display (LCD) to display data, while some have used IoT and mobile applications. The power has been supplied to these systems using conventional electricity sources. With all these automated systems, users just have to worry about refilling the water storage when it goes down [4-6]. The main limitation of those systems is that they do not facilitate fertilizer supply. So the fertilizer supply has to be done manually for indoor potted plants. Since supplying the right amount of fertilizer at the right time is essential for plant health, just automating the water supply might not be enough for the users. Additionally, these systems typically use a single threshold value of soil moisture to control the water pumps. This may not be suitable for indoor plants, which often require the soil to dry completely before watering.

A better approach would be to use an automated system that can supply both water and fertilizer for indoor plants, using two threshold values to identify dry and wet soil. Therefore, the main aim of the system discussed here is to automate the process of supplying water and liquid fertilizer to indoor potted plants while not depending on conventional electricity sources. It also aims to conserve water and fertilizer by delivering them to the plants only when needed. So the system will promote both plant health and cost effectiveness.

2.0 EXPERIMENTAL

2.1 Functional requirements of the system

A comprehensive background study was conducted on indoor plants, analyzing their water, fertilizer, and other requirements to identify and determine the functional requirements of the system. The functional block diagram of the system is shown in Figure 2.1.

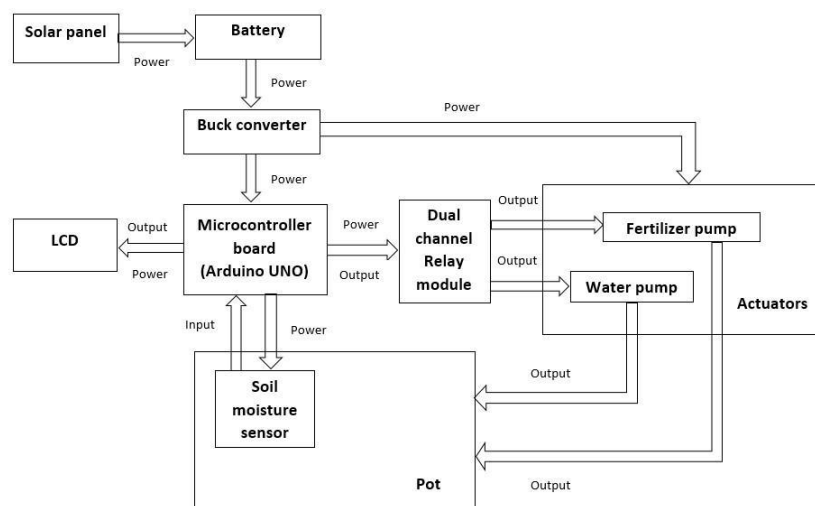


Figure 2.1: Block diagram of the system

Moisture content in the pot is measured using the soil moisture sensor and the obtained analog value is fed to the Arduino board. Based on the input data, the Arduino board determines whether water or fertilizer is needed to be supplied to the plant. When the soil moisture level falls below a predetermined threshold value, the corresponding channel of the relay module is activated to switch on the water pump to supply water to the soil. Once the soil moisture level reaches an adequate predefined level, the pump is switched off. The fertilizer pump is activated

after a defined number of watering cycles, operates for a predefined period, and then is switched off. The moisture content and status of the soil are displayed on an LCD. Additionally, the LCD indicates when the water and the fertilizer pumps are operating. Output from the battery pack is stepped down using a buck converter and provided to power the Arduino board and the pumps. The Arduino board powers the soil moisture sensor, the relay module, and the LCD. The battery pack is charged using a solar panel. The system also includes a separate circuit to identify low liquid levels in the water and liquid fertilizer storages.

2.2 Hardware implementation

According to the functional requirements, the components required for the system were carefully selected and assembled to form the automated system. Arduino UNO board was selected as the microcontroller unit of the system. MH-Sensor-Series soil moisture sensor, HW-383 dual channel relay module, and 16x2 LCD were connected to the Arduino board. Two BI0002051 mini submersible pumps were connected to the relay module and the power supply. The power supply was given to the system using three 18650 3.7 V 2000 mAh Li-ion rechargeable cells connected in series via the XR-121 BMS. The 12 V output of the battery pack was connected to the input of the

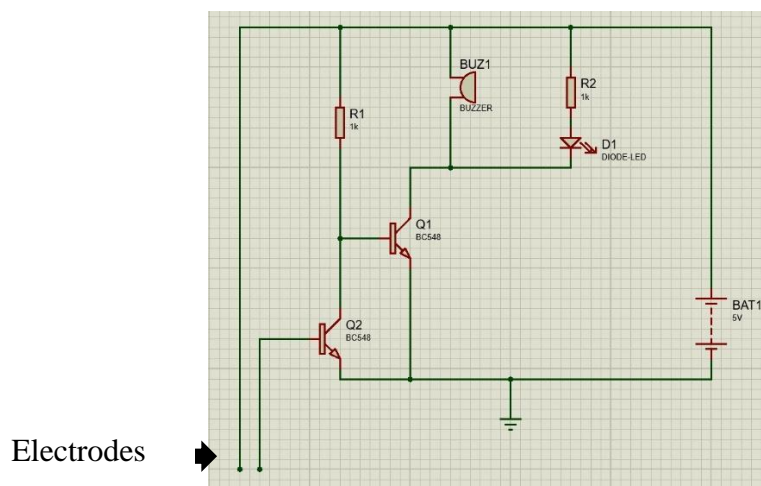


Figure 2.2: Low liquid level indication circuit

XY-3606W buck convertor to get 5 V outputs which were used to supply power to the motors and the Arduino board. The battery pack can be recharged using a solar panel. A separate circuit was designed to indicate the low liquid levels in the water and fertilizer storages as shown in Figure 2.2 using two BC548 transistors, two 1 K Ω resistors, a buzzer, and an LED. Electrodes should be kept inside the storage at a level to be identified as the low liquid level.

2.3 Software development

A complete software program was developed using Arduino IDE to operate the system as required. The soil moisture sensor was calibrated by mapping analog values for completely dry and completely wet soil to 0% and 100% of soil moisture respectively. The soil mix used for calibration included 50% coconut fiber, 25% sand, and 25% compost. The period of supplying fertilizer was calculated using the average flow rate of the pumps. The values obtained were

updated in the program. The data flow diagram for the visual representation of the system operation is shown in Figure 2.3.

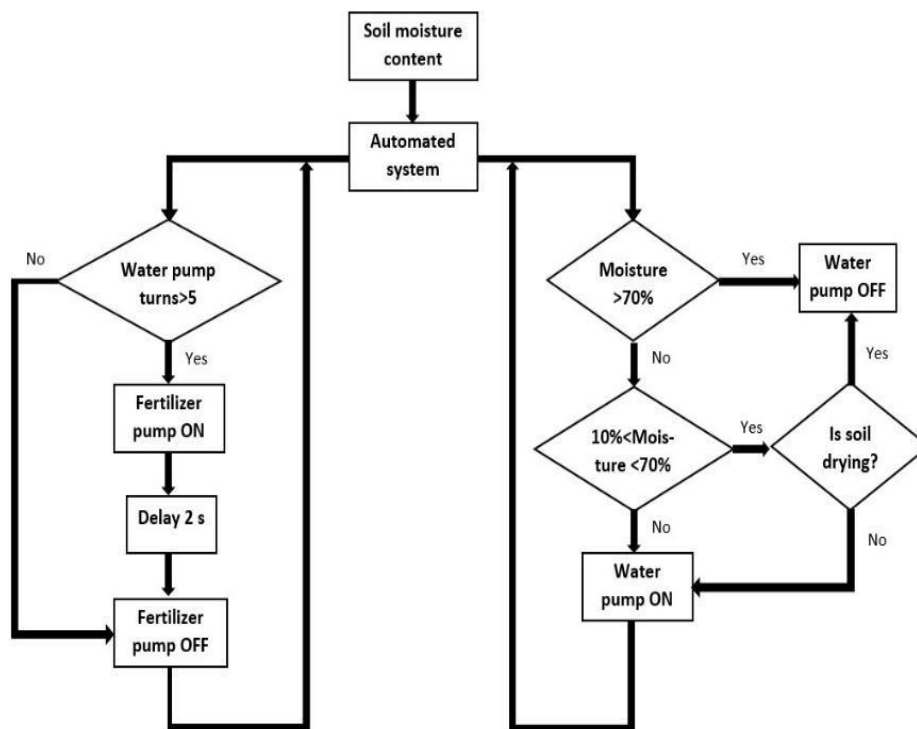


Figure 2.3: Data flow diagram of the system

2.4 Testing of the system

Before testing the system, the temperature and humidity of the test environment were measured using a DHT11 sensor. Then, the developed program was uploaded to the assembled system and it was tested to validate its functionality and accuracy. The same soil mix used for the calibration of the sensor was used for testing. To validate the functionality of the water pump, soil samples with varying soil moisture levels were used. The soil samples include dry soil, partially wet soil, and completely wet soil. The soil moisture sensor probes were inserted into the samples and the system's response was observed. To verify the fertilizer pump's operation, a water container was used. The soil moisture sensor probes were repeatedly immersed in and removed from the water, and the system's behavior was monitored. The fertilizer pump should activate after a predefined number of watering cycles and operate for the determined ON period. The low liquid level indicator was tested by inserting the electrodes in an empty container and then filling it with water. Through these tests, the functionality of the system was successfully demonstrated.

3.0 RESULTS AND DISCUSSION

3.1 Verification of system functionality

The final design of the system was constructed as shown in Figure 3.1. The system was calibrated and tested under a specific environment. The temperature and humidity of the test environment were 30.2 °C and 72% respectively. The lower soil moisture threshold value was selected as 10% and the upper soil moisture threshold value was selected as 70%.

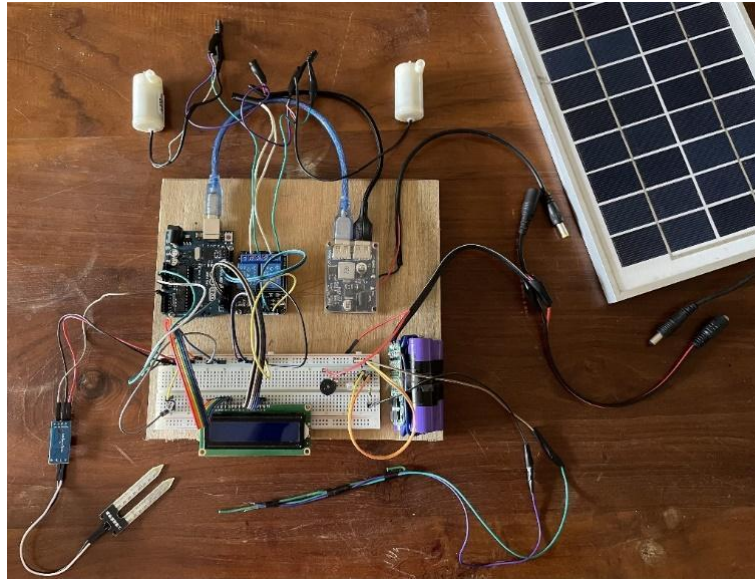


Figure 3.1: Final design of the system

When the soil moisture sensor was inserted in soil samples with different moisture content, the ON/OFF status of the water pump and the content displayed on the LCD are shown in Table 3.1.

Table 3.1: Operating status of the system for water pump control

Soil sample	LCD status	Water pump status
Dry soil	Moisture:8% Dry & watering.	ON
Partially wet soil	Moisture:48% Good & watering.	ON
Completely wet soil	Moisture:92% Soil is wet.	OFF

When the system was tested for fertilizer pump control, the fertilizer pump turned ON after 5 turns of water pump activations, operated for 2 seconds, and turned OFF. ON status and OFF status of the fertilizer pump were displayed on the LCD. When the low liquid level indicator circuit was tested, the obtained results for the ON/OFF status of the buzzer and the LED are shown in Table 3.2.

Table 3.2: Operating status of the low liquid level indicator

Status of container	Buzzer status	LED status
Empty	ON	ON
Filled with water	OFF	OFF

3.2 The reliability and accuracy of the system's performance

Environmental factors such as temperature and humidity, sensor calibration, and other errors that might occur during the operation may affect the performance of the system. Higher temperatures lead to increased water loss from the soil, while higher humidity levels promote moisture retention within the soil. The combined effects of temperature and humidity on water demand can be effectively monitored by assessing soil moisture content regularly. This approach eliminates the need to consider both temperature and humidity separately, simplifying plant care. By calibrating the soil moisture sensor using the actual soil mixture and in the same environment where the plant would be placed, users can obtain accurate and reliable readings of soil moisture content, ensuring optimal watering schedules and promoting plant health. To guarantee accurate watering and drying cycles and prevent system malfunctions the system compares the current soil moisture reading with the previous reading. However, occasional sensor malfunctions may lead to inaccurate readings, potentially disrupting the watering cycle.

3.3 Advantages and limitations of the system

The designed system offers a solution for automating the care of indoor potted plants, providing both water and liquid fertilizer to ensure their optimal growth and well-being. This system significantly reduces the need for manual intervention, saving time and effort for users. By identifying the plants' needs and delivering the appropriate amount of water and fertilizer at the right time, the system promotes resource conservation. Moreover, its reliance on solar energy for charging aligns with the principles of sustainability and reduces dependence on conventional energy sources making it cost-effective. The system's design is easy to operate making it user-friendly. Overall, the proposed automated system presents a practical solution for managing indoor potted plants, offering numerous benefits for both users and the environment.

While the designed system offers numerous advantages, it does have certain limitations that should be considered. The system currently relies on a predetermined fertilizer schedule based on water cycles, which may not accurately reflect the plant's exact nutrient needs. Environmental conditions such as temperature and humidity can also affect the performance and accuracy of the system since they affect the calibration of the sensor. The current system was designed for a single plant and may not be suitable for different plant types with varying water and nutrient requirements. Moreover, the system's user interface is relatively limited, providing primarily output data rather than interactive controls. The system's watering and fertilizing thresholds are currently fixed in the programming code. Addressing these limitations would further enhance the effectiveness of the automated system.

4.0 CONCLUSION

Solar powered automatic watering and liquid fertilizer supplying system for indoor potted plants was successfully designed and constructed. The system was designed to automate the process of supplying water and liquid fertilizer to indoor potted plants, reducing the need for manual plant care and making it more convenient for users. The system was tested under different conditions and was found to respond exactly as expected. It could identify the moisture content in soil and activate the pumps to supply water and liquid fertilizer as intended by the user. To fully evaluate the system's performance and identify areas for improvement, long-term tests need to be carried out. By following approaches like incorporating a Real Time Clock (RTC) module to improve the fertilizing schedule, modifying hardware and software

program to make the system compatible with multiple plants, and incorporating a more interactive user interface the system can be improved to make it more versatile for the use of indoor planting. Overall, the designed system provides a good solution for automating care for indoor plants.

ACKNOWLEDGEMENTS

Authors wish to thank the Department of Electronics, Faculty of Applied Sciences, Wayamba University of Sri Lanka for the support and guidance given while carrying out this research.

REFERENCES

- [1] Nicolaisen, A., Gorer, R. (eds.). *The Pocket Encyclopaedia of Indoor Plants in Colour*. London: Blandford Press, 1970. E-book.
- [2] Sharma, P., Thaneshwari, Sachin, T.M., Akram, S.M., Indoor gardening for aesthetic and healthy lifestyle. *The Pharma Innovation Journal* 10/5, (2021), 382-389.
- [3] De Vries, S., Hermans, T., Langers, F., Effects of indoor plants on office workers: a field study in multiple Dutch organizations. *Frontiers in Psychology* (2023), doi: 10.3389/fpsyg.2023.1196106.
- [4] Nu, Y.Y., Lwin, S.S., Maw, W.W., Automatic Plant Watering System using Arduino UNO for University Park. *International Journal of Trend in Scientific Research and Development (IJTSRD)* 3/4, (2019), 902-906.
- [5] Abhishek, V., Akash, R., SUDHA, P.N., Automatic Plant Watering System Using Arduino. *International Journal of Innovative Research in Technology (IJIRT)* 8/3, (2021), 260-262.
- [6] Venkatesh, P., Manojkumar, R., Rajesh, R., Venkatesh, N., Design and Fabrication of Automatic Plant Watering System. *International Journal of Research Publication and Reviews* 4/4, (2023),5145-5149.

WEATHER FORECASTING BASED AUTOMATED SWITCHING SYSTEM FOR HYBRID PV SYSTEMS

U.I.K. Perera*, Y.A.A. Kumarayapa

Department of Electronics, Wayamba University of Sri Lanka, Kuliyapitiya, Sri Lanka

*ivanthakasunperera@gmail.com

ABSTRACT

Recent years have seen a significant increase in the popularity of integrating renewable energy sources into home power networks, especially in the form of hybrid solar power systems. Changeover, switch in between PV system to a grid power source, has historically been accomplished manually. This may result in ineffectiveness, constant concentration and attention from humans, energy waste, and serious interruptions to the power supply. An intelligent Internet of Things (IoT)-based navel switching system for hybrid home solar power systems is presented to address these issues. This system automates the two-way switching process by using real-time monitoring of the solar system's battery voltage, the weather, and the amount of energy used in the home. The system combines several sensors and actuators with the help of a CPU that processes data to create a cloud-based monitoring platform that collects information and determines which power source is best for the home at any given time. Python was used to program the Raspberry Pi 3 Model B, which served as the basis for all of the procedures. The Voltage Detection Sensor module was used to test the battery's voltage, while the SCT013 60A/1V Sensor module was used to assess the household's power consumption. The application programming interface "openweathermap.org" is used to track local weather forecasts. These factors are included to give priority to using the PV system when the conditions are right, such high irradiance and clear skies. A 1.8-inch 128x160 TFT LCD Color Display at the station was used to display all the updated parameters for the system, including weather, internet access availability, power source consumption, battery voltage level, and mode of changeover (auto/manual). All of the previously listed criteria can be remotely tracked with the use of the website developed for this research study.

Keywords: Automated, Changeover, Hybrid solar energy harvesting systems, Internet of Things

1.0 INTRODUCTION

Transitioning to a sustainable and ecologically friendly energy harvesting and efficient utilization of power has become a global priority. In this environment, the integration of renewable energy sources, notably solar power electricity, into domestic power systems has gained substantial popularity. Two major challenges with photovoltaic (PV) generation systems are the conversion efficiency of electric power generation is becoming exceptionally low on those conditions (9–17%), the amount of electricity generated by solar arrays and varies constantly with weather conditions and in low irradiation conditions. Photovoltaic (PV) systems are primarily used in two configurations: stand-alone (household, street lighting, recreational vehicles (RVs) and camping, electric cars, boating, and marine applications) or grid-connected (residential and commercial PV hybrid systems) [1].

Grid-connected photovoltaic systems, are composed of PV arrays that are linked to the grid via a power conditioning unit and are intended to run in parallel with the utility grid [2]. The cost of an all-in-one power conditioning unit is expensive (about LKR 110, 000- LKR 280, 000) due to their integrated design and additional features [3]. A more economical setup can be obtained by combining separate units of charge controllers, inverters, and changeover switches.

A changeover switch is utilized in the above system, alternate between the PV system and grid power. Such a system provides an uninterrupted and consistent flow of electricity to the devices of home appliances connected to it.

The main objective of design and construction of an IoT based changeover to switch automatically between the grid and PV system based on the weather forecast, load power consumption, and battery voltage level. The IoT platform allows for real-time monitoring of the system.

2.0 EXPERIMENTAL

There are three primary processes in the implemented system: Weather Forecasting Data Monitoring, Load Power Measuring, and Battery Voltage Measuring then switching and displaying according to the measured parameters.

2.1. Weather Forecasting Data Monitoring.

All the weather forecasting data for the Kuliyaipitiya area (latitude=7.4688 and longitude=80.0401) were obtained through the JSON file by sending the following ‘GET’ request to the ‘OpenWeather’ API and saved it into a configuration file.

GET Request:

<https://api.openweathermap.org/data/2.5/forecast?lat=7.4688&lon=80.0401&units=metric&appid=8422dff2e1655bb932f888f2e5eXXXXX>

2.2. Power Measuring of the load.

The current drawn by the load was measured using the SCT013 Current Transformer sensor. It was connected to the Raspberry Pi board via ADS1115 16-bit 4-channel ADC. Power consumption was calculated by measuring the Root mean square (RMS) current through the inverter, using the equation 2.2.1. It is necessary to apply the RMS formula and capture instantaneous current values across the whole cycle of the waveform to obtain the RMS current [4].

$$I_{rms} = \sqrt{\frac{i_1^2 + i_2^2 + i_3^2 + \dots + i_n^2}{n}} \quad [2.2.1]$$

Where; I_{rms} = root mean square (rms) current

i_1^2 = Instantaneous currents

n = Number of samples

The voltage of an AC inverter is typically fixed and can be found in the inverter manufacture's specifications or by measuring it directly with a voltmeter. Power can be calculated using I_{RMS} and measured voltage values using equation 2.2.2.

$$P_{rms} = V \times I_{rms} \quad [2.2.2]$$

Where; P_{rms} = Root mean square (RMS) power

V = Output voltage of the inverter

I_{rms} = Root mean square (RMS) current

Calculated power values were saved into a configuration file for later use.

2.3. Measuring of the Battery Voltage.

The voltage of the battery was measured using the voltage sensor. It was connected to the Raspberry Pi board via ADS1115 16-bit 4-channel ADC. Calculated voltage values were saved into a configuration file.

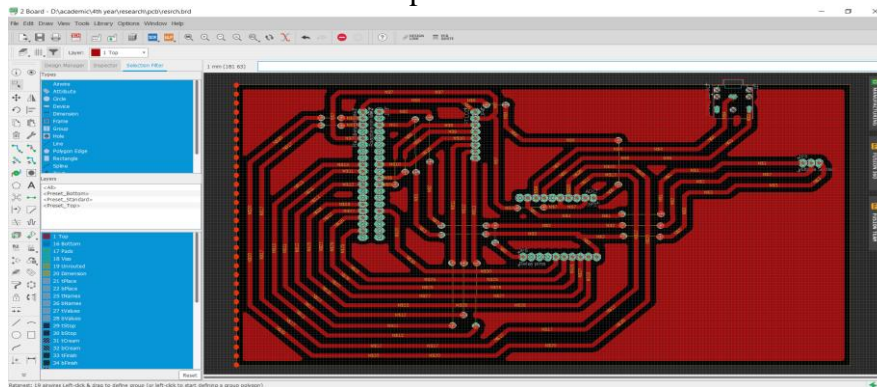
2.4. Displaying on TFT LCD.

The 1.8-inch 128*160 TFT SPI serial LCD color display was used to show the parameters with a GUI.

2.5. IoT Monitoring

All the parameters saved into the configuration file were uploaded to the MongoDB database using POST requests via JSON files. All the parameters in the MongoDB database were read using GET requests via JSON files. Those parameters were displayed using the web interface.

PCB was fabricated to assemble all the components.



(a)

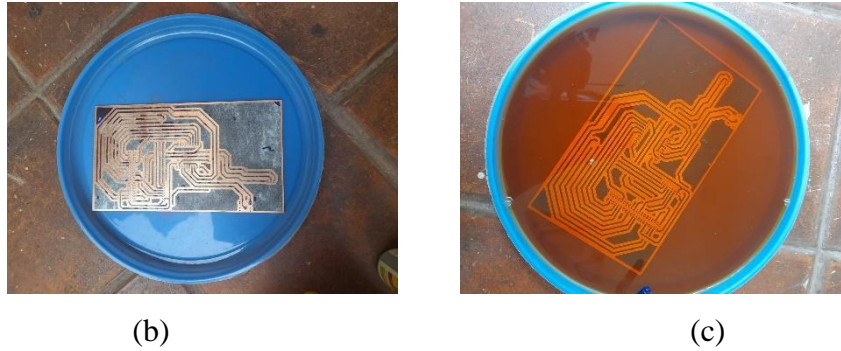


Figure 2.1: Designed and fabricated PCB for the changeover

3.0 RESULTS AND DISCUSSION

The prototype of the proposed changeover is implemented design is shown in Figure 3.1.

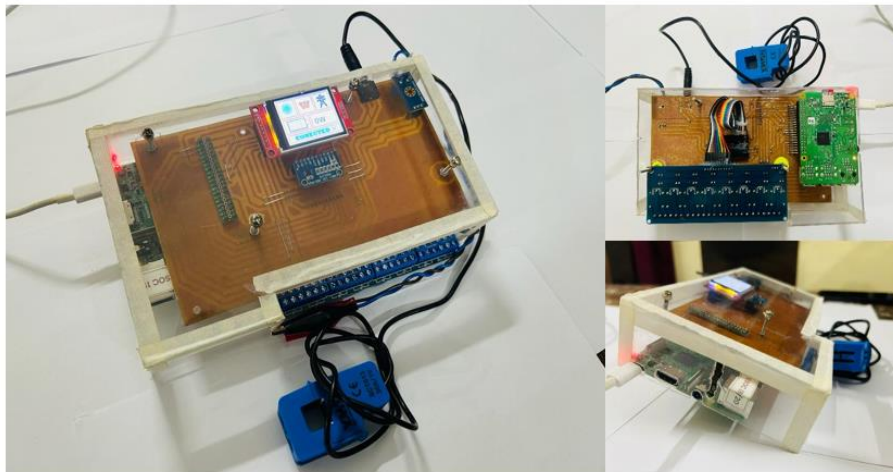


Figure 3.1: Prototype of the Automatic changeover

3.1. Switching process according to Weather Forecasting

The weather forecast monitoring program retrieves the weather forecast data from a JSON file, as shown in Figure 3.2.a. It then sets the variable 'WeatherVal' according to the given instructions, as shown in Figure 3.2.b.

```

99 weather_data = get_weather_now('Kuliyapitiya', openwe
100 weather data forcast = get weather forcast('Kuliyapit
Shell
City: Kuliyapitiya
Weather focatst1: Rain
Weather_des focatst1: moderate rain
Weather focatst1: 501

Weather focatst2: Rain
Weather_des focatst2: moderate rain
Weather focatst2: 500
-----
City: Kuliyapitiya
Weather focatst1: Rain
Weather_des focatst1: moderate rain
Weather focatst1: 501

Weather focatst2: Rain
Weather_des focatst2: moderate rain
Weather focatst2: 500
-----
vvalue of 'WeatherVal' is 1
\-----end-----//
    
```

(a)

```

79
80 if(idVal>=802 and idVal <=804):
81     WeatherVal=0
82 elif(idVal>=500 and idVal <=531):
83     WeatherVal=1
84 elif(idVal==801):
85     WeatherVal=2
86 elif(idVal==800):
87     WeatherVal=3
88
89 #print(WeatherVal)
90 return WeatherVal
91
    
```

(b)

Figure 3.2: (a) Given instructions and (b) Displays the weather forecast data that was read by the weather forecast monitoring program.

The TFT LCD GUI is updated and displays the appropriate weather icon based on the variable values as shown in figure 3.3.

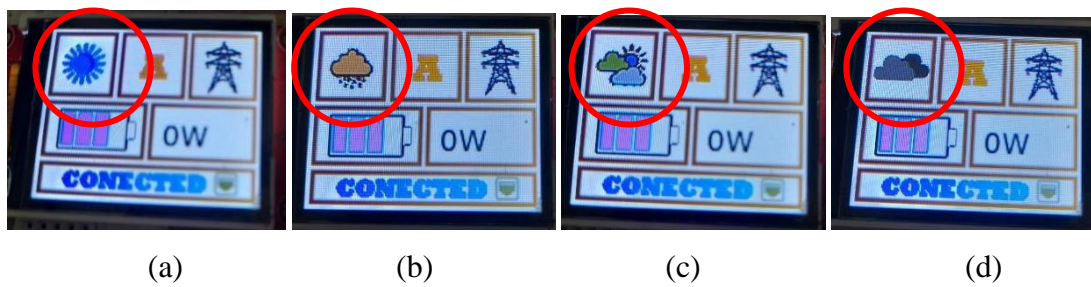


Figure 3.3: Display updates based on (a) sunny, (b) rainy, (c) sun with cloud, (d) cloudy weather condition

The switching between the grid and inverter occurred based on weather conditions as shown in Figure 3.4.

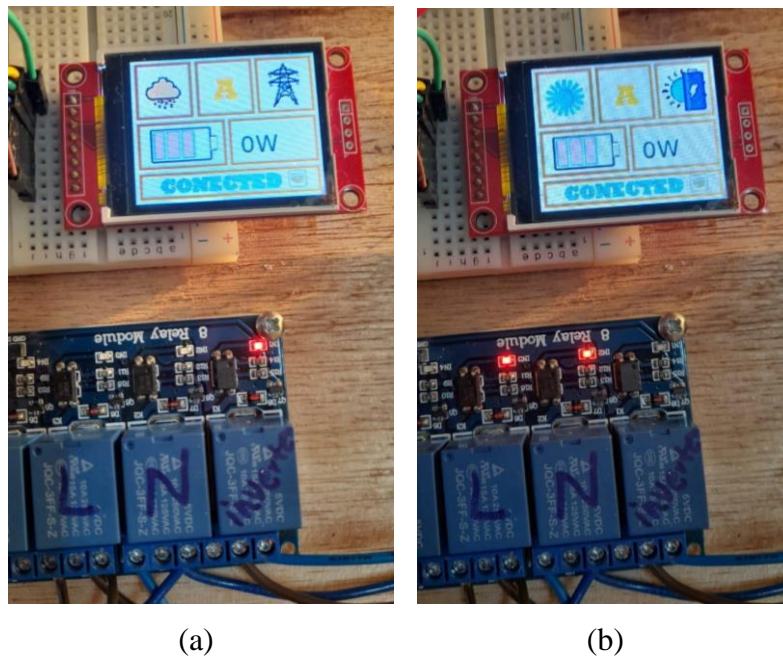


Figure 3.4: Power supply switched between the grid and inverter based on weather condition

As shown in Figure 3.4.a, when the weather condition is ‘rainy’, the changeover was switched to the grid, and the inverter is switched OFF (Red LED on the last relay module is turned ON for such indication). As shown in Figure 3.4.b, when the weather condition is ‘sunny’, the changeover was switched to the PV system, and the inverter was switched ON.

Simultaneously the IoT web interface is updated and displays the appropriate weather icon and power source based on the variable values as shown in Figure 3.5.

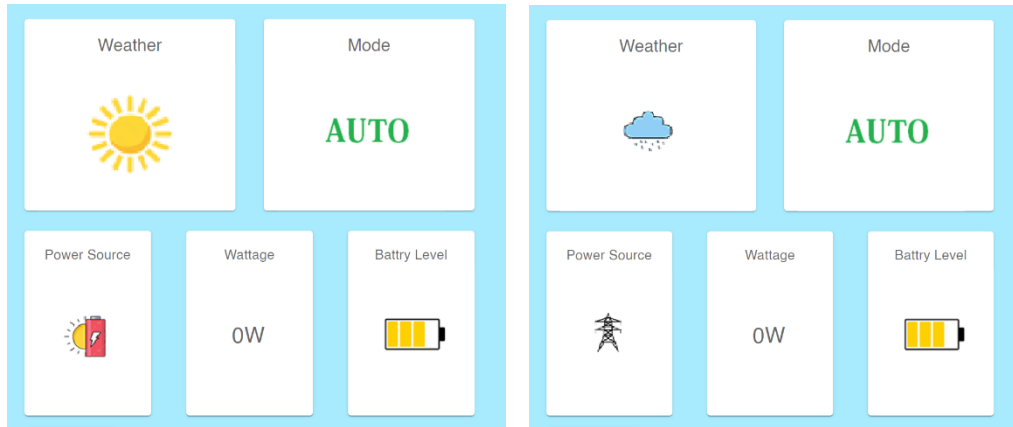


Figure 3.5: Web interface updates based on weather conditions and power source data

3.2 Switching process according to power consumption.

The switching between the grid and inverter occurred based on the power consumption of the load as shown in Figure 3.6.

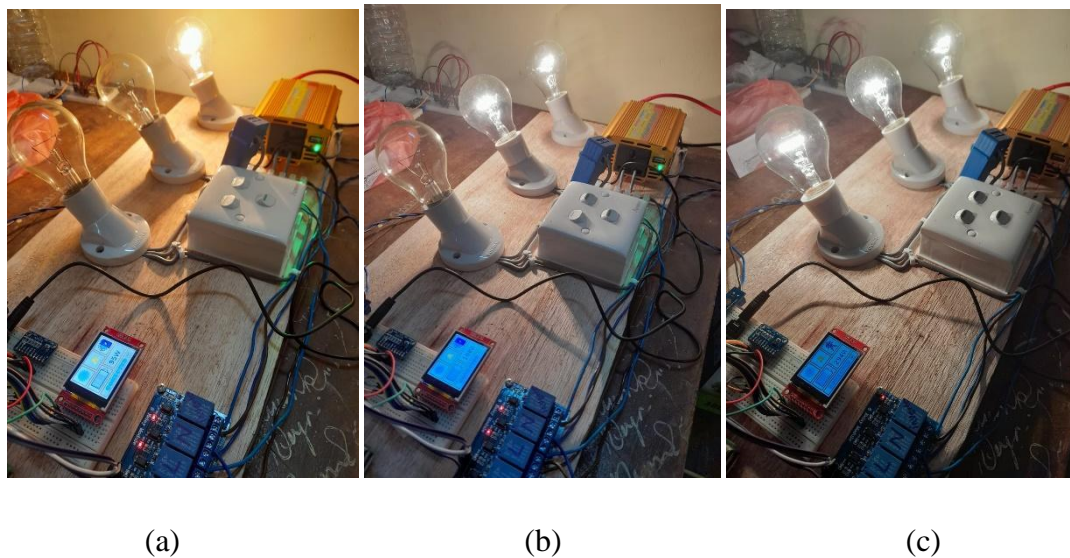


Figure 3.6: Power source is switched between the grid and inverter based on load power consumption
As shown in Figures 3.6.a and 3.6.b, when the power consumption is below the reference power value (250W in this demonstration), the changeover was switched to the inverter, and the inverter was switched ON (Red LED on the last relay module was turned ON for indication). Also, it showed in the TFT LCD. As shown in Figure 3.6.c, when the power consumption is above the reference- power, the changeover is switched to the grid, and the inverter is switched OFF and indicated it on the LCD. Simultaneously the IoT web interface is updated as shown in Figure 3.7.

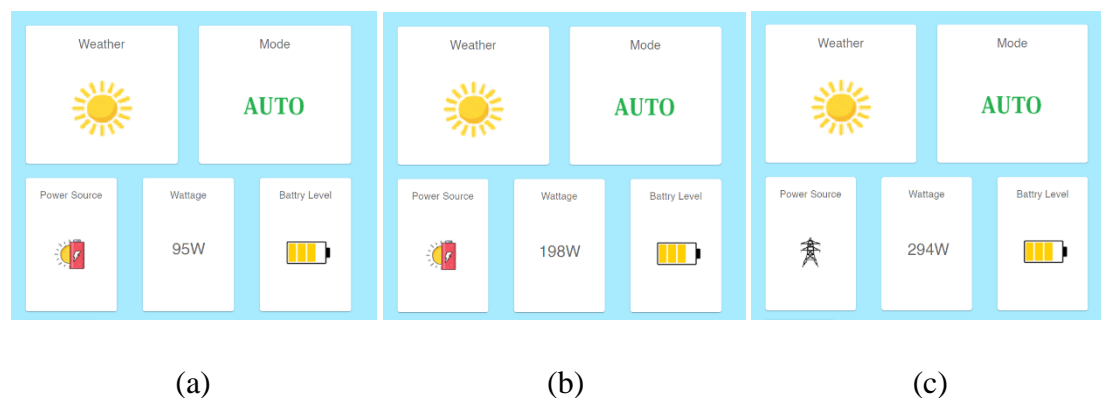


Figure 3.7: IoT web interface is updated according to load power consumption

The design and implementation of our system effectively demonstrated its capability to alternate between the grid and the inverter based on power demand and weather conditions. The system was equipped with a TFT LCD GUI and an IoT web interface that could be updated using weather forecast data from a JSON file. By monitoring the power consumption of the load, the system was able to switch between using the grid and the inverter as a power source. The system's performance was impressive and it proved to be efficient in controlling power consumption.

4.0 CONCLUSION

The need of switching to a sustainable energy system is growing more important as the Earth's resources get more limited and the world's energy consumption keeps rising. With its availability and advantages for the environment, solar energy is the promising energy replacement for traditional energy sources. One way to optimize energy use and reduce reliance on the grid is to develop a solar system changeover switch based on weather forecasting data. The prepared switch can smoothly switch between solar and grid power, guaranteeing a dependable and economical energy source, by integrating weather forecast data.

The primary objective of this project is to develop an IoT-based automatic changeover switch for domestic purposes, switching between the grid and PV system, based on weather forecasting data. Accurate weather forecasting data was obtained by accessing the 'OpenWeather' API, which was used to develop the changeover system. Additionally, this system collects data on the power consumption of the load and the level of voltage in the battery. These data are uploaded to a MongoDB database in Real-time. The IoT web interface allows for device monitoring by retrieving data from the database.

Hence this system can be used to enhance the efficiency and reduce the maintenance cost of the PV system. In future studies, data can be collected about solar energy generation from panels to develop an analysis model for forecasting switching patterns without third-party platforms.

ACKNOWLEDGEMENTS

Authors would be grateful to the lecturers and staff at the Department of Electronics, faculty of Applied Sciences Wayamba University for their guidance in research and laboratory facilities.

Authors would be grateful to the members of the Electronics Society for maintaining a collection of valuable electronics components and circuitry parts, which have aided us in this research and that of other electronics undergraduates.

REFERENCES

- [1] Sağlam Ş., Meteorological parameters effects on solar energy power generation, WSEAS Trans. Circuits Syst., vol. 9, no. 10, pp. 637-649, 2010.
- [2] Rashid M. H., *POWER ELECTRONICS HANDBOOK DEVICES, CIRCUITS, AND APPLICATIONS*, 3rd Ed., USA, Elsevier Inc.,717-720, 2011.
- [3] IMEX Energy products prices, <https://imexsolar.lk/shop/>, (Accessed 2023-11-29).
Bhattacharya S. K., Debashis De, Basic Electrical And Electronics Engineering I (For Wbut), India, Pearson Education, 149, 2010.

COMBINED POWER SYSTEM USING A LI-POLYMER BATTERY, SUPERCAPACITOR BANK AND SOLAR CELLS FOR A DRONE

T.K.C.Samarasinghe*, K.P. Vidanapathirana

Department of Electronics, Wayamba University of Sri Lanka, Kuliyaipitiya, Sri Lanka

*chamil.samarasingh98@gmail.com

ABSTRACT

Commercial drones are utilized to do some special tasks, but their battery time affects the completion of tasks. To overcome these limitations combined or hybrid power system technologies are tested. During the designing process of new power system mechanisms, several facts have to be considered due to the drone's architecture. The proposed system was designed as a combined power system using Li-polymer (LiPo) battery, supercapacitor bank (SCB) and solar cells. This design mainly has two power sources a LiPo battery and SCB. Solar cells are used to charge the SCB. In this design, SCB and solar cells are considered as one unit. Within the combined power system mechanism only one power source is taken into action. Two power sources are not simultaneously active. Some interchanging mechanism is needed between two power sources based on their charging rate (voltage value). To proceed with this interchanging mechanism switching circuit was designed using a voltage measuring sensor, MOSFET, and Arduino UNO board. This switching circuit helps to measure the voltage values of two power sources using the voltage measuring sensor. These two power sources have active regions which can power up the motors properly. The proposed combined power system model can be used in commercial drones but needs some modifications. These modifications will depend on the drone's specifications and power consumption. Under normal atmospheric conditions, the SCB can reach a predefined maximum charged state (4 V) within 1 to 2 minutes and Power can be supplied to the motors for at least 95 seconds from a predefined maximum charged state (4 V) to a predefined minimum voltage (1 V) through a SCB (while charging).

Keywords: Supercapacitor, MOSFET, LiPo

1.0 INTRODUCTION

A drone is a flying robot that can be controlled through a wireless remote controller and main controlling unit. Most drones are made for special purposes, such as fertilizing, mapping, delivering, videography, etc. Drones require power sources, such as a battery, fuel, or other suitable sources, to fly and have a frame, motors, and propellers.

Drone frames are often composed of lightweight composite materials to minimize weight and improve maneuverability [1,2]. Drones are not only flying devices but also do some special tasks. Battery-powered drones are widespread nowadays. But it has the drawback of less flying time. Normally, drones need battery capacities to ranging from 200 mAh to at least 20,000 mAh.

Most drones use Li-polymer (LiPo) batteries as a power source. These batteries are charged through a special type of charger, which takes a considerable time compared with the drone's

complete flying time when using a fully charged LiPo battery. These batteries are charged at the ground level and cannot be charged while the drone is flying [3].

Supercapacitors (SC) is an energy storage system that stores energy based on their electrochemical properties. Compared with conventional dielectric capacitors, SC has higher power density and specific capacitance. These systems can efficiently release energy with a high-power density over a relatively short time. SC has an unsatisfactorily low energy density, a low amount of energy stored per unit weight, higher dielectric absorption, and a higher rate of self-discharge than an electrochemical battery, despite having benefits like a better lifecycle and higher power density. When a SC is shorted, it quickly discharges due to its low internal resistance. According to the mechanism of the drone and the SC types wired-based solar panel architecture is the most efficient for charging purposes. During the daytime, the SC can be charged continuously when it is flying. It is very beneficial for the drone performance. Most of the presently used charging methods cannot charge their power sources while flying [4,5].

Design of a combined power system needs some switching mechanism to switch between two power sources. It needs a high-speed switching circuit to achieve the highest performance. While designing this switching mechanism need to consider some important factors. Because drones can handle a limited amount of weight.

2.0 EXPERIMENTAL

2.1 Charging time of a supercapacitor using a solar cell

A simple circuit has been developed using an ESP32 board and a voltage measuring sensor to obtain charging time and corresponding voltage values. Using this circuit, an Excel sheet can be updated at specified time intervals. Various types of SCs are available in the market. In this study, the primary focus was on the weight and voltage values of the SC. Consequently, the following circuit (Figure 2.1) was designed to identify the most efficient SC for this study and Figure 2.2 shows a charging time comparison of three button-type SCs.

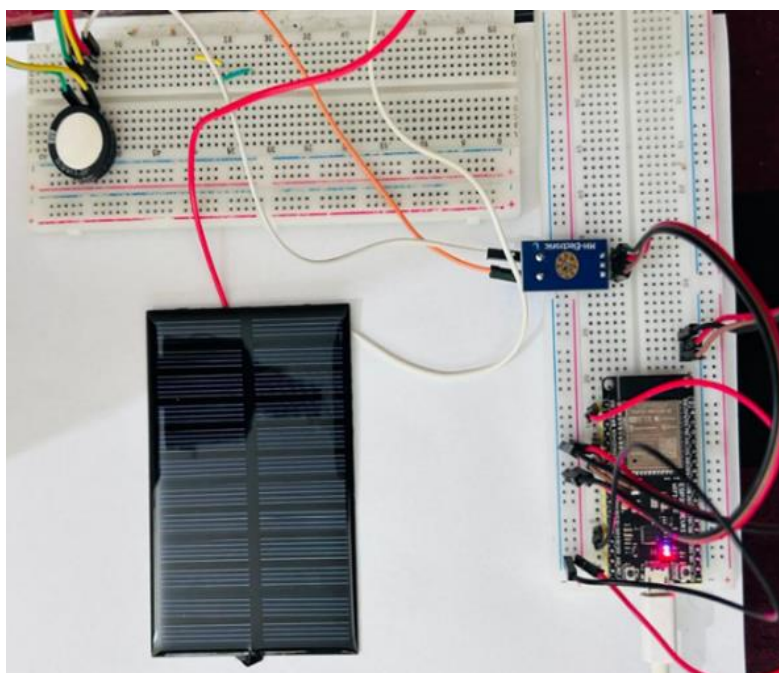


Figure 2.1: SC charging time and voltage monitoring circuit

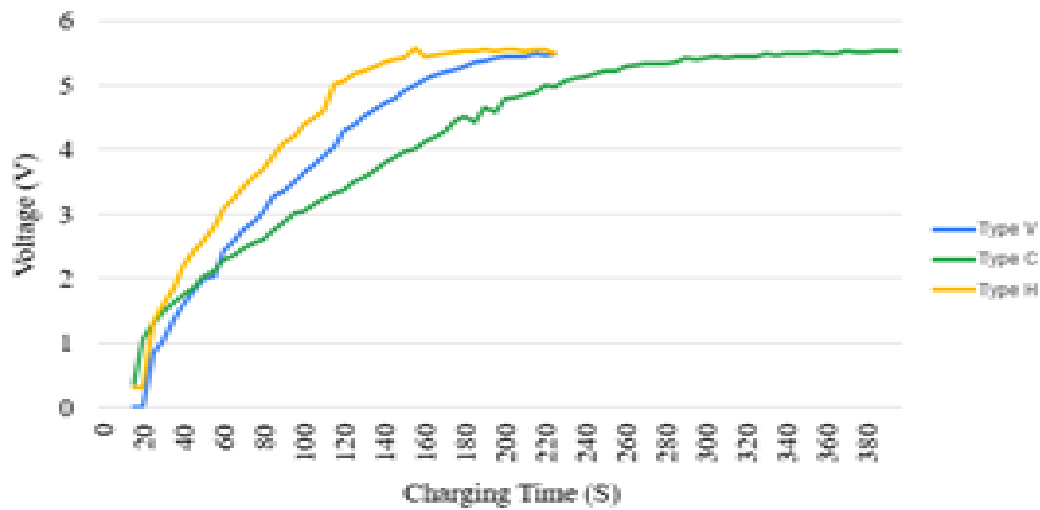


Figure 2.2: Charging time comparison of different SC types

2.2 Supercapacitor discharging time measurement with DC coreless motor

The setup in Figure 2.3 was designed to measure the discharging characteristics of the SCs through a DC-coreless motor.

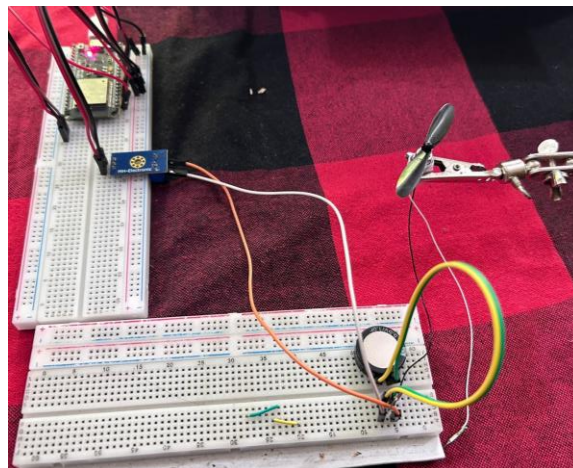


Figure 2.3: SC discharging time and voltage monitoring circuit

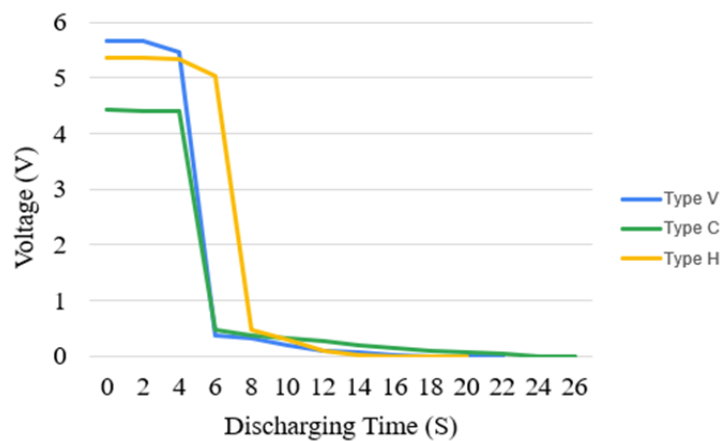


Figure 2.4: Discharging time comparison of SC types

2.3 Supercapacitor bank (SCB)

By analyzing the charging (Figure 2.3) and discharging (Figure 2.4) times of SCs, it was determined that drones require more than one SC to fulfill their power requirements. Based on results obtained a SCB was designed. It was determined that the H-type SC exhibited the highest efficiency (relatively less charging time and high discharging time). Due to this efficiency, a SCB was created utilizing parallelly connected six H-type SCs. Figure 2.5 depicts the structure of the SCB.



Figure 2.5: Supercapacitor bank

Based on the results shown in Figure 2.2, it was observed that a single solar cell was not sufficient for the SCB. Consequently, combined solar cells as in Figure 2.6 were designed, with eight solar cells being connected in parallel.



Figure 2.6: Combined solar panel design

2.4 Switching circuit

The switching circuit formed the basis of the entire study. The switching part was primarily controlled through the MOSFET. Depending on the command signal provided using the Arduino Uno board, the MOSFETs were operated. Figure 2.7 shows a complete model (switching circuit) with two power sources. The operation of the switching mechanism depends

on predefined maximum and minimum voltage values. Practically, these voltage values were measured using a voltage-measuring sensor. The measured values matched the predefined values, initiating the starting of the switching process. The predefined voltage values were integrated into a code using a trigger point. The activation of the SCB throughout the predefined period was facilitated by the trigger point.

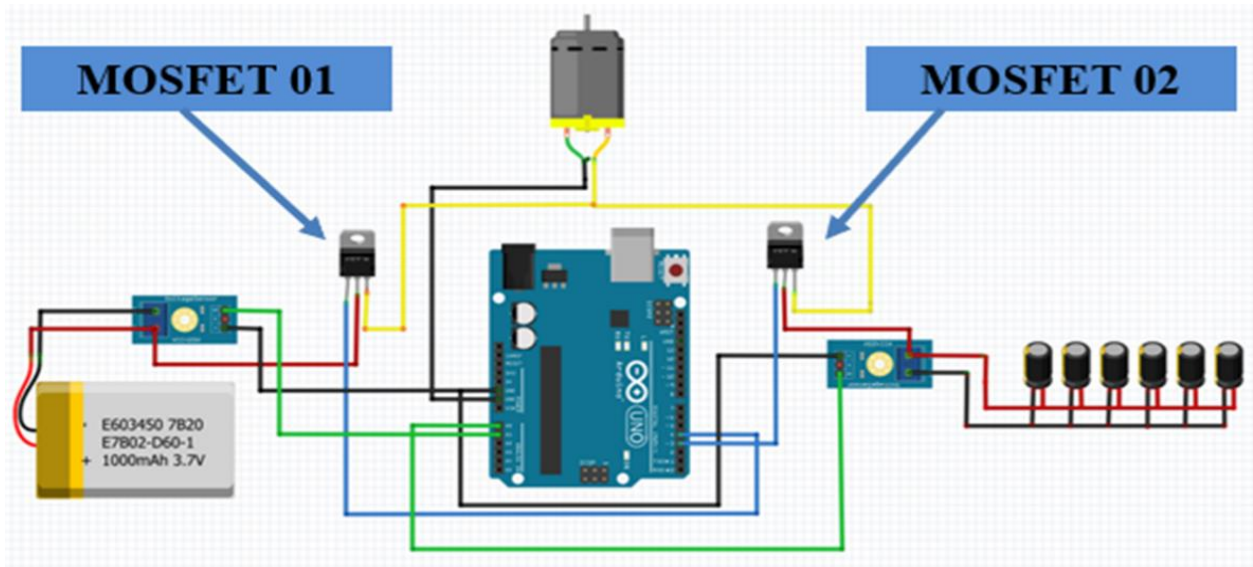


Figure 2.7: Schematic diagram of the switching circuit

3.0 Results and Discussion

Promising outcomes in enhancing the operational efficiency of the drone were demonstrated by the combined power system, which integrated a LiPo battery, a supercapacitor bank (SCB), and a solar cell. Main focus of this study was to flying time extension, adaptability to different power sources, and overall reliability of the system.

LiPo batteries, in comparison with other available power sources for drones, are widely utilized for both commercial and military drones. Distinctive advantages and challenges are presented within the field when SCs are considered as a potential power source for drones. Which is often attributed to their exceptionally high discharge rate. SC technology is characterized by its rapid charging and discharging capabilities, resilience to overcharging, and capacity to mitigate DC bus voltage fluctuations significantly. The operational flexibility of SCs spans a wide range of temperatures, making them suitable for diverse flight conditions and environments. However, their optimal application in drone systems involves their integration either as an additional power source or as part of a hybrid system alongside the other high-energy-density sources [6].

Under normal atmospheric conditions, the SCB can reach a predefined maximum charged state (4 V) within 1 to 2 minutes (Figure 3.1).

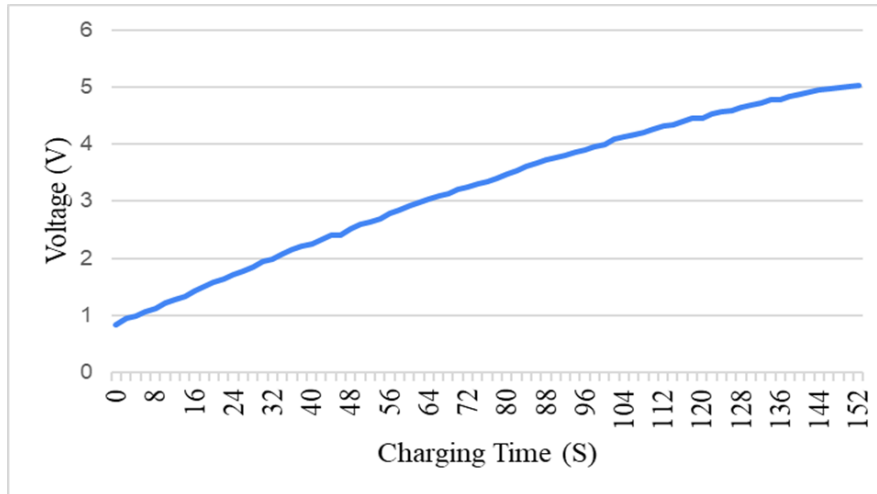


Figure 3.1: Charging time (through the combined solar cells design) curve of SCB

Power can be supplied to the motors for at least 95 seconds (Figure 3.2) from a predefined maximum charged state (4 V) to a predefined minimum voltage (1 V) through a SCB (while charging).

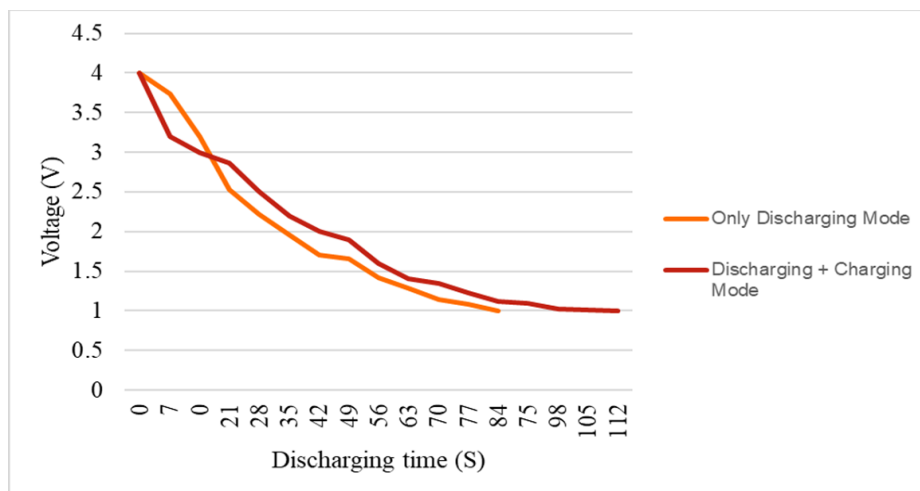


Figure 3.2: Discharging time comparison of SCB

Within this study discharging + charging mode helps to control the discharging rate of the SCB. Here the charging and discharging processes were simultaneously run to get high-efficiency results.

In this study, creating a combined solar cell structure is deemed necessary to achieve a sufficient charging rate for the SCB. The primary objective in designing the combined solar cells is to attain a high current and nearly 6 V voltage. To accomplish this, solar cells were connected in parallel, aiming to maximize the current output.

Within this combined power system, the discharging and charging processes of the SCB occur simultaneously. Due to this architecture, the SCB and the combined solar cells-based charging unit were considered as a single unit. While high-power solar panels are available, certain limitations are present within this system. Typically, high-power solar panels tend to be very

large, making it impractical to integrate them directly into the drone in contrast, the combined design allows for separation, enabling easy attachment to the four arms of the drone. This separation does not impact their connection; rather, it solely influences their physical structure. Consequently, the combined solar cell design is highly suitable for drones.

4.0 CONCLUSION

This study proposed a new solution to extend drone flying time using a combined mechanism of power source and part of the power source can be charged while the drone is flying. According to this study LiPo battery, SCB, and solar cells are combined to generate power. SCB and combined solar cells design act as one unit. SCs have a high charging rate. Using that feature, SCB can charge to their sufficient voltage level within one to two minutes. Based on the voltage values measured through the voltage sensors, the switching mechanism starts based on the microcontroller command and MOSFET. In this model, when SCB starts to supply power to motors it can cautiously supply for around 95 Seconds. Within this system, charging and discharging processes are occurred simultaneously. As a result of this simultaneous process, the discharging rate of the SCB can be controlled.

ACKNOWLEDGEMENTS

The authors would like to express sincere gratitude and appreciation to academic and other staff of the Department of Electronics, Faculty of Applied Sciences, Wayamba University of Sri Lanka for the support provided during the study.

REFERENCES

- [1] Daley, S., What Is a Drone? Uses of Drones and Definition., <https://builtin.com/drones> (Accessed 2023-11-05).
- [2] Luckovich, B., Earls, A.R., Drone (UAV), IoT Agenda, 2021, <https://www.techtarget.com/iotagenda/definition/drone> (Accessed 2023-11-05).
- [3] Media, S., 6 energy sources powering today's commercial drones, Shearwater Aerospace publication, <https://www.shearwater.ai/post/6-energy-sources#:~:>(Accessed 2023-11-05).
- [4] Raza, W., et al., Recent advancements in supercapacitor technology, *Nano Energy*, vol. 52, 2018, 441–473, doi: 10.1016/j.nanoen.2018.08.013.
- [5] Paravannoor, A., *Supercapacitors and their applications: Fundamental*. CRC Press, 2023. E-book
- [6] Boukoberine, M. N., Zhou, Z., Benbouzid, M., Power Supply Architectures for Drones - A Review, IECON Proc., *Industrial Electron. Conf.*, 2019, 5826–5831, doi: 10.1109/IECON.2019.8927702

DRYING NATURAL RUBBER (LATEX) SHEETS BY USING A SOLAR PANEL

W.M.S.M. Weerasinghe*, G.A.K.S. Perera

Department of Electronics, Wayamba University of Sri Lanka, Kuliypitiya, Sri Lanka

*shashimadhu9616@gmail.com

ABSTRACT

Rubber is a valuable agricultural product in Sri Lanka, with the country being one of the major exporters of natural rubber in the world. Drying rubber sheets is a critical step in the rubber production process that involves removing excess moisture from the sheets to increase their durability, quality and value of the final product. Traditionally, in our country, rubber sheets are dried using sunlight. But during some days, intensity of sunlight differs. So, it is not possible to dry rubber sheets properly. Some may dry unequally. In less sunny days, rubber sheets may get moldy. Also, some days it rains several times. Then people have to put the rubber sheets outside and take it again and again, thus wasting time and energy. One of the large-scale drying methods is storing rubber sheets in a sealed room. The air in the room is heated by sending hot water through steel pipes. Rubber sheets are dried in hot air. But this method is expensive. So, this project was aimed at designing a setup to use solar energy via a solar panel to dry rubber sheets.

Solar panels are installed to capture sunlight and via the electricity produced by panels, fans are powered convert to facilitate the drying process. Rubber sheets are placed in a chamber and with the fans, moisture is reduced speeding up the evaporation process. When compare with the widely used traditional drying method, this design is more efficient and effective. Also, it is suitable for all scales of rubber producers.

Keywords: Natural rubber, Rubber sheets, Solar panel

1.0 INTRODUCTION

Rubber is one of Sri Lanka's major export crops, since the time immemorial. And also, Sri Lanka is one of the major rubber-producing countries globally [1]. Sri Lanka is the seventh-largest exporter of rubber in the world. In 2022, country exported 80,955,644 kg of rubber, generating export revenue of USD 1.02 billion. Rubber production in Sri Lanka is expected to decline by 15% in 2023 to around 60 million kilograms, mainly due to unfavorable weather conditions and labor shortages. The government of Sri Lanka has launched the Rubber Industry Master Plan 2023-2027 to revitalize the rubber industry and achieve an export target of USD 4.4 billion by 2024[2].

Rubber is grown mainly in districts like Kalutara, Kegalle and Rathnapura. It is done as large scale as well as medium/small scales. About large portion of the rubber comes from small farmers plantation.

Natural rubber is an elastic material obtained from the sap of rubber trees (*Hevea brasiliensis*). Its production process begins with tapping the latex from rubber trees. Once the latex is collected in cups, it is put into large buckets. Then, it is put into trays and mixed with acid (methanoic acid) for coagulation. After being processed into thin sheets, the rubber sheets undergo a two-step drying process. First, they are spread out and exposed to sunlight to

evaporate excess moisture. Once partially dried, the rubber sheets are transferred to a smokehouse for fumigation.

In Sri Lanka, rubber sheets are typically dried in the sun. However, there are days when the amount of sunlight varies. As a result, rubber sheets may mold and some rubber sheets may not dry evenly on less sunny days as depicted in Figure 1.1 and 1.2. Additionally, people have to put the rubber sheet outside and take it inside repeatedly on days when it rains a lot, which wastes their time and energy.



Figure 1.1 Molded rubber sheet



Figure 1.2 Unequally dried rubber sheets

In the large-scale drying method, the rubber sheets are stored in a sealed room where the drying process is facilitated by heating the air. This is achieved by circulating hot water through strategically placed steel pipes in the room. The high temperature of the air improves the evaporation of moisture from the rubber sheets, and speeds up the drying process. The sealed environment helps maintain consistent drying conditions, contributing to the efficiency and uniformity of the overall drying process. But this method is very expensive and need more man power to roll rubber sheets. Energy-saving, time-saving, and low-cost by drying rubber sheet using solar panels.

2.0 EXPERIMENTAL

2.1 Block diagram of the design

Figure 2.1 illustrates the block diagram of the design for drying rubber sheets using a solar panel.

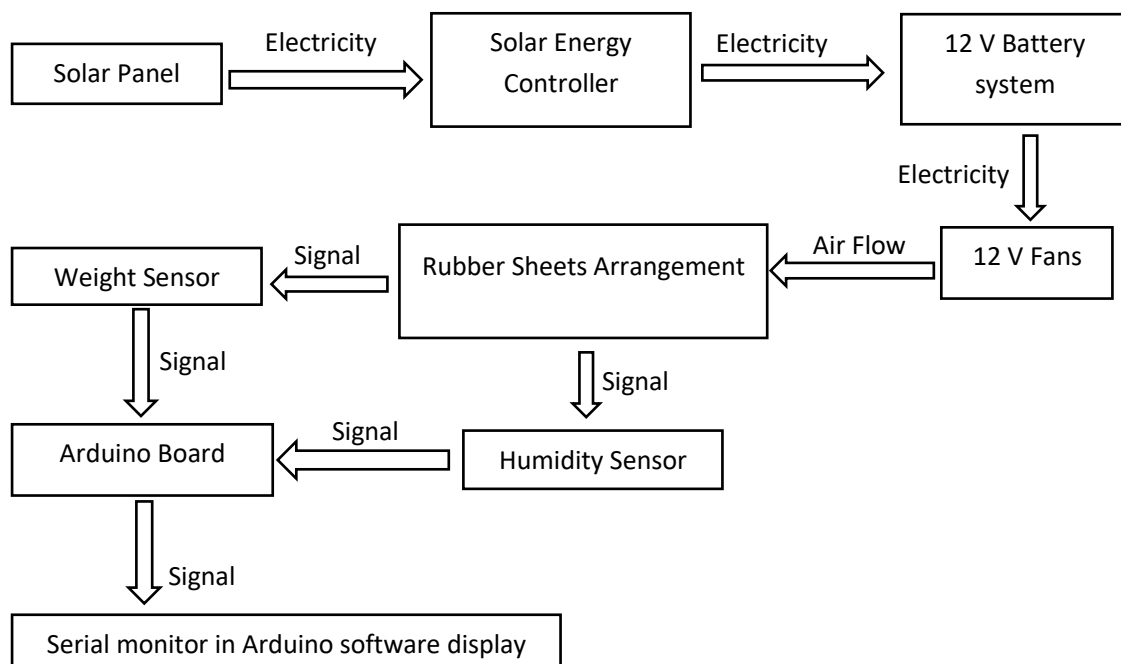


Figure 2.1: Block diagram of the design

Electricity generated by the solar panel is controlled to charge 12 V battery via the controller which was available with the solar panel. Fans are operated assisting drying of rubber sheets. To check the system functionality, drying process was observed with a weight sensor and a humidity sensor.

2.2 Procedure

Figure 2.1 shows the complete design. The solar-powered rubber sheet dryer was set up in a location with ample daylong sunlight. The sheets were cleaned properly to remove any dirt that may affect the drying process. Then, those were arranged with space between them on wooden strips for optimal airflow as illustrated in Figure 2.3. Next, the solar panel was mounted for maximum sun exposure and connected to a solar charge controller and battery. 12 V fans were powered by the battery and were installed to circulate air throughout the dryer. Finally, a weight sensor and a humidity sensor were connected to the Arduino Uno board, allowing the drying process to be monitored via the serial monitor. When the desired weight reduction and the humidity level were indicated the complete dryness, the rubber sheets were removed and stored in the smokehouse.

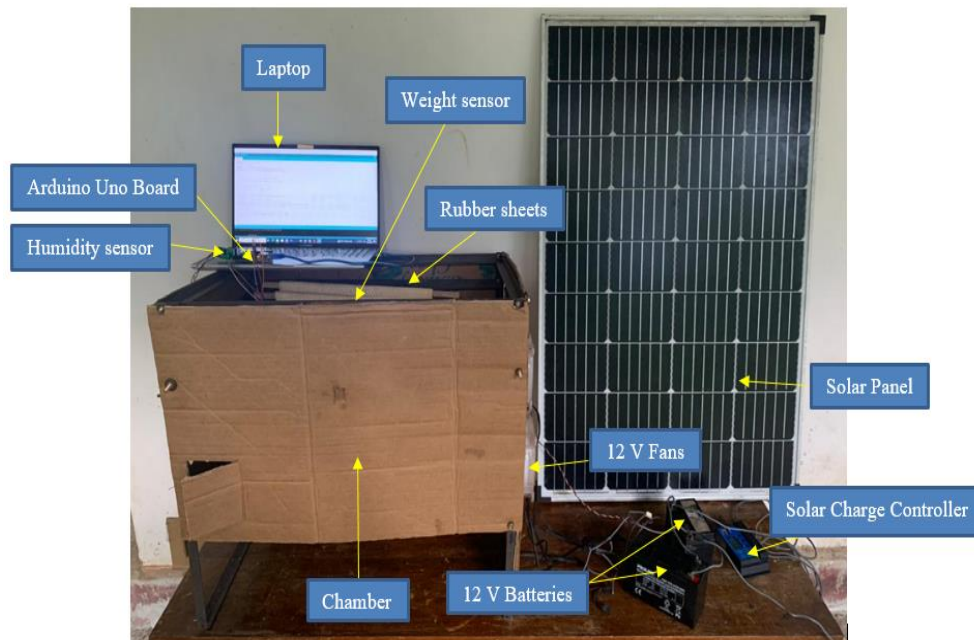


Figure 2.2: Full experimental setup



Figure 2.3: Experimental setup of chamber

3.0 RESULTS AND DISCUSSION

3.1 Data presentation

3.1.1 Data of traditional drying method

10 rubber sheets were taken and dried using the traditional method. It took three days for this purpose. At the beginning and when appropriate to put in the smoke house, the weight of rubber sheets was measured. Those data are in the below table.

Table 3.1 Weight change when using the traditional drying method

Sample	Weight of the rubber sheet before drying(g)	Weight of the rubber sheet after drying(g)
1	626	468
2	606	430
3	558	380
4	590	434
5	554	398
6	588	420
7	580	420
8	606	440
9	584	420
10	588	420
Total weight	5880	4230

Average weight reduced percentage per sheet = $(5880 - 4230) / 5880 * 100\% = 28\%$

Time duration for achieving this level of drying is 3 days.

3.1.2 Data of solar drying method

Four rubber sheets were taken and dried using the solar drying method. It took 12 hours for this purpose. At the beginning and when appropriate to put in the smoke house, the weight of rubber sheets was measured. This drying process was started at 10.00 am. Those data are in the below table.

Table 3.2 Data of solar drying method

Sample	Weight (g) at 10.00A.M	Weight (g) at 12.00 Noon	Weight (g) at 02.00 P.M	Weight (g) at 04.00 P.M	Weight (g) at 06.00 P.M	Weight (g) at 08.00 P.M	Weight(g) at 10.00 P.M
1	554	518	490	467	451	438	432
2	542	507	479	457	441	428	424
3	510	480	456	436	421	408	404
4	590	545	512	488	469	455	450
Total Weight	2764						1960

Average weight reduced percentage per sheet = $(2764 - 1960) / 2764 * 100\% = 29\%$

3.1.3 Output of humidity sensor

Table 3.3 Output of humidity sensor

Time	Humidity
10.00 A.M	73%
10.05 A.M	74%
10.10 A.M	75%
10.15 A.M	76%
10.20 A.M	77%
10.25 A.M	78%
10.30 A.M	79%
10.35 A.M	80%
10.40 A.M	81%
10.45 A.M	82%
10.50 A.M	83%
10.55 A.M	84%
11.00 A.M	85%
11.10 A.M	86%
11.25 A.M	87%
11.40 A.M	88%
12.00 A.M	89%
01.00 P.M	88%
02.30 P.M	87%
04.15 P.M	86%
06.15 P.M	85%
08.00 P.M	84%
10.00 P.M	83%
01.00 A.M	83%

With this humidity reduction which took place within about 12 hours, it was observed a proper drying state of rubber sheets. Figure 3.1 shows two rubber sheets dried using this system.



Figure 3.1 Dried Rubber sheet from Solar-powered drying system

When comparing with Figure 1.1 and 1.2, above figure shows the high quality of the dried rubber sheet from solar powered drying system.

From 10.00 A.M to 3.00 P.M, solar panel was able to generate electricity and battery was fully charged to 12 V by 3.00 P.M. During the measurements were taken, fans were operating in the same level with the battery power. This evidences that fans can be operated for more than 12 hours with a full charge of the battery.

4.0 CONCLUSION

Solar-powered drying method of natural rubber sheets emerges as a system changer, providing a clear advantage over traditional methods. Solar drying produces superior quality rubber with consistent drying, requires little manpower to operate, and improves brand image by appealing to environmentally conscious consumers.

While the initial investment cost of solar panels may be higher than traditional drying equipment, the long-term benefits of solar-powered drying systems outweigh the upfront expenses. The cost savings from reduced electricity consumption, coupled with the environmental and brand reputation benefits, can translate into significant gains for rubber processing facilities.

In conclusion, drying natural rubber (latex) sheets using solar panels is a viable and sustainable approach that offers both environmental and economic benefits. As solar technology advances and becomes more prevalent, this technique is poised to play an increasingly important role in the rubber industry, contributing to a cleaner and more sustainable future for rubber manufacturing.

ACKNOWLEDGEMENTS

The authors would like to express their appreciation to the Department of Electronics, Faculty of Applied Sciences, Wayamba University of Sri Lanka, Kuliypitiya, Sri Lanka.

REFERENCES

- [1] United Nations ESCAP. Country study on Sri Lanka using global value chain analysis: the industrial rubber and electronic products sectors. Bangkok: United Nations publication; 2011.
- [2] Sri Lanka Rubber Secretariat. Sri Lanka rubber industry development master plan 2017-2026. Battaramulla; 2017.

REDUCING HOUSEHOLD ELECTRICITY CONSUMPTION WITH A SMART MONITORING SYSTEM

U.T. Nanayakkarawasam* ,W.A.S. Wijesinghe

Department of Electronics, Wayamba University of Sri Lanka, Kuliypitiya, Sri Lanka

*umesh.nanayakkarawasam@gmail.com

ABSTRACT

High electricity bills are a significant issue for many households in Sri Lanka. To address this, the present study aimed to minimize household power consumption by developing an IoT-based system for monitoring electricity usage. This system measures the power consumption of devices connected to power sockets and sends the data to a Wi-Fi server. If daily consumption exceeds predefined thresholds, warning and danger LEDs are activated. The system provides real-time consumption data, which users can access through a mobile app, allowing them to monitor and conserve electricity. The app also enables users to set daily target values and update the Arduino code, adding a dynamic aspect to the system. Its user-friendly design increases its accessibility to a wide range of users. However, the effectiveness of the system relies on user engagement, which could be improved in future implementations of the mobile application.

Keywords: Power Socket, Daily Target, Smart Monitoring, IoT

1.0 INTRODUCTION

In the modern world, energy efficiency has become a vital concern for sustaining our environment. With the growth of population and technological advancements, energy consumption has increased rapidly. Moreover, in Sri Lanka, rising electricity costs are a significant issue faced by households. Therefore, reducing household electricity consumption is crucial to conserve energy and reduce electricity bills. Different electrical appliances used in households have different electricity consumption [1]. Understanding the power consumption of different electrical devices can direct consumers to optimize current usage.

There is currently no effective method for monitoring household power consumption that provides specific details about the energy usage of individual appliances. The electricity bill is made based on the values generated by the electricity meter at the end of the month. It is difficult to check the electricity meter reading daily. Another drawback is not being able to measure the current usage of each electrical appliance. Having a power monitoring system enables the users to monitor and conserve energy before receiving the electricity bill. Previous studies have identified that internet of things (IoT) systems can be used to measure energy consumption.

An IoT-based meter reading system has been developed for domestic power consumption billing [2]. Another study designed a power monitoring application that measures energy consumption and provides real-time feedback to the user via a web interface [3], A smart power meter monitoring system was developed with home automation using IoT. The system aims to improve energy efficiency by providing real-time feedback to users and enabling remote

control of appliances [4]. IoT energy monitoring system was designed to measure the energy consumption of household appliances and provide real-time feedback to users enabling users to identify energy-intensive appliances and make more informed decisions about energy usage [5].

The main objective of this study is to develop a smart monitoring system using a microcontroller and several sensors that can optimize household electricity consumption. The proposed system provides an answer to the question of how power monitoring devices can be designed, implemented and optimized to effectively monitor household electricity usage.

2.0 METHODOLOGY

This study developed a power socket which measures and uploads the electricity power consumption of household electrical devices. The power socket was built using a current transformer (CT) sensor, a small circuit with two warning LEDs and NodeMCU. At the first stage, calibration of the CT sensor was carried out. Then the obtained data from the CT sensor was passed to the NodeMCU through an analogue pin. Next, the data obtained from the NodeMCU were uploaded via Wi-Fi into a cloud server.

The NodeMCU board was designed to get the total power consumption for 15 minutes. Every 15 minutes, the total consumption value is uploaded to the cloud server. Simultaneously, at every 15 minutes, NodeMCU checks whether this total current consumption value exceeds the threshold values of the warning limit and danger limit. Two separate values for the warning limit and danger limit were defined in the Arduino board. These threshold values were the maximum values that could be consumed for a day. When the values exceed the predefined warning limit or danger limit, respective LED bulbs will power on. Two bulbs, a yellow one for the warning limit and a red one for the danger limit were installed to the power socket. This socket was designed to store total value for 24 hours. After 24 hours the value is set to 0.

The same process recurs daily. This total value helped to determine whether the daily power consumption has exceeded the predefined warning limit or danger limit. To define the threshold values was performed manually, first, the current consumption of previous months was obtained and the average current usage value was determined in units/kWh. As electricity usage increases by 30 units, the fee charged also increases. If we can control the electricity usage, electricity bills can be reduced. Hence, in this study, it was planned to set a predefined target. The predefined targets were set based on past electricity bills. The power consumption for three previous electricity bills was obtained. Then the average value of those three previous months was divided by 30 to obtain the daily power consumption. It was divided by 30 assuming a month has 30 days. This value was used to set threshold values. The threshold values for warning limit and danger limit were set using the arduino code.

Usually, houses have devices that have various electricity usage such as 5 A, 15 A, 30 A etc. Hence, electrical devices that may consume high electric power or the devices that are often used were selected. This system selected these sockets to the group power consumption based on load. The power socket measures the power consumption of devices and then the data is sent to the server. Additionally, the main line's current was also measured. These details could be viewed by the user via the mobile app.

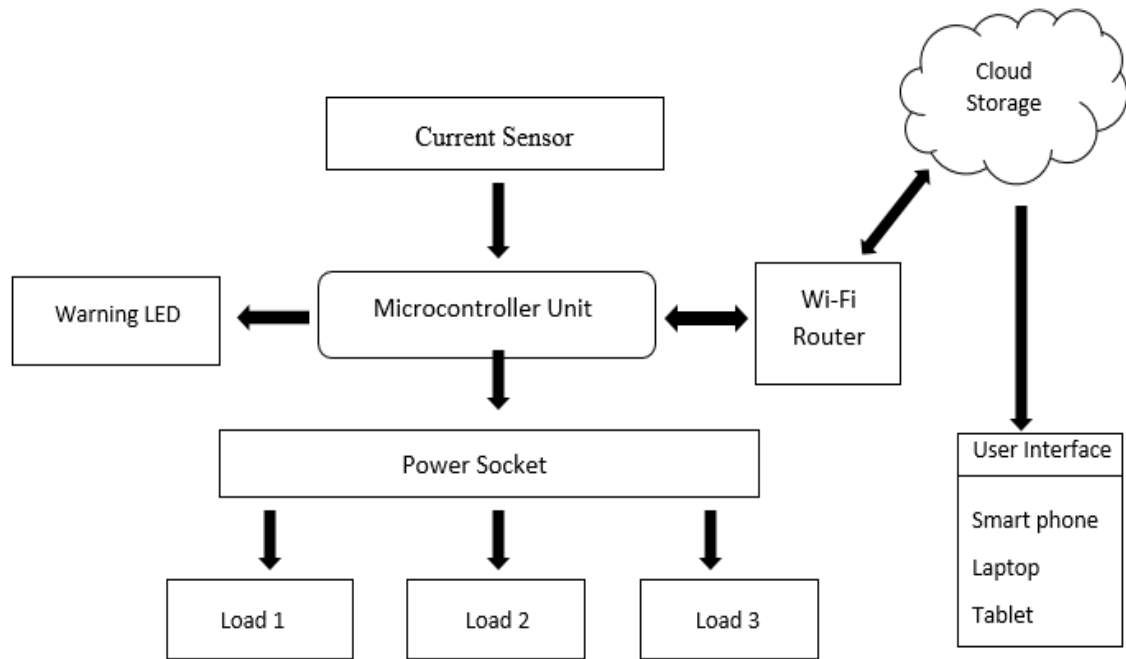


Figure 2.1: Block diagram of the system (Source: Author compile)

2.2. Circuit Diagram

The Figure 2.2 below illustrates the circuits of the CT sensor, NodeMCU and a small circuit with two warning LEDs. The CT sensor was connected to the NodeMCU through the analog input (A0) pin. A₀ pin has a voltage range of 0 to 33V. The two LEDs were connected to the NodeMCU through resistors.

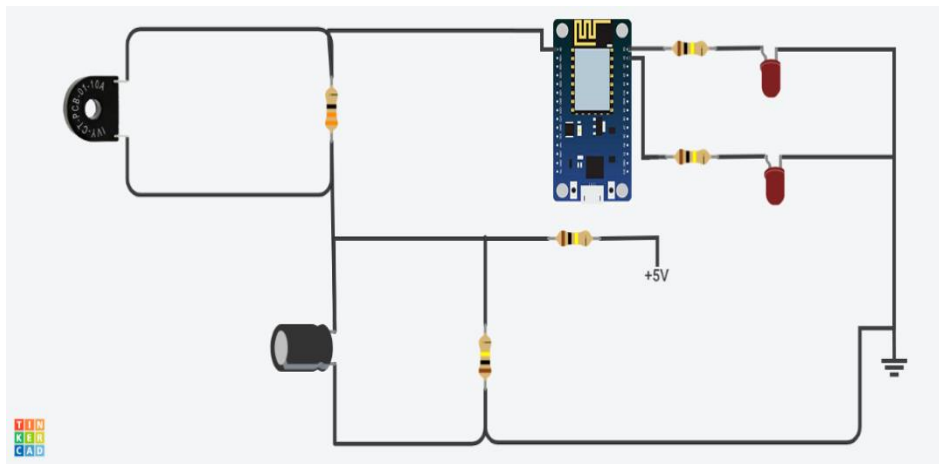


Figure 2.2: Circuit diagram of the power socket (Source: Author compile)

2.3. Software and Network Architecture

The Figure 2.3. below depicts how the device connects with the web server via Wi-Fi. Read API and Write API enable the data transfer. The Wi-Fi module used in this was ESP8.

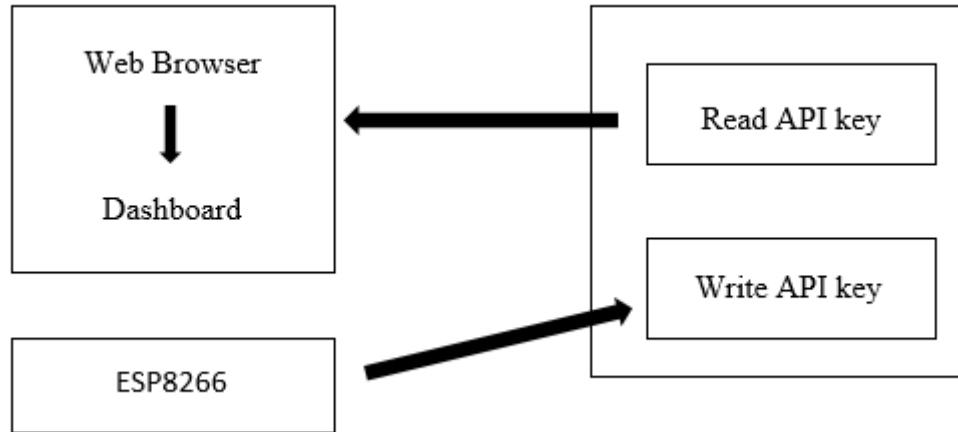


Figure 2.3: Software and network architecture (Source: Author compile)

The client is the owner or person who wants to know the power consumption. Dashboards of the systems were viewed through web browsers on the client side. Also, the Wi-Fi module acted as a client and it sent data to the server. Client-side web-based dashboards were implemented using HTML and CSS. Two interfaces were designed and they are user login and dashboard. As depicted in Figure 2.4.

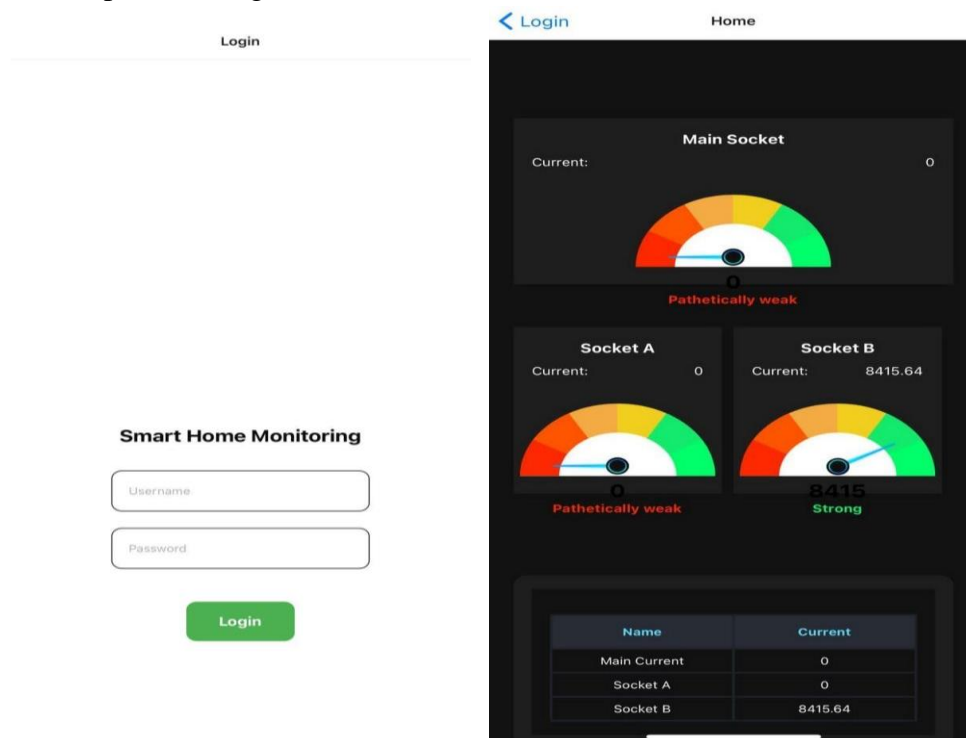


Figure 2.4: Login interface and dashboard (Source: Author compile)

3.0 RESULTS AND DISCUSSION

3.1. Design Overview

This study developed a smart monitoring system using a microcontroller and CT sensors to optimize household electricity consumption. Figure 3.1 shows the final design of this study including one main socket and two other sockets that can be connected to any electric device.

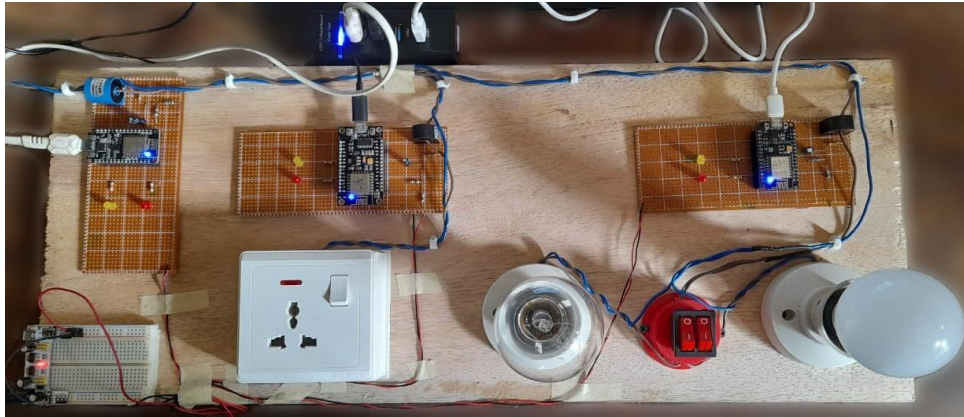


Figure 3.1: Final design of the system

3.2. ThingSpeak Server

The data measured through the system was uploaded to the ThingSpeak server. The prototype was designed to upload values once every minute. Simultaneously, it checked whether the total value exceeded the warning limit and danger limit. Once every ten minutes the total value of the prototype was set to be 0. The ThingSpeak dashboard shows the graph of the sockets that have connected. Figure 3.2 shows the real time updated data on the Thingspeak server. Two graphs were generated for one socket. One graph illustrates the power usage of a device per second. The other graph shows the total power consumption of the socket every 10 minutes.

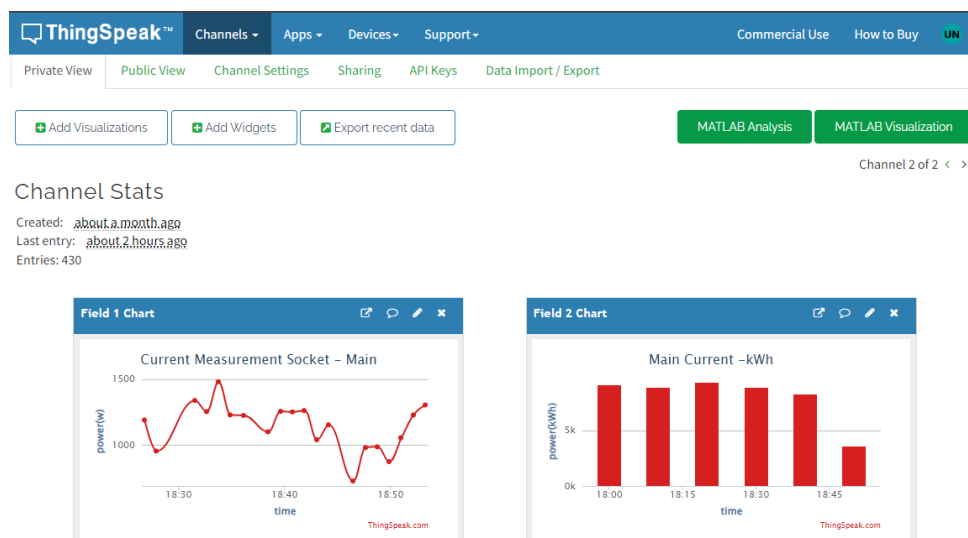


Figure 3.2: Realtime updated data on the ThingSpeak server (Source: Author compile)

4.0 CONCLUSION

Today, many electricity users face the problem of increased electricity bills. This led to the problem of how power monitoring devices can be designed to optimize household electricity consumption. The system provided details of electricity consumption and the users could view the details. Accordingly, they could disconnect devices that consume high electricity and reduce use of those devices. This study successfully developed a smart monitoring system that optimizes household power consumption. The prototype developed in this study provided real-time data on electricity consumption. It allowed users to monitor and control energy usage. This experiment can be further developed by improving the mobile application with additional features that make the system more effective. Designing an auto power-off system that powers off devices when limits are exceeded may not be always practical in real life as some devices are essential in our lifestyle. This system is highly dependent on user engagement. This is a limitation of the study. Future work can be performed to evaluate the effectiveness of smart monitoring systems on power consumption and electricity bills using a sample. Furthermore, the mobile application can be developed to set targets and send alerts to users. The developed system was user-friendly, making it accessible to a wide range of users. The system contributes to the conservation of energy and the sustainability of the environment.

ACKNOWLEDGEMENTS

The authors would like to express their gratitude to the Academic Staff of the Faculty of Applied Sciences, Wayamba University of Sri Lanka for their expert advice and guidance.

REFERENCES

- [1] Ahsan, S. M., Khan, H. A., Hussain, A., Tariq, S., & Zaffar, N. A. (2021). Harmonic Analysis of Grid-Connected Solar PV Systems with Nonlinear Household Loads in Low-Voltage Distribution Networks. *Sustainability*, 13(7), 3709. <https://doi.org/10.3390/su13073709>
- [2] Muhamad, N. A., Kum, T. L., Peng, A. S., & Ja'afar, S. B. M. (2023). IoT-based meter reading for domestic power consumption billing. In *AIP Conference Proceedings* AIP Publishing LLC, Vol. 2643, No. 1, p. 040010-.
- [3] Surriani, A., Pradana, A. B., Arrofiq, M., Putra, J. T., Budiyanto, M., & Subekti, L. (2020). Design of Power Monitoring Application. In *IOP Conference Series: Materials Science and Engineering* IOP Publishing, Vol. 722, No. 1, p. 012069-.
- [4] Raj, K. D., Aadhithya, K., Indrajaya, N., & Srinivas, S. (2021). Smart power meter monitoring system with home automation using IoT. In *AIP Conference Proceedings*, AIP Publishing LLC, Vol. 2407, No. 1, p. 020031-.
- [5] Chooruang, K., & Meekul, K. (2018). Design of an IoT Energy Monitoring System. <https://doi.org/10.1109/ictke.2018.8612412>

ANALYZE INDOOR ENVIRONMENT QUALITY USING IOT BASED MONITORING SYSTEM

J.K.A.T.R. Jayasuriya*, J.M.J.W. Jayasinghe

Department of Electronics, Wayamba University of Sri Lanka, Kuliyapitiya, Sri Lanka

*thrishul.jayasuriya20@gmail.com

ABSTRACT

The rapid advancements in Internet of Things (IoT) technology have paved the way for innovative solutions in various domains, including environmental monitoring. This research focuses on the development and implementation of an IoT-based monitoring system to comprehensively analyze the indoor environment. The proposed system incorporates a network of sensors strategically deployed within indoor spaces to collect real-time data on various environmental parameters. The primary objectives of this research include the design and deployment of a robust IoT infrastructure, the integration of diverse sensors for monitoring parameters such as temperature, humidity, air quality, air pressure and light intensity, and the development of analytical tools for processing and interpreting the collected data. The monitoring system aims to provide a holistic view of indoor environmental conditions, enabling users to understand and optimize factors affecting comfort, health, and energy efficiency. Key components of the research include the selection and calibration of sensors, the establishment of a secure and scalable communication network, and the development of algorithms for data fusion and analysis. The research use the indoor environment standards in Sri Lanka to predict and respond to dynamic changes in the indoor environment. By leveraging the capabilities of IoT technology, this research contributes to the creation of intelligent indoor environments that are adaptive and responsive to the needs of occupants. The insights gained from the analysis of the collected data can inform decision-making processes related to building management, energy conservation, and occupant well-being. The findings of this research have implications for a wide range of applications, including smart homes, offices, healthcare facilities, and educational institutions. Ultimately, the integration of IoT-based monitoring systems for indoor environments holds the promise of fostering sustainable and user-centric spaces, enhancing overall quality of life and contributing to the advancement of smart building technologies.

Keywords: Indoor Environment, Air Quality, Air Quality Monitoring

1.0 INTRODUCTION

Indoor Environmental Quality (IEQ) stands as a keystone in shaping the well-being and productivity of individuals within the confines of built environments. A truly favorable indoor setting goes beyond simple shelter, including optimal air quality, comfortable thermal conditions, adequate lighting, and minimal noise levels. These elements collectively use a profound impact on the physical health, mental function, and emotional well-being of occupants. Scientifically linked to various health issues such as respiratory problems, allergies, and fatigue, poor IEQ not only risks individual health but also resonates through the realms of concentration, decision-making, and overall job satisfaction, influencing productivity both in workplaces and educational settings [1,2].

The significance of IEQ extends beyond the individual, resonating with broader social imperatives. In a world increasingly familiar to sustainability, well-designed indoor

environments are recognized for their potential to contribute to energy efficiency and reduced environmental impact. Thoughtful considerations such as prioritizing natural lighting, implementing efficient ventilation systems, and employing sustainable building materials not only support healthier living and working spaces but also usher in lower energy consumption and a reduced environmental footprint. In essence, the growing emphasis on IEQ aligns with global aspirations for environmentally responsible and flexible built environments. As societies continue to prioritize creating spaces that are not only habitable but also health-enhancing and sustainable, IEQ emerges as an integral component in the pursuit of a harmonious and forward-thinking built environment, where the immediate comfort and health of occupants are interconnected with the broader global agenda of environmental management [3].

An Indoor Environment Quality (IEQ) monitoring system, encompassing the evaluation of air quality, temperature, humidity, light intensity, and air pressure, is of paramount importance for enhancing the overall well-being, comfort, and productivity of occupants within indoor spaces. The comprehensive monitoring of these key parameters serves as a proactive approach to creating a conducive indoor environment. Firstly, the scrutiny of air quality is critical, considering that poor air quality is linked to various health issues, including respiratory problems and allergies. By monitoring and addressing pollutants such as carbon dioxide, volatile organic compounds (VOCs), and particulate matter, the system plays a pivotal role in maintaining clean air, thereby contributing significantly to the creation of a healthier and more productive indoor setting [4].

Equally essential is the monitoring of temperature and humidity, as these factors directly influence occupant comfort. Maintaining optimal levels through continuous monitoring not only ensures a pleasant indoor atmosphere but also mitigates potential health issues and prevents the growth of mold and allergens. The system's attention to these parameters reflects its commitment to fostering an environment that prioritizes the physical comfort and well-being of occupants. Furthermore, the monitoring of light intensity becomes crucial in promoting occupant well-being and productivity. By ensuring spaces are adequately illuminated, the system helps reduce eye strain and cultivates a positive mood. The consideration of natural circadian rhythms in proper lighting design contributes not only to the overall health of occupants but also positively influences sleep quality. Lastly, the system's oversight of air pressure differentials underscores its role in effective ventilation, preventing the buildup of indoor pollutants and ensuring a continuous supply of fresh air[5]. This controlled air pressure not only supports overall indoor environmental quality but also plays a vital role in the safe operation of equipment and influences important fire safety measures, reinforcing the system's multifaceted significance in maintaining a safe, healthy, and productive indoor environment [4].

The existing research on IoT-based Indoor Air Quality (IAQ) monitoring systems lacks comprehensive monitoring of crucial environmental parameters. Previous studies either omit variables like temperature, humidity, light intensity, and air pressure or lack alert systems with buzzers and LEDs. In contrast, our research innovatively integrates all these parameters, ensuring a more holistic and effective indoor environment monitoring system [6]. This system, capable of real-time monitoring and internet connectivity, presents a valuable advancement for small spaces, offering a comprehensive solution with alerts for enhanced user awareness and management.

The absence of an Indoor Environment Quality (IEQ) monitoring system gives rise to a host of challenges and problems, spanning from a lack of environmental awareness to inefficiencies in

resource management. Without a monitoring system in place, building occupants and facility managers may be unaware of the prevailing indoor environmental conditions, potentially resulting in discomfort, health issues, and decreased productivity. Health and comfort problems, stemming from poor indoor air quality, uncomfortable temperatures, inadequate lighting, and imbalanced air pressure, can adversely impact the overall well-being of building occupants. Additionally, the inability to respond promptly to sudden changes in environmental conditions, such as increased pollutant levels or unexpected temperature fluctuations, poses a significant limitation [7]. The absence of real-time monitoring further complicates resource management, making it challenging to optimize energy usage for heating, ventilation, and air conditioning (HVAC) systems, potentially leading to unnecessary energy consumption and increased operational costs. Moreover, the potential for building-related illnesses increases in the absence of monitoring, as factors like mold growth, poor ventilation, or the accumulation of indoor pollutants may go unnoticed [8]. Lastly, energy inefficiency looms large, as buildings may operate sub optimally without the ability to adjust systems based on real-time data, resulting in higher energy consumption, an increased carbon footprint, and undue strain on energy resources.

Design and implement a comprehensive Indoor Environment Quality (IEQ) Monitoring System to ensure optimal and healthy indoor conditions [9]. The system will monitor and analyze key environmental parameters, including air quality, temperature, humidity, light intensity, and air pressure, with the aim of creating a comfortable, safe, and productive indoor environment [10]. There are no IoT based indoor environment monitoring system to monitor above five parameters. The system implements with IoT technology to monitoring personal computer and mobile phones with monitoring air quality, temperature, humidity, light intensity and air pressure.

2.0 EXPERIMENTAL

The NodeMCU ESP8266 wifi development board is used as the main controlling unit of the system. The NodeMCU, centered on the ESP8266 SoC, is an open-source IoT development environment with built-in CPU, RAM, and WiFi. Ideal for IoT projects, it contrasts with Arduino, offering simplicity for hobbyists but lacks the varied CPUs and extensive flexibility found in Arduino, which supports different chips, memory, and programming environments, resulting in variations among vendors.

The MQ135 air quality sensor is a semiconductor gas sensor designed to detect and quantify various gases, including ammonia, alcohol, benzene, smoke, and carbon dioxide. Operating at 5V with a 150mA power consumption, it requires a 20-second preheating for accurate results. Suited for air quality monitoring, it's particularly sensitive to smoke, benzene, CO₂, NH₃, NO_x, making it cost-effective for applications involving the detection and monitoring of hazardous gases. Its digital output pin signals when gas concentration exceeds the set threshold, and the analog pin provides a voltage output representing the gas level.

The DHT11 sensor module combines temperature and humidity sensing, delivering a calibrated digital output. Featuring a calibrated humidity and temperature complex with high dependability and long-term stability, it provides extremely accurate readings. The module integrates an 8-bit microcontroller for fast response, housed in a 4-pin package with resistive humidity and NTC temperature components. Utilizing single-wire communication, the DHT11 transmits data in a time-specific pulse train, making it a reliable choice for precise environmental monitoring.

A cheap and small atmospheric sensor breakout that measures temperature, barometric pressure, and altitude without taking up much room is the BMP280 Barometric Pressure and Altitude Sensor I2C/SPI Module. Basically, this little breakout can tell you everything you need to know about atmospheric conditions. Among its many uses, the BMP280 Breakout is intended for use in home automation, weather forecasting, indoor and outdoor navigation, and even personal health and wellness monitoring.

The LDR Light Sensitive Module is used to measure light intensity and detect its presence. When there is light, the module's output increases, and when there isn't, it decreases. Potentiometers can be used to change the signal detection sensitivity.

The Arduino Integrated Development Environment (IDE) is a user-friendly software platform tailored for Arduino microcontroller boards' code development. Offering syntax highlighting and auto-indentation, it structures programs into setup for initialization and loop for execution. The IDE features a library manager for easy code library integration, a Serial Monitor for debugging, and a Board Manager for selecting and installing Arduino board profiles. Supporting cross-platform compatibility, it encourages community collaboration through forums and documentation, making it popular in electronics and maker communities.

Blynk is a versatile IoT cloud service empowering the creation of IoT applications for microcontrollers. It offers a user-friendly mobile app and cloud service, simplifying the development of customizable dashboards for remote monitoring and control. Compatible with ESP8266, it adapts to various projects, and Blynk's virtual pins and widgets facilitate seamless communication between devices and the mobile app, enabling users to design interactive interfaces effortlessly within the Internet of Things (IoT) ecosystem.

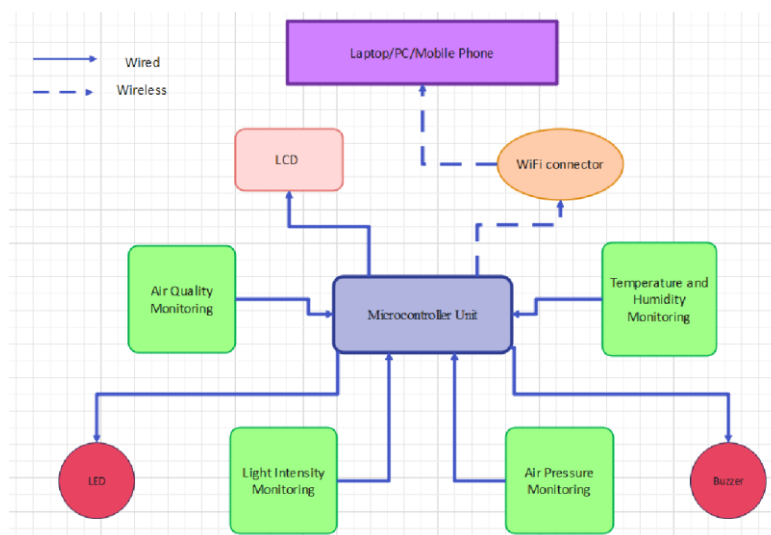


Figure 2.1: Block Diagram of the system

The system incorporates temperature and humidity monitoring using the DHT11 sensor, activating LED and buzzer based on levels. Air quality is tracked by the MQ135 sensor, with LED and buzzer responding to levels, and readings displayed in ppm on an LCD. Light intensity monitoring, using an LDR module, controls LED based on ambient light and displays messages on the LCD. Atmospheric pressure is monitored via the BMP280 sensor, with pressure displayed in kPa. Data from sensors are internet-connected through NodeMCU

ESP8266, enabling a web-based interface for visualizing indoor environment factors with an alert system.

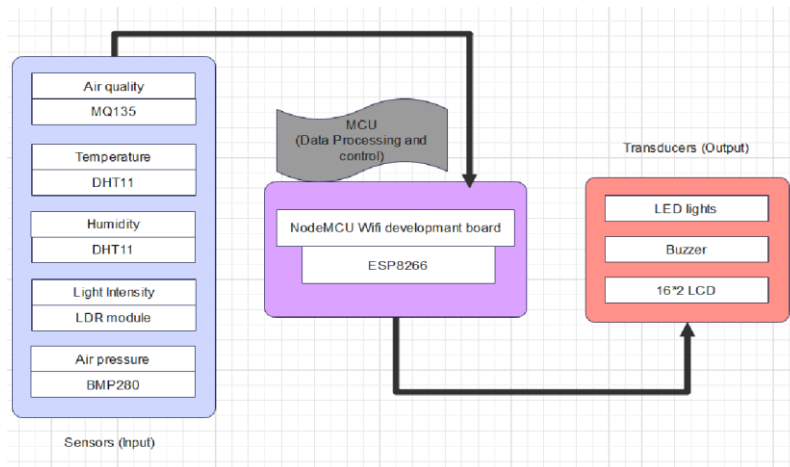


Figure 2.2: Input-output device connection

Analyze the indoor environment of the twenty sample living rooms in the areas using the monitoring system.

3.0 RESULTS AND DISCUSSION

The data provided by the sensors such as air quality, temperature, humidity, and air pressure could be viewed live in these gauges. The live values are indicated in the middle of the gauges. Graphs were visualized the fluctuation of sensor data.



Figure 3.1: Web dashboard of the system

Develop the prototype of the system with connecting sensors as inputs, and LCD, buzzer and LEDs as outputs.

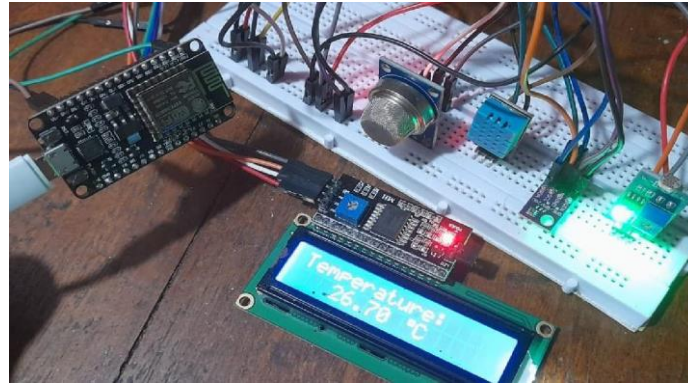


Figure 3.2 Prototype of the system

In the Figure 3.3 shows, the changing of temperature in the living rooms of the houses in the areas. The standard value shows in the red line.

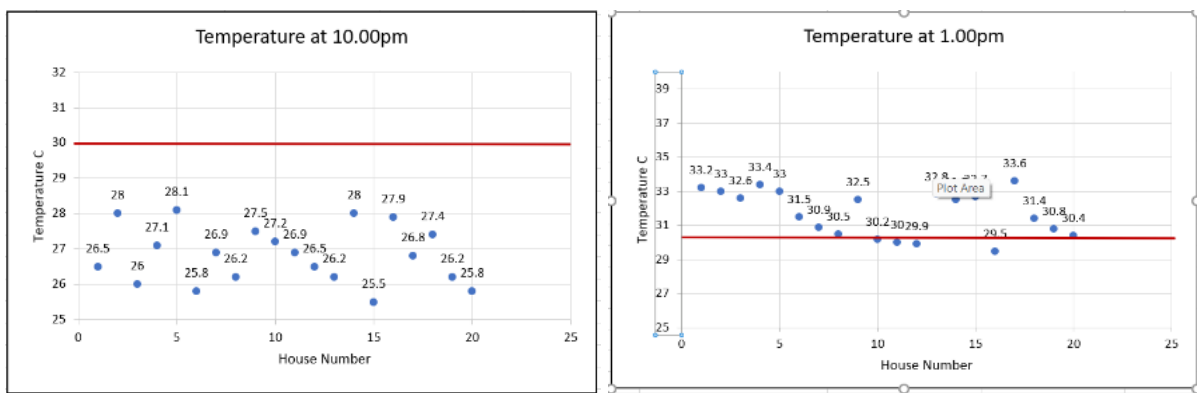


Figure 3.3 Changing of temperature

In the Figure 3.4 shows, the changing of humidity in the living rooms of the houses in the areas. The standard value shows in the red line.

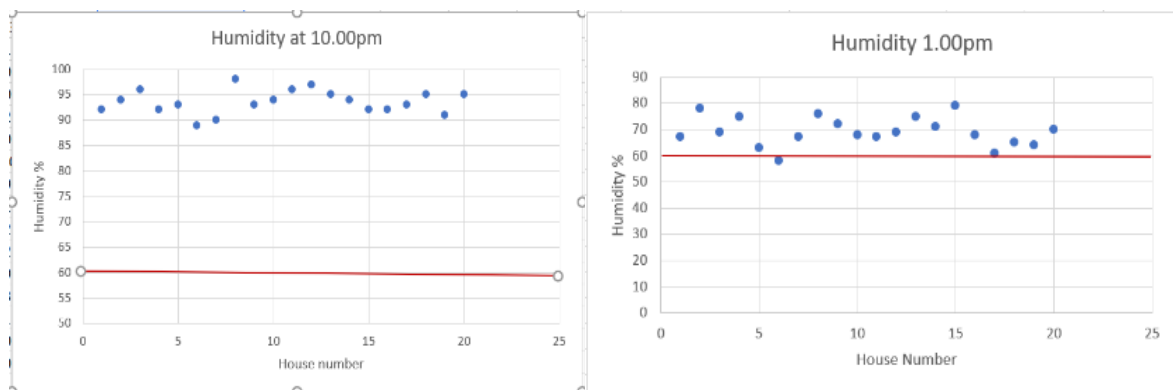


Figure 3.4 Changing of humidity

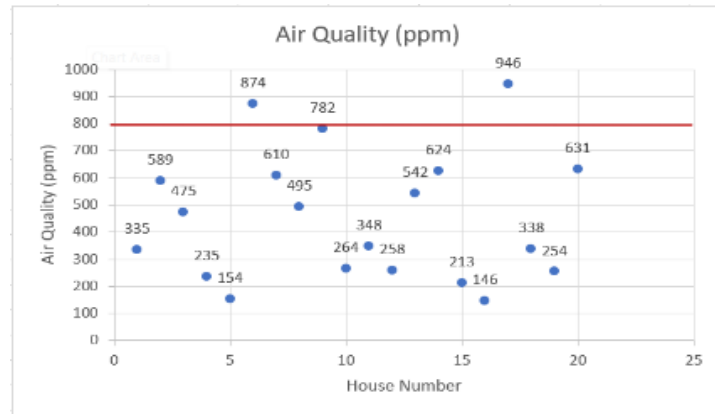


Figure 3.5 Changing of air quality

Figure 3.5 depicts air quality fluctuations in living rooms; the red line indicates the standard PPM. Two rooms exceed the standard, while others maintain good air quality. Figures 3.3 shows temperature variations exceeding standards in daytime but within limits at night. Figures 3.4 reveals humidity fluctuations, surpassing standards at night and remaining optimal during the day.

4.0 CONCLUSION

In conclusion, the research on analyzing the indoor environment using an IoT-based monitoring system has provided valuable insights into the dynamic nature of indoor conditions. The implemented system effectively captured and analyzed data related to air quality, temperature, humidity, air pressure and light intensity in living spaces. Identified fluctuations, such as temperature exceeding standards during the day and humidity surpassing limits at night, emphasize the need for adaptive environmental management. The findings underscore the potential for informed decision-making in building management, energy efficiency, and occupant well-being. This research contributes to the ongoing evolution of smart and sustainable indoor environments, highlighting the significance of IoT technology in enhancing our understanding and control of indoor spaces. Future work could further refine algorithms, integrate predictive models, and explore real-time interventions for optimizing indoor environments.

ACKNOWLEDGEMENTS

The authors would like to express their sincere gratitude to everyone who helped to carry out this project successfully.

REFERENCES

- [1] J.C., Zhang, J.F., Feng, Y. and Guo, J.X., The study and application of the IOT technology in agriculture, In 2010 3rd international conference on computer science and information technology, Vol. 2, pp. 462-465.
- [2] Kamal, Raj, Microcontrollers: Architecture, Programming, Interfacing and System Design, 1st edition, Prentice Hall Press, 2009
- [3] Singh, P.Y., 2019. Internet of Things and Nodemcu A review of use of Nodemcu ESP8266 in IoT products. Journal of Emerging Technologies and Innovative Research (JETIR), 1085, p.8.

- [4] Gokhale, P., Bhat, O. and Bhat, S., Introduction to IOT, International Advanced Research Journal in Science Engineering and Technology, 5(1), pp.41-44.
- [5] Kuria, K.P., Robinson, O.O. and Gabriel, M.M., 2020. Monitoring temperature and humidity using arduino nano and module-DHT11 sensor with real time DS3231 data logger and LCD display. Health Hyg, 6(7), p.8.
- [6] Srivastava, D., Kesarwani, A. and Dubey, S., 2018. Measurement of Temperature and Humidity by using Arduino Tool and DHT11. International Research Journal of Engineering and Technology (IRJET), 5(12), pp.876-878.
- [7] A. R. Biswas and R. Giaffreda, "IoT and cloud convergence: Opportunities and challenges," 2014 IEEE World Forum on Internet of Things (WF-IoT), 2014, pp. 375-376, doi: 10.1109/WF-IoT.2014.6803194.
- [8] Putri, M. and Aryza, S., 2018. Design of security tools using sensor Light Dependent Resistor (LDR) through mobile phone. Int. J. Innov. Res. in Comp. and Comm. Eng, 4(10), pp.168-173.
- [9] Interfacing BMP280 with Arduino to Read Pressure, Temperature, and Altitude. Article of IoT design pro website (2020). <https://iotdesignpro.com/projects/interfacing-bmp280-with-arduino-to-read-pressure-temperature-and-altitude> (Accessed 02-11-2023)
- [10] Fioccola, G.B.; Sommese, R.; Tufano, I.; Canonico, R.; Ventre, G. Polluino: An efficient cloud-based management of IoT devices for air quality monitoring. In Proceedings of the 2016 IEEE 2nd International Forum on Research and Technologies for Society and Industry Leveraging a Better Tomorrow (RTSI), Bologna, Italy, 7–9 September 2016.

RESEARCH ON ENHANCING THE PERFORMANCE OF VLC-BASED IMAGE TRANSMISSION AT LOW BIT RATE

K.B.M.N. Neranjan*, Y.A.A. Kumarayapa

Department of Electronics, Wayamba University of Sri Lanka, Kuliypitiya, Sri Lanka

*maheshanirmal@gmail.com

ABSTRACT

A thorough investigation into the application of Visible Light Communication (VLC) for image transmission is presented in this research, utilizing a distinctive combination of hardware and software components. The hardware setup includes two ESP32 microcontrollers, with LED/Laser diodes are used as transmitters and Light Dependent Resistors (LDR) / Infrared (IR) photodiodes used as receivers. Additionally, Optical-electronics low-based communication, a cost-effective technique utilizing optoelectronic devices for free-space transmission, is incorporated in the study. The encoding of an image into Base 64 format using Python and its transmission as a string using a light-emitting device programmed with Arduino IDE (C++) were explored. Various transmission methods, including the use of multiple LEDs, were investigated, with a 59cm transmission distance demonstrated when employing 8 LEDs. The research also delves into 1-bit serial and 8-bit parallel communication methods. A substantial focus of the research is placed on the evaluation of the accuracy of LDR and IR photodiode receivers, with an emphasis on their performance under varying light intensities. The modulation technique adopted in the experiment is On-Off Keying. A key discovery of the research is the exceptional performance of the Laser diode as a transmitter. Due to its coherent beam, the Laser diode ensures zero data loss during transmission and facilitates direct interaction with the LDR surface. This configuration results in an impressive 100% accuracy rate and an outstanding transmission distance exceeding 300 meters, surpassing other configurations significantly. The significance of the research is further enhanced by the incorporation of optical-electronics low-based communication, introducing a low-cost technique utilizing optoelectronic devices for free space transmission. Consequently, valuable insights into the application of VLC for image transmission are provided by this research, offering a comprehensive evaluation of various hardware and software components, transmission methods, and receiver accuracy. The substantial potential of VLC technology in wireless communication is emphasized by these research observations, paving the way for future research in this domain with more advance research facilities.

Keywords: Visible Light Communication (VLC), Free Space Transmission, Opto-electronic devices, Low-Cost Communication

1.0 INTRODUCTION

Within the context of conventional wireless communication, formidable obstacles were encountered due to the intrinsic constraints associated with sending pictures and videos at low bandwidth [1]. When working with high-resolution photographs or films that required significant bandwidth resources, this became very difficult [1]. This research study focuses on low bit rate transmission for various reasons, including efficiency, power consumption, real-world applications, challenging environments, and innovation. Low bit rates are ideal for bandwidth usage, battery-operated devices, IoT devices, and remote sensors. Overcoming challenges like maintaining image quality and dealing with transmission errors can lead to

advancements in VLC technology. This study contributes to making wireless communication more efficient, reliable, and accessible, opening new possibilities for VLC in various applications. Retransmitting photos was a typical solution to avoid transmission failures, but it came with its own set of problems: image quality was deteriorated, and important information was lost. Every retransmission not only used more bandwidth but also added to the overall power consumption, which was particularly problematic for devices that ran on batteries. Moreover, a number of parameters, such as the kind of data transmission, the number of devices in use, and the selection of light-emitting devices, had a complex impact on the functionality of systems for visible light communication (VLC) [2].

It became clear that ensuring proper image transmission was a significant task that needed to be carefully considered, especially at low bit rates [3]. Precise light intensity measurement was another challenge. Although tools existed for this purpose, their precision might not have been as good as that of equipment used by professionals to measure light [4].

These complex issues were the focus of this research, which aimed to improve the efficiency of VLC-based picture transmission at low bit rates [5]. The knowledge acquired from this research may influence VLC technology advancements in the future, advancing the sector as a whole. The study's goals were met, and the lessons gained opened up new avenues for research and development in VLC systems. Consequently, this effort provided a strong basis for future work in the dynamic and developing field of VLC [6].

This study explored the challenges of traditional wireless communication, focusing on the low-bandwidth transfer of high-resolution images, and explored Visible Light Communication (VLC) as a potential solution. The research was based on Maxwell's equations, which provided knowledge about light propagation [7].

This research study utilizes the following theories in practical way.

1. Gauss's law for electricity: $\nabla \cdot \mathbf{E} = \rho / \epsilon_0$
2. Gauss's law for magnetism: $\nabla \cdot \mathbf{B} = 0$
3. Faraday's law of induction (and Lenz's law): $\nabla \times \mathbf{E} = -\partial \mathbf{B} / \partial t$
4. Ampère's circuital law (with Maxwell's addition): $\nabla \times \mathbf{B} = \mu_0 \mathbf{J} + \mu_0 \epsilon_0 (\partial \mathbf{E} / \partial t)$

Where:

- E is the electric field
- B is the magnetic field
- ρ is the electric charge density
- J is the current density
- ϵ_0 is the permittivity of free space
- μ_0 is the permeability of free space [7]
-

The study also looked into the characteristics of light-emitting components, namely SYD1230 laser diode modules and white LEDs. Light from white LEDs, which were just blue LEDs with a phosphor-coated lens, was produced in the 450–460 nm wavelength range. In contrast, the red laser beam produced by the SYD1230 laser diode module had a wavelength of 650 nm. The electroluminescence concept underlay the operation of both of these devices.

The goal of the research was to increase the efficiency of VLC-based picture transmission at low bit rates. It offered insightful information about how several factors affected how well VLC systems operated, the difficulties in measuring light intensity precisely, and the

possibilities for breakthroughs in VLC technology. The results of this experimental study provided fresh low-cost avenues for future work in the dynamic and developing field of VLC.

2.0 EXPERIMENTAL

2.1 Research design

In Figure 2.1, a transmitter circuit design diagram was presented, featuring a basic electronic connection for control and operation. The illustration showcased a light-emitting device connected to an ESP-32 microcontroller IDE, a versatile and powerful device that could be programmed to control the operation of the device, such as an LED or laser diode.

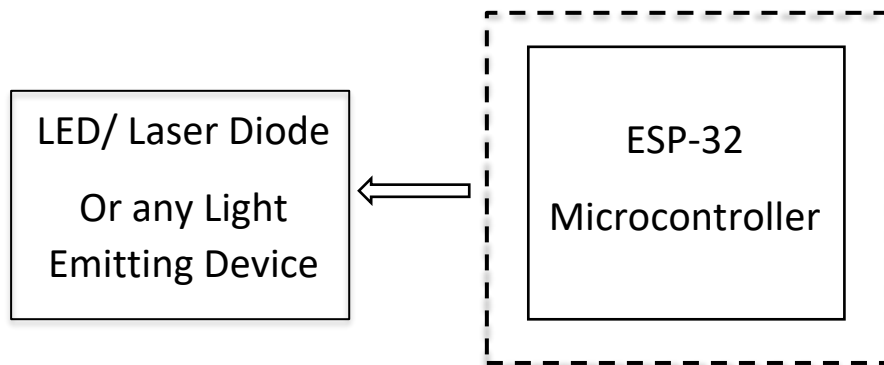


Figure 2.1: The experimental Transmitter block diagram

In Figure 2.2, a receiver circuit design diagram was presented, displaying a basic electronic connection for control and operation. In this representation, a light-sensitive device, such as an LDR or photodiode, was depicted as being connected to an ESP-32 microcontroller. The ESP-32 microcontroller IDE, recognized for its versatility and power, could be programmed to process signals received from the LDR or photodiode [8].

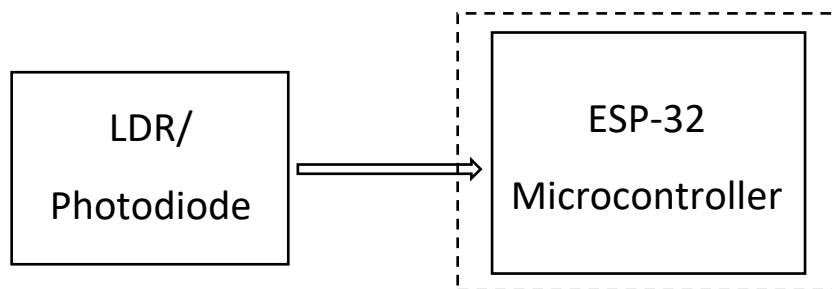


Figure 2.2: Receiver block diagram

2.2 Research Procedure

The systematic process of transmitting an image was outlined in the flow chart presented in Figure 2.3. The process commenced with an image being captured or added, encoded into base 64 format, transmitted, received, and subsequently decoded back to its original form. This sequence of operations was reiterated in four steps, thereby concluding the entire process. Serving as a visual aid, the flow chart facilitated an understanding of the operations involved in the transmission of an image, encompassing the stages from image capture or addition to the

final output following reception and decoding. The clear and concise representation of the process enabled users to comprehend the sequential operations integral to image transmission.

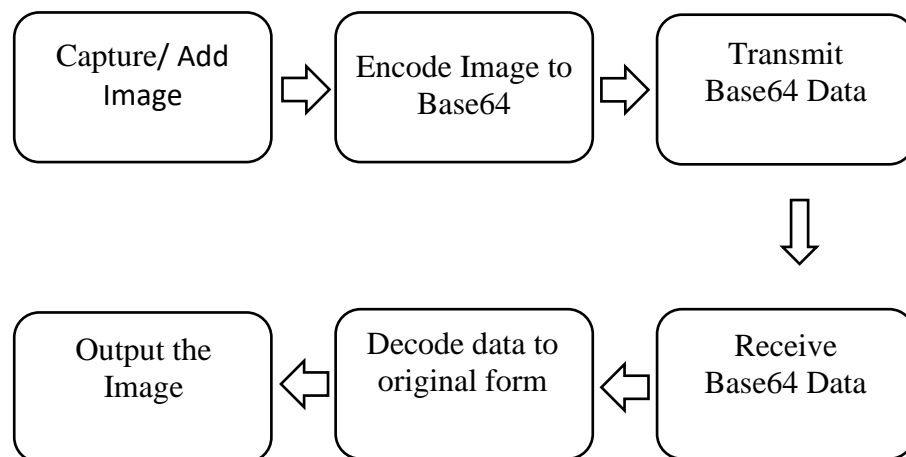


Figure 2.3: Receiver block diagram

2.2.1 Data preparation in the experimental setup

The format of this data was Base64, a binary-to-text encoding scheme used for data integrity, ASCII compatibility, memory efficiency, and universal support. It ensures integrity and reliability of image data in Visible Light Communication systems, facilitating data preparation and decoding processes.

The string data that had to be transmitted was transformed into Base64 format during the data preparation procedure. Binary data could be represented in an ASCII string format using the Base64 binary-to-text encoding technique. When transferring data over networks or storing data, this conversion was quite helpful. This could be done in Python by utilizing built-in modules that offered functions for Base64 encoding and decoding. This guaranteed that the data wouldn't be altered while being transported.

Used for data decoding, converting Base64-encoded digital data back to its original format ensured comprehensible and suitable processing for analysis as well. Also, coding included an initialization of a camera, a frame capture, and a closing of the OpenCV window [9].

2.2.2 Transmitting and receiving image data through VLC

The ESP32 WROOM module was used to set up a Visible Light Communication (VLC) system. LEDs/ Laser Diodes were used as a transmitter, and Light Dependent Resistor (LDR) and IR photodiodes were used as a receiver to transmit and receive data through variations in light intensity [8]. The transmission and reception of data were controlled by ESP-WROOM-32 microcontrollers.

The transmitter setup involved a light source, image processing, data compression, modulation, and power supply. The VLC transmitter circuit included components for modulating the analog signal, and the transmitter had to be positioned for unobstructed line-of-sight communication.

The receiver setup included a photodetector, amplification and filtering, demodulation, signal processing, data decompression, and output display or storage. The transmitter used LEDs for low cost and power consumption, while the receiver used a photodetector, amplifiers, filters, demodulation, signal processing, and data decompression [8].

Furthermore, techniques like Serial communication and parallel communication were used, where a complete byte (eight bits) could be sent at once, with each bit corresponding to a different LED. Compared to serial communication, this sped up the transfer of data. The amount of delay reduction resulting from sending a string using this method was contingent upon the string's length and the bit-by-bit transmission time [10].

2.3 Performance evaluation with the low cost VLC setup

The process of data comparison involved comparing decoded data with the original transmitted data, ensuring successful transmission. The system's performance was evaluated based on the success of data transmission and the quality of the received data, considering factors like transmission rate, accuracy, and transmission latency.

3.0 RESULTS AND DISCUSSION

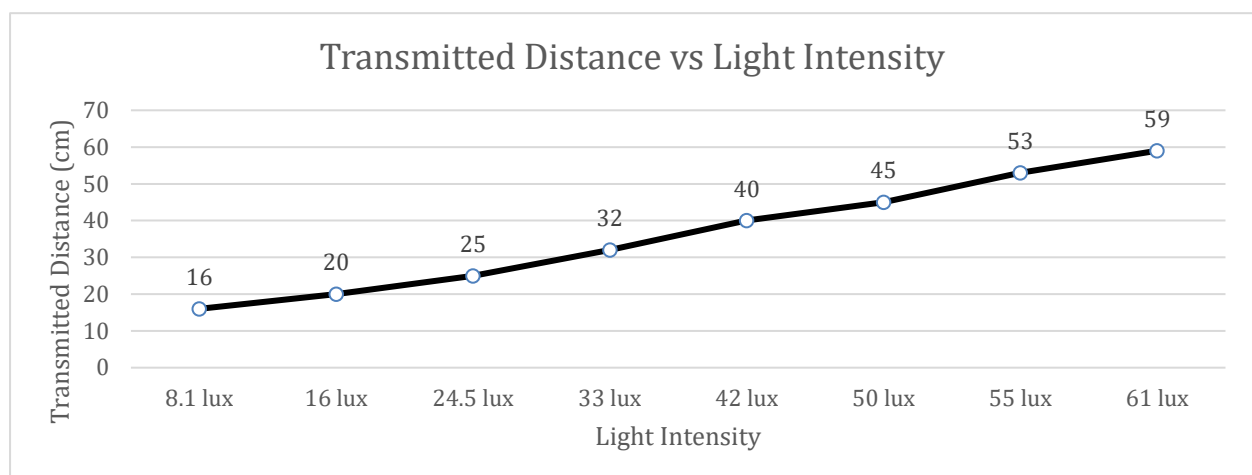


Figure 3.1: Relationship between light intensity and Transmitted distance

The relationship between light intensity and transmitted distance was depicted in Figure 3.1. Light intensity, measured in lux, was represented on the x-axis with values from 8.1 lux to 61 lux. The y-axis denoted the transmitted distance in centimeters, ranging from 0 to approximately 70 cm. Data points on the graph corresponded to measurements of light intensities and their respective transmitted distances. These points were interconnected by a blue line, signifying the trend of the data.

A positive correlation was observed from the graph, indicating that an increase in light intensity was associated with an increase in the transmitted distance. This trend was represented by the ascending line moving diagonally from left to right.

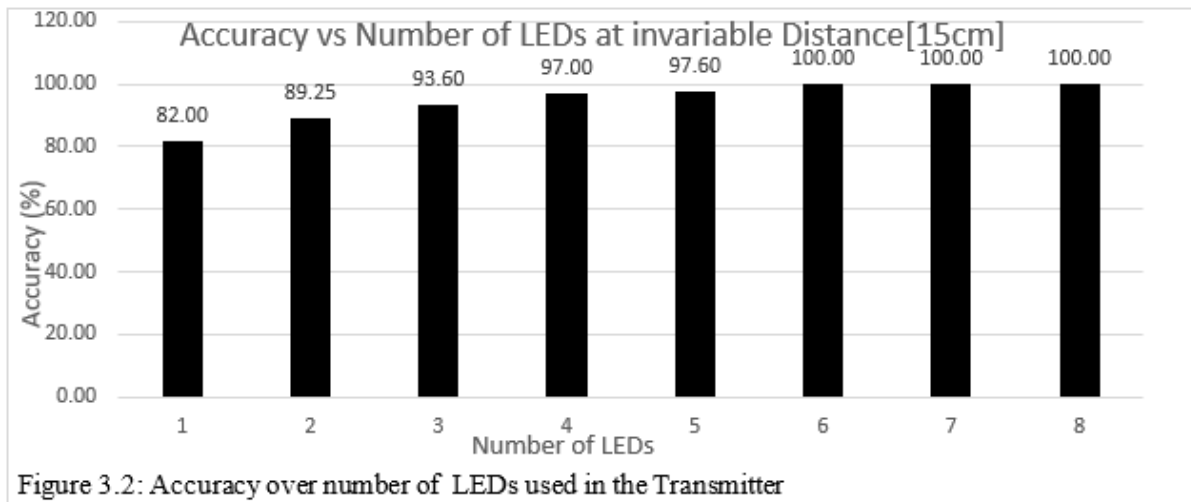


Figure 3.2: Accuracy over number of LEDs used in the Transmitter

Figure 3.2 showed the relationship between the number of LEDs in a transmitter and transmission accuracy at a 15cm distance. The graph showed that accuracy increased with more LEDs, reaching 89.25% with 2 LEDs, 93.60% with 3 LEDs, 97.50% with 4 LEDs, and stabilized at 100% from 5 to 8 LEDs.

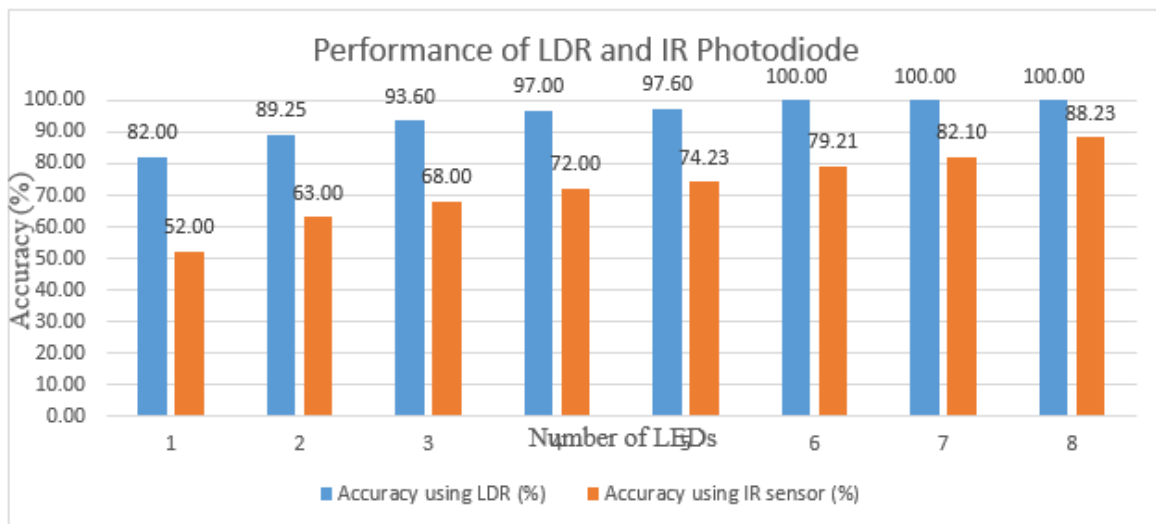


Figure 3.3: Performance of LDR and IR photodiode

Figure 3.3 provided a comparative analysis of the accuracy achieved using Light Dependent Resistors (LDR) and Infrared (IR) sensors in a system with varying numbers of LEDs. The number of LEDs, ranging from 1 to 8, was represented on the x-axis. The y-axis indicated the accuracy in percentages, spanning from 0 to 100%.

Each set of bars in the graph corresponded to the accuracy achieved with a specific number of LEDs. The blue bars represented the accuracy using LDRs, while the orange bars represented the accuracy using IR sensors. The heights of the bars revealed that both types of sensors showed varying levels of accuracy depending on the number of LEDs, with both having their peaks and troughs.

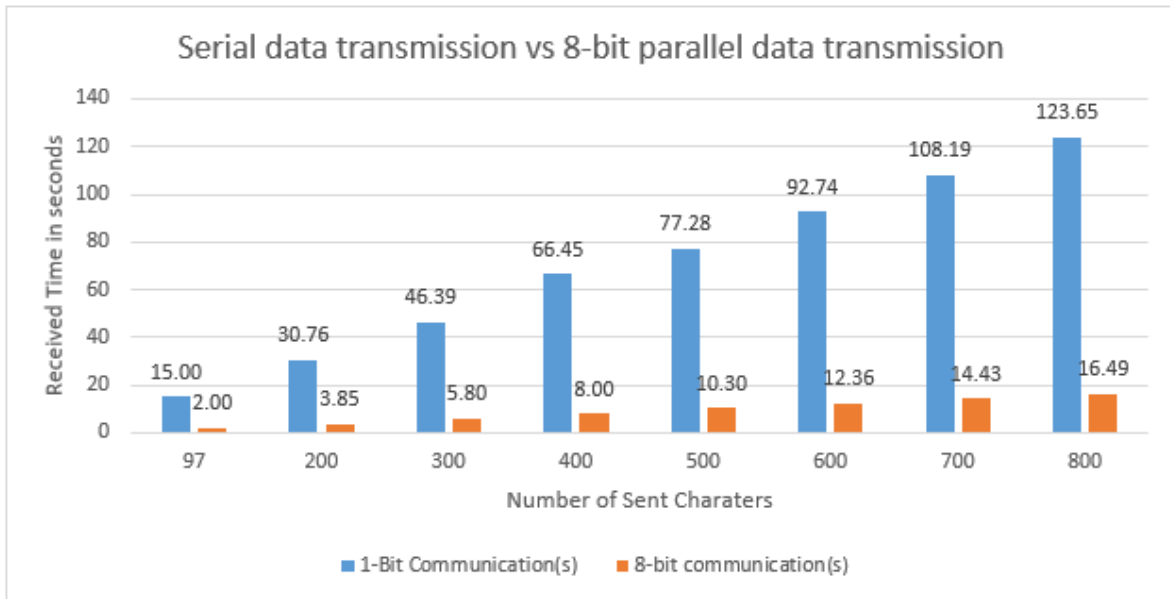


Figure 3.4: Serial communication vs 8-bit parallel communication

Figure 3.4 compared the time taken to receive data using 1-bit and 8-bit communications. The graph showed that as the number of characters sent increased, so did the received time for both types of data transmissions. However, 8-bit communication consistently took longer. This comparative analysis helped understand the performance of different communication methods.

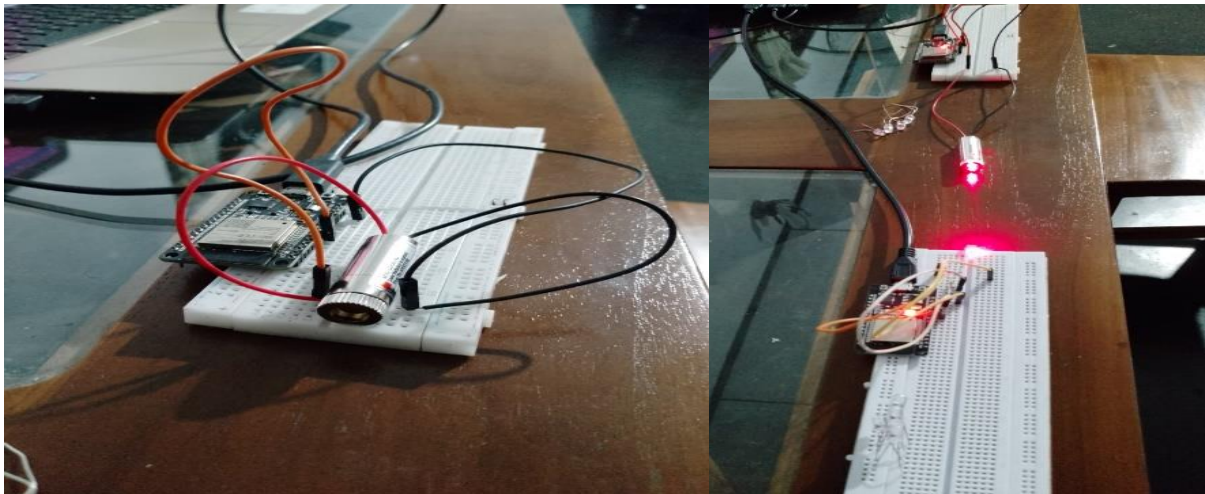


Figure 3.5: Laser Diode Circuit design

Our extensive experiments involved various configurations of LEDs and LDRs. However, the Laser diode emerged as the most effective component for our purpose. The Laser diode (Figure 3.5), due to its coherent beam, ensured no data loss during transmission and could directly interact with the LDR surface. This resulted in an impressive 100% accuracy rate and a transmission distance exceeding 300 meters, significantly outperforming other configurations. These results underscored the potential of Laser diodes in enhancing the performance of Visible Light Communication (VLC) systems, particularly in scenarios requiring high accuracy and long transmission distances. The coherence of the Laser diode beam played a crucial role in this superior performance, paving the way for further exploration and utilization of Laser diodes in VLC systems.

3.1 Discussion

Laser diode is the most suitable transmitter for Visible Light Communication (VLC) systems, achieving 100% accuracy. The Light Dependent Resistor (LDR) was the most effective receiver, accurately detecting and interpreting light signals. The Base64 format was used for data encoding and decoding, ensuring data integrity. A parallel transmission method was the most suitable method, reducing data transfer delays. The VLC system achieved a maximum transmission distance of over 300 meters, demonstrating its potential for long-range communication. The study recommends further research on laser diode performance, Python coding, hardware improvements, environmental factors, real-time image transmission, and security measures. These findings could influence future advancements in VLC technology, opening up new possibilities for its use in various applications. However, the LUX Light Meter App should be replaced with professional light measuring devices due to its lack of functionalities.

4.0 CONCLUSION

The research study was undertaken to analyse the performance of Visible Light Communication (VLC) systems using various configurations of LEDs and LDRs. Despite challenges like Python coding and hardware limitations, significant progress was made. The Laser diode demonstrated exceptional performance, consistently delivering 100% accuracy and an impressive transmission distance exceeding 300 meters. This was attributed to its coherent beam, preventing data loss and allowing direct interaction with the LDR surface. The findings highlighted the potential of Laser diodes in improving VLC system performance and suggested future research to address challenges and explore innovative solutions. The study opened new avenues for exploration and innovation in VLC systems.

ACKNOWLEDGEMENT

The author expresses gratitude as a student of the Faculty of Applied Sciences at Wayamba University. The supervisor is acknowledged for invaluable guidance, unwavering support, and insightful counsel in completing the research. Lecturers and staff at the Faculty of Applied Sciences are recognized for providing foundational knowledge. The author emphasizes that the study's success is attributed to the collective support and guidance of these individuals.

REFERENCES

- [1] Ryunosuke Kurimoto, Yoshihito Imai, T. Ebihara, K. Mizutani, N. Wakatsuki, *Design of efficient and compact visible light communication using low-speed image sensor and MEMS mirror*, (2017) DOI:10.1109/GCCE.2017.8229354
- [2] A. Sobhy, Shaimaa ElSayed, A. Zekry, *Enhancing the performance of optical VLC system based on asymmetric symmetric subcarriers OFDM*, (2019) DOI:10.1002/dac.4226
- [3] H. L. Minh, W. Popoola, Zhengyuan Xu, *Techniques for Enhancing the Performance of VLC Systems*, (2017) DOI:10.1201/9781315367330-6
- [4] Ratan Kumar Mondal, Nirzhar Saha, Y. Jang, *Performance enhancement of MIMO based visible light communication*, (2014) DOI:10.1109/EICT.2014.6777901

- [5] Yang Xinqu, *Image Transmission System Based on Visible Light Communication*, (2015) <https://www.semanticscholar.org/paper/Image-Transmission-System-Based-on-Visible-Light-Xinqu/1008f53bc6938b7c827cba3752210223d36c2db3>
- [6] Priyanka, M. Singh, Mandeep Singh, Harpuneet Singh Gill, Sehajpal Kaur, Hardeep, *Performance estimation of image transmission in indoor visible light communication system based on variable pulse position modulation*, (2022) DOI:10.1002/dac.5303
- [7] Frederick David Tombe, *Maxwell's Original Equations*, (2011), https://www.Researchgate.net/publication/302966559_Maxwell's_Original_Equations
- [8] Suchismita Debata, Rupa Mantoliya, Veena Sahithi, V. R. Kolluru, *Implementation of IoT based smart street light intensity control system using IR and LDR sensors*, (2018) DOI:10.14419/ijet.v7i2.7.10605
- [9] Isnar Sumartono, Andysah Putera Utama Siahaan, Arpan, *Base64 Character Encoding and Decoding Modeling*, (2016), https://www.researchgate.net/publication/311715821_Base64_Character_Encoding_and_Decoding_Modeling
- [10] Vishnu Mahohan, *How to Write Parallel Multitasking Applications for ESP32 using FreeRTOS & Arduino - CIRCUITSTATE Electronics*, (2022) ,<https://www.circuitstate.com/tutorials/how-to-write-parallel-multitasking-applications-for-esp32-using-freertos-arduino/>

SMART ELEPHANT CHASING AND WARNING SYSTEM

A.A.P.P. Navoda*, K.P. Vidanapathirana

Department of Electronics, Wayamba University of Sri Lanka, Kuliypitiya, Sri Lanka

*pasindupavan617@gmail.com

ABSTRACT

The Human-Elephant conflict in Sri Lanka poses significant challenges, leading to socio-economic problems. To address this issue, the implementation of an Elephant Chasing and Warning System is proposed as an effective means of reducing conflict incidents. This system aims to mitigate crop damage, property destruction, and human injuries or fatalities by providing timely warnings of elephant presence and initiating measures to deter them. Existing approaches, ranging from traditional electric fences to contemporary technological solutions, exhibit limitations and complexities. In response, this study introduces a wireless sensor network-based detection system, integrating a warning and chasing mechanism. Utilizing a microwave radar sensor module, the intrusion of elephants is detected, triggering a warning system that sends SMS alerts to pertinent authorities, including property owners, the wildlife department, and local police stations. Additionally, the system offers diverse deterrent options, such as activating a siren emitting frequencies intolerable to elephants, flashing Red-Blue lights, and activating an electric fence. The versatility of this comprehensive system extends to a wide array of applications, covering the detection and warning of elephant intrusions across varied contexts. Application of the system covers wider aspects of detecting and warning of elephant intrusions such as on village forest boundaries, rail tracks, and on roadsides.

Keywords: Human-Elephant conflict, Chasing and Warning System

1.0 INTRODUCTION

1.1 Human-Elephant conflict

The conflict between humans and elephants (HEC) in Sri Lanka is not a contemporary issue. It has existed since the beginning of human settlements and agriculture close to elephant habitats. Elephant assaults mostly affect farming communities in arid zones and impoverished people living near forest boundaries in undeveloped countries. The most common forms of attacks include crop raiding, village raiding, when dwellings are raided and destroyed in search of rice and salt, and unexpected roadside attacks. When looking at the overall number of elephant deaths attributable to human activity, 574 elephants died by shooting, and 105 elephants died via electrocution between 2005 and 2010 [1]. An estimated 71 fatalities among humans and numerous property losses are reported each year as a result of elephant assaults [2].

1.2 Literature review

Over time, several techniques and frameworks have been created to tackle the HEC. Elephants are physically and mentally separated from electric fences. However, it did not resolve the problem or provide HEC with a stand-alone solution. Scientists devised and built the electrification fence intrusion detection and warning system alerts. Nevertheless, a significant restriction on physical access to the system for maintenance and repair following an intrusion is included in the alert system. A technique is available for tracking elephants with radio collars to obtain their Global Positioning System (GPS) coordinates and suggested an Radio-Frequency Identification (RFID) device for elephant detection. Its poor position update rate and limited short-range detecting capabilities are its drawbacks [3]. A method to detect elephant incursion along the margins of forests using real-time picture capture was established when systems with visual and image processing approaches were adopted. There were restrictions on the field of view, camera angle, and lighting for vision-based devices for recognize the elephant [3].

1.3 Objectives of the project

The primary objectives of this Smart Elephant Chasing and Warning System are to enhance safety measures upon detecting the presence of elephants and once an elephant is detected, the system will promptly activate an electric fence to create a secure barrier, ensuring the safety of both elephants and nearby human communities. Simultaneously, a loud siren will be activated, serving as an audible deterrent to guide elephants away from populated areas. The system will also trigger a powerful flashlight, increasing visibility and alerting communities to the potential presence of elephants. Furthermore, the system will send crucial information to relevant authorities, facilitating swift response and coordination to manage the situation effectively to mitigate human-elephant conflicts and promote a safer coexistence in shared habitats.

2.0 EXPERIMENTAL

The below Figure 2.1 shows the block diagram of the system.

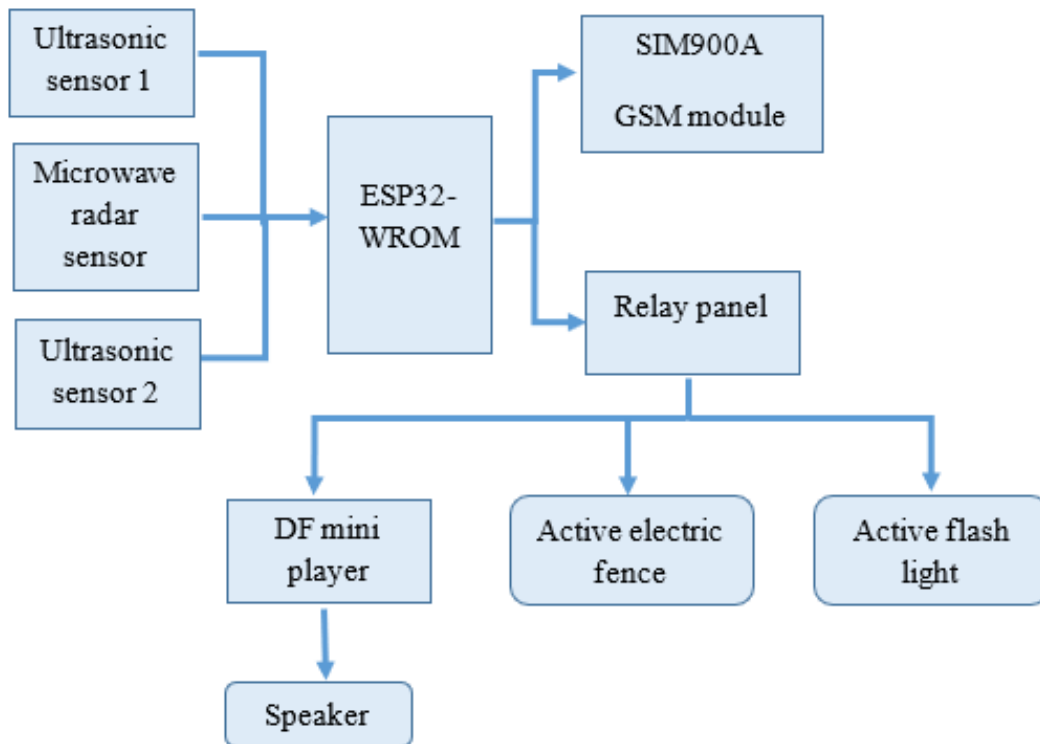


Figure 2.1: Block diagram of the system

The microcontroller always gets input signals of the two ultrasonic sensors and microwave radar sensor. Here, two ultrasonic sensors are used in order to improve the detection accuracy & if the signals of two ultrasonic sensors (distance sensor) and microwave radar (motion sensor) were high, the microcontroller sends an output signal to GSM module and relay panel. Then GSM module sends the SMS to authorized people. Also, it activates the electric fence, flash light and DF mini player.

The speaker emits the sound of swarming bee, activating the electric fence and flashing the light (red & blue) which will help to chase elephants. This is the elephant chasing part of the project. Sending the SMS to authorized people is the warning part of the system. Figure 2.2 shows the flow chart of the system.

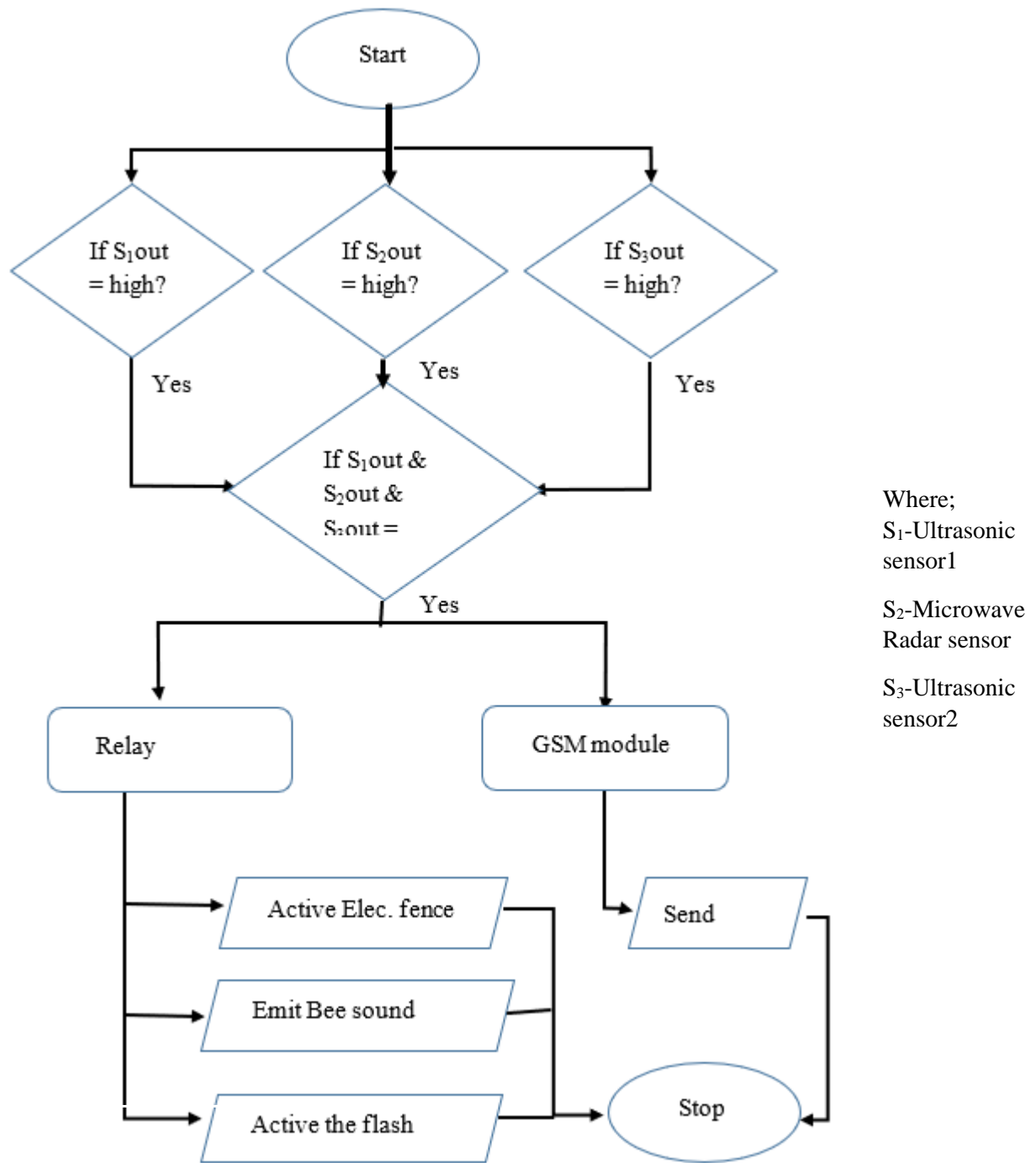


Figure 2.2: Flow chart of system

The modules, components and software used to develop the system are explained in the next sections.

2.1 XYC-WB-DC microwave radar sensor

Microwave radar sensor is electronic devices that measures the motion of a target object by emitting microwaves, and converts the microwaves into an electrical signal as high level 3 V and low level 0 V. It has 5-8 meters detection distance and 5.8 GHz operating frequency [4].

This was used to get an output signal, if the sensor detects any motion in a selected distance range.

2.2 HY-SR05 Ultrasonic sensor

Ultrasonic sensor is an electronic device that measures the distance of a target object by emitting ultrasonic sound waves, and converts the reflected sound wave into an electrical signal. Ultrasonic wave travel faster than the speed of audible sound [5]. Two HY-SR05 Ultrasonic sensors are used in the system designed, considering elephants' height, to get output signals if the sensors detect any object

2.3 Node MCU (ESP32-WROOM)

ESP32-WROOM is a Wi-Fi module that is more and more popular among hardware developers. In addition, the price is very affordable. This is a versatile Wi-Fi module coming as SOC (system on chip), which can be programmed directly to ESP32-WROOM without requiring an additional microcontroller [6]. The Node MCU (ESP32-WROOM) is the controller of the system designed. It sends a signal to the relay panel based on the output from the two ultrasonic sensors and the microwave radar sensor in order to activate the system.

2.4 SIM900A GSM module

The GSM 900A module is a wireless communication device designed to operate within the GSM 900 frequency band, a widely-used spectrum for mobile communication services in various regions. This module facilitates versatile communication capabilities, including SMS messaging, voice calls, and potentially data communication [7]. This was used to send text messages to the authorized people once the system is activated.

2.5 DF mini player

The DF mini player is a super cheap MP3 Player that can be play files from a SD card, USB storage devices and NOR flash. It has an integrated 3W amplifier that can be used to build a standalone mono speaker [8]. This was used to play mp3 file of swarming bee sound.

2.6 Flash light

The red and blue flash lights are used because the elephants are afraid of the red and blue colors [9].

2.7 Arduino software

The Arduino software, also known as the Arduino IDE (Integrated development environment) is a user-friendly platform that facilitates the programming and development of projects using Arduino boards [10].

2.8 Detection system

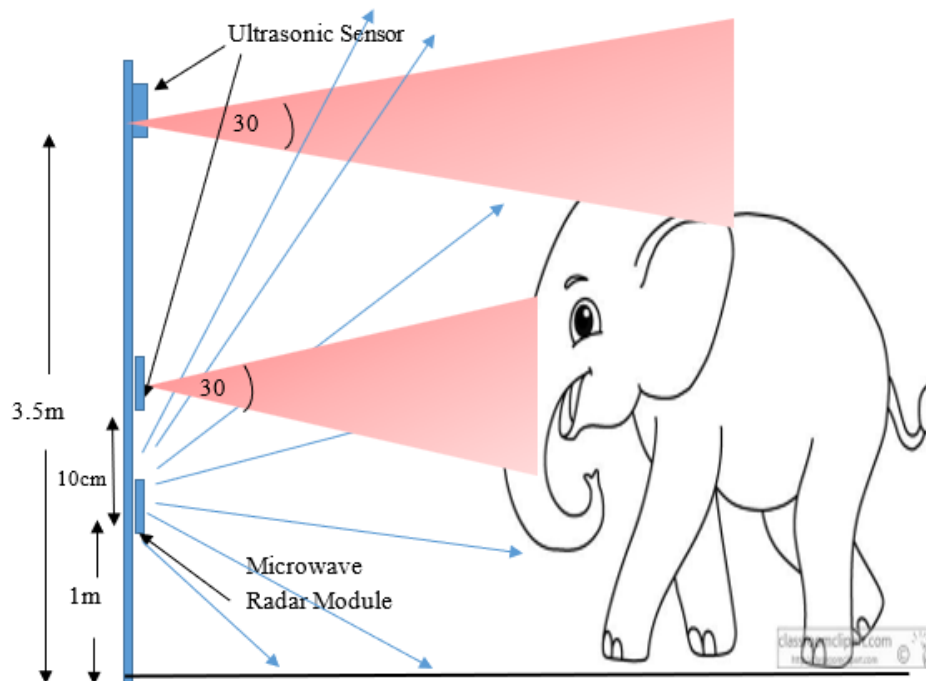


Figure 2.3: Detection system

In optimizing the detection module, it is assumed that baby elephants do not move alone without herd and if moved, the threat from baby elephants is minimum. Based on that assumption the optimized height of sensor placement is done for the worst case of detecting an intrusion of an elephant. In the elephant detecting system, the elephant detection was done by placing the microwave radar sensor and two ultrasonic sensors strategically placed above ground level. The microwave radar sensor has 5-8 m detection range and 5.8 GHz operating frequency. The motion was detected by this microwave radar sensor [4]. It was mounted in 1 m above the ground level shown in Figure 2.3.

Normally male and female elephant's height is between 2-3.5 m [2]. According to this measurement, one ultrasonic distance sensor was mounted 3m above the ground level and other ultrasonic sensor was mounted a little above 1m to detect the body. The ultrasonic sensor has a detection range between 2-4.5 m, 40 kHz sound frequency and a 15-degree measurement angle [5].

The logic for elephant detection involves examining the output values of both sensors. When the output values of both the microwave radar and ultrasonic sensors are high, signaling simultaneous detection, the system concludes that an elephant is present, triggering the activation of the chasing and warning mechanisms. Conversely, if the output of one sensor is high while the other remains low, it is assumed that no elephant is detected, and the system remains inactive.

The system just used a sound of swarming Bee as a sound frequency because the aim of the project is just to warn and chase the elephants away, not to do any kind of harm to them. The sound of swarming Bee is selected because the elephants are afraid of the particular sound and they normally do not get near to the particular sound source [11].

3.0 RESULTS AND DISCUSSION

The system was planned to make using PIR and IR sensors, but could not use the PIR sensor because its sensitivity is too high so that it can sense any kind of motion despite big or small. As examples, the PIR sensor can sense the motion of a little fly as well as a tiny little motion of a tree leave and etc. The reason is that the PIR sensor having a low operational frequency. And, could not use the IR sensor because it has just a 2-30 cm detection range and it is not sufficient to detect an elephant. Therefore, the system was built using 2 ultrasonic sensors and one microwave radar sensor. The results of the test done using the system are shown in the below table.

Table 1: Detection test with objects

Object	Number of tests	Number of detected	Detection rate (%)
Dog	5	0	0
Car	5	0	0
Elephant	8	7	87
Cow	5	1	20

Dogs and Cars are having a 0% of detection rate while cows are having a 20% detection rate. The cow's detection was happened because of a flying bird near the upper ultrasonic sensor at the same time the cow gets near to the lower ultrasonic sensor and the microwave radar sensor. Therefore, in order to resolve this error, changing the delay resister in the microwave radar sensor is crucial. The elephants are having an 87% successful detection rate. The 8 tests were done at various conditions such as at day time, at night time, when the elephant is asleep and using different distances and etc.

Here, the detection range of the ultrasonic distance sensor can be increased by upgrading it to FST700-CS01 long distance ultrasonic sensor. Also, the detection range of microwave radar sensor can be increased by upgrading it to HB100 long distance microwave motion sensor.

An example for the text messages received is mentioned below in Figure 3.1.

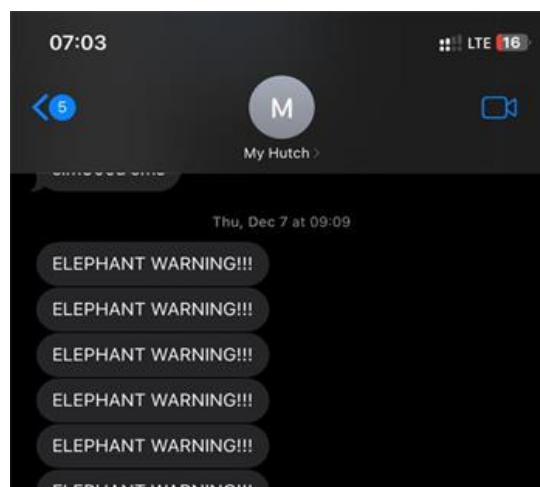


Figure 3.1: SMS warning from GSM

4.0 CONCLUSION

HEC is known to be a major socio-economic problem in Sri Lanka causing fatal damage for both humans and elephants. Protecting the lives and properties of people as well as conserving elephants was the focus of this project. Thus, the Elephant chasing and warning system was successfully designed as a possible effective solution to minimize HEC. The design consists with microwave motion sensor and ultrasonic distance sensor for the identification from far and GSM based SMS alerting is used for warning system. Emitting swarming bee sound, activating electric fence and activating flash light are used for chasing the elephants. The detection system was tested and a general detection rate of 87% was observed. This system can be further enhanced by adding long distance motion sensors. Finally, a possible solution for minimizing HEC in rural areas of Sri Lanka was provided as the outcome of this project.

ACKNOWLEDGEMENT

The authors would like to thank all the staff of the Department of Electronics, Faculty of Applied Sciences, Wayamba University of Sri Lanka, and others who have supported to make this study a success.

REFERENCES

- [1] Köpke, S. et al. (2021) Human–elephant conflict in Sri Lanka: A critical review of causal explanations, MDPI. Available at: <https://www.mdpi.com/2071-1050/13/15/8625> (Accessed: 30 October 2023).
- [2] current status of Asian elephants in Sri Lanka - researchgate. Available at: https://www.researchgate.net/publication/258286914_Current_Status_of_Asian_Elephants_in_Sri_Lanka (Accessed: 22 October 2023).
- [3] elephant intrusion detection, deterrence and warning ... - AC. Available at: http://ir.kdu.ac.lk/bitstream/handle/345/2943/FOE%20Proceedings%20Body%20Ver03_16.pdf (Accessed: 22 October 2023).
- [4] e-Gizmo (no date) *Build software better, together, GitHub*. Available at: <https://github.com/e-Gizmo/XYC-WB-DC-Microwave-Radar-Motion-Sensor-Module/blob/master/xyc-wb-dc.pdf> (Accessed: 30 November 2023).
- [5] Nicholas_N (2020) *Distance measurement with an ultrasonic sensor hy-SRF05, Hackster.io*. Available at: https://www.hackster.io/Nicholas_N/distance-measurement-with-an-ultrasonic-sensor-hy-srf05-64554e ,(Accessed: 30 November 2023).
- [6] Teja, R. (2021) *ESP32 pinout: ESP-WROOM-32 pinout, ElectronicsHub*. Available at: <https://www.electronicshub.org/esp32-pinout/>, (Accessed: 30 November 2023).
- [7] Fahad, E. (2022) *GSM SIM900A with Arduino complete guide with GSM based projects examples, Electronic Clinic*. Available at: <https://www.electronicclinic.com/gsm-sim900a-with-arduino-complete-guide-with-gsm-based-projects-examples/> ,(Accessed: 30 November 2023).

- [8] Lab, S. (2023) *How to use the DFMINI player MP3 module with Arduino: Arduino, Maker Pro*. Available at: <https://maker.pro/arduino/projects/how-to-use-the-dfmini-player-mp3-module-with-arduino>, (Accessed: 30 November 2023).
- [9] *Elephants see red as a risky colour*, *NZ Herald*. Available at: <https://www.nzherald.co.nz/nz/elephants-see-red-as-a-risky-colour/KQ7JQDFGSWJDTKLHJU3YD5NIFM/#:~:text=Scientists%20from%20the%20University%20of,red%20%2D%20and%20their%20body%20scent>. (Accessed: 15 December 2023).
- [10] Team, T.A. (no date) *Software, Arduino*. Available at: <https://www.arduino.cc/en/software/> (Accessed: 30 November 2023).
- [11] King, L. E. et al., 2018. Wild Sri Lankan elephants retreat from the sound of disturbed Asian honey bees. *Current Biology*, 28(2)

DESIGN AND ANALYSIS OF A FILTER NETWORK FOR IMPROVED TV SIGNAL QUALITY

D.H.L. Zoysa*, J.M.J.W. Jayasinghe, T. Premathilake

Department of Electronics, Wayamba University of Sri Lanka, Kuliypitiya, Sri Lanka

*dhlzoysa@gmail.com

ABSTRACT

The research aims to address the challenges of maintaining optimal TV signal quality in Sri Lanka. The investigation looks at variables affecting TV signal quality, including weather conditions, external interference, and the role of TV signal amplifiers in augmenting signal strength. The research focuses on the design and analysis of a suitable filter network integrated into the amplification system, elucidating the function of filters in signal processing. The study acknowledges real-world complexities and practical implementation considerations, highlighting the resilience of the developed filter network through rigorous simulations and experiments. The results show a significant enhancement in TV signal quality, validating the efficacy of the proposed filter network. The study begins by identifying unwanted TV signal ranges in Sri Lanka, followed by designing a strategic filter network circuit for their elimination. Through careful experimentation, these steps conclude in a substantial improvement in TV signal quality. The outcomes not only address local challenges but also contribute to global discussions, providing practical solutions for Sri Lankan broadcasting and influencing worldwide advancements in TV signal amplification.

Key words: Signal Enhancement, Filter Network, Broadcast Technology

1.0 INTRODUCTION

1.1 Overview

The introduction sets the stage for a comprehensive exploration of TV signal quality in Sri Lanka. It outlines the profound transformations in television broadcasting, connect against persistent challenges. This research is introduced with a focus on addressing these challenges. The importance of TV antennas and amplifiers in enhancing signal quality becomes evident as we navigate through the presentation. Friss transmission concepts are touched upon, laying the groundwork for understanding the complexities of signal propagation. An exploration of factors influencing TV signal quality offers a contextual backdrop, guiding the audience into the heart of the research objectives.

1.2 Research Objective

The research undertakes a comprehensive exploration of TV signal amplifiers and the development of an optimized filter network. It begins by measuring the frequency response of the amplifier, focusing on upper and lower frequency limits within the input bandwidth using advanced equipment like spectrum analyzers. The study then scrutinizes the relationship between input bandwidth and TV signal quality, analyzing parameters like signal to Noise Ratio (SNR) and interference. Emphasizing proactive design, the research crafts a tailored filter network to selectively allow desired frequencies while eliminating unwanted signals. The final phase involves a rigorous evaluation of the filter network's performance, assessing its ability

to enhance signal quality. This multifaceted approach positions the research at the forefront of advancing TV signal processing technologies.

2.0 EXPERIMENTAL

2.1 Measure Frequency Response:

The objective entails a comprehensive examination of the TV signal amplifier's frequency response. The aim is to precisely quantify and delineate the upper and lower frequency limits within the input bandwidth [1]. Utilizing advanced measurement techniques and tools such as spectrum analyzers, this phase seeks to provide a detailed understanding of the amplifier's responsiveness across various frequencies.

2.2 Analyze Input Bandwidth Effects on Signal Quality

The research aims to delve into the intricate relationship between input bandwidth and TV signal quality. This involves a systematic analysis of SNR, distortion, and interference within the amplified signal. By scrutinizing these critical parameters, the objective is to discern how variations in input bandwidth directly influence the overall quality of the TV signal, providing insights into potential trade-offs and optimization strategies [3].

2.2.2 Frequency allocation in Sri Lanka

Telecommunications Regulatory Commissions of Sri Lanka (TRCSL) oversees the frequency distribution for television transmission in Sri Lanka. To ensure the accurate design and optimization of the filter circuit, it is imperative to access detailed information on TV signal frequencies allocated by the TRCSL. The TRCSL, as the authoritative body overseeing frequency management, holds crucial data on the specific frequency bands dedicated to television broadcasting in the country. The accuracy of our filter circuit design shifts on obtaining these details, allowing us to tailor our circuit to the allocated frequency ranges and optimize its performance for improved TV signal quality.

The TV frequency ranges can be identified from the Table of National Frequency Allocation [10].

Table 2.1: Table of National Frequency Allocation

Frequency (MHz)	Region
54 – 68	Fixed mobile broadcast
174 – 223	Fixed mobile broadcast
223 – 230	Radio navigation fixed mobile broadcast
470 – 806	Fixed mobile broadcast

The unwanted frequency ranges identified in the TV signal amplifier's amplification spectrum are less than 54 MHz, 68 MHz to 174 MHz, 230 MHz to 470 MHz, and above 806 MHz

2.3 Designing filter network to eliminate unwanted signal

The objective focuses on the proactive design of a filter network tailored to the TV signal amplifier's input frequency range. The emphasis lies in crafting a filter network with meticulous attention to detail, leveraging appropriate configurations and component values. The goal is to create a robust filtering system capable of selectively allowing desired frequencies while efficiently eliminating unwanted signals, addressing issues such as atmospheric interferences and distortions [6].

The cutoff frequency is typically defined as the frequency at which the power of the signal is reduced to half of its original value. This corresponds to a decrease of 3 dB, or a 70.7% magnitude of the input signal. The quality factor is defined as the ratio of the center frequency of a resonant system to the bandwidth around that frequency. And a low Q factor gives a broad band (wide) bandwidth or a high Q factor gives a narrow band (small) bandwidth.

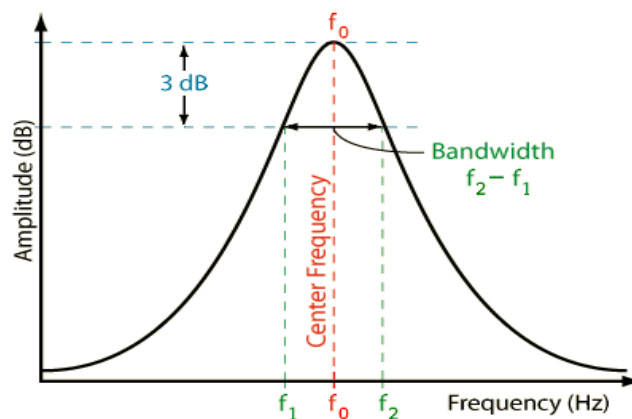


Figure 2.1: Cutoff Frequency

Center Frequency (f_0) is frequency at which the notch filter provides maximum attenuation to the unwanted signal.

$$Q = R_1(C_1 + C_2)R_1R_2C_1C_2 \text{ -----(1)}$$

$$f_0 = \frac{1}{2\pi\sqrt{R_1R_2C_1C_2}} \text{ -----(2)}$$

Quality Factor (Q)

A measure of the filter's selectivity. Higher Q values result in narrower notches.

$$Q = \frac{\sqrt{R_1R_2C_1C_2}}{R_1(C_1+C_2)} \text{ -----(3)}$$

Bandwidth (BW):

The range of frequencies around the center frequency where the notch filter operates.

$$BW = \frac{f_0}{Q} \text{ -----(4)}$$

Low Cutoff Frequency (f_L) and High cut off frequency (f_H)

$$f_L = \frac{f_0}{\sqrt{1+\frac{1}{4Q^2}}} \text{ -----(5)}$$

$$f_H = f_0 \times \sqrt{1 + \frac{1}{4Q^2}} \text{ -----(6)}$$

A notch filter is an electronic device designed to reduce or eliminate a specific range of frequencies, known as the notch frequency, while allowing all other frequencies to pass through with minimal attenuation. It creates a "notch" in the frequency response, effectively suppressing signals within a narrow band. This filter is commonly used to eliminate unwanted interference or noise at a specific frequency in audio, radio, and communication systems.

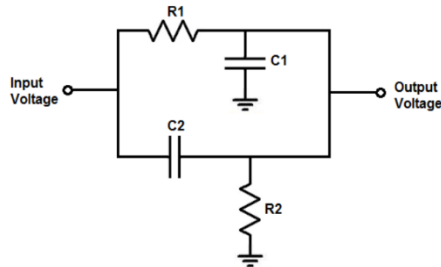


Figure 2.2: Wideband Notch Filter circuit diagram

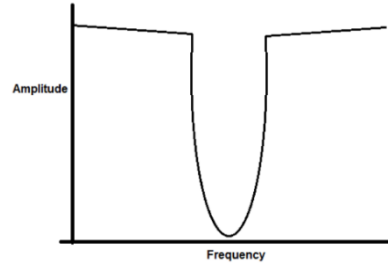


Figure 2.3: Amplitude vs Frequency Graph

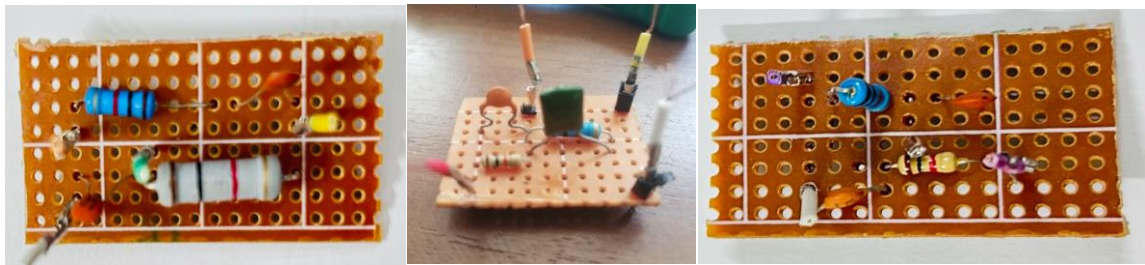


Figure 2.4: Designed Notch filters

2.4 Evaluate Filter Network Performance:

Following the design phase, this objective involves a thorough evaluation of the performance of the design. The investigation looks at variables affecting TV signal quality filter network. Measurement metrics will include the network's ability to attenuate unwanted signals effectively and its overall impact on improving signal quality in the amplified TV signal. This stage is crucial for validating the practical efficacy of the designed filter network and gauging its real-world applicability in enhancing the viewer experience.

3.0 RESULTS AND DISCUSSION

3.1 Spectrum Analyzer Observations



Figure 3.1: Antenna 01



Figure 3.2: Antenna 02

The TV signal amplifier exhibits a noteworthy amplification range spanning from 50 MHz to 900 MHz, showcasing its versatility in handling a broad spectrum of frequencies. At the pivotal frequency of 588 MHz, the amplifier achieves a peak gain of 9.22 dBm, indicating its effectiveness in enhancing signal strength. These findings hold profound implications for the optimization of the filter network design, offering valuable insights into tailoring the filter for maximum efficiency within the targeted frequency band, thereby contributing to an overall improvement in TV signal performance.

3.2 Spectrum Analyzer Observations before and after connecting filter circuit (64 MHz-174 MHz Frequency Range): Filter 01

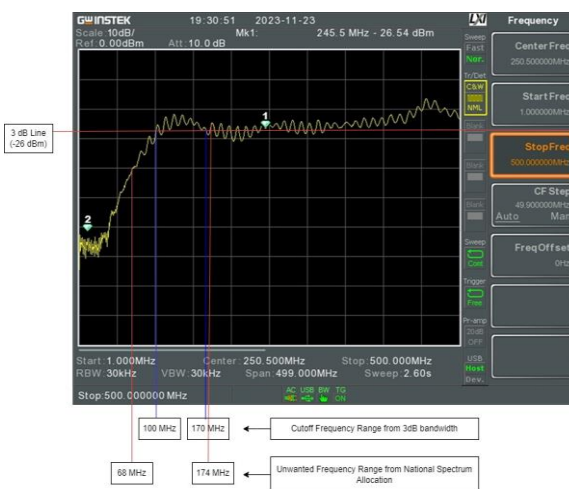


Figure 3.3: Spectrum Analyzer Output before connecting Filter 01 (64 MHz-174 MHz)



Figure 3.4: Spectrum Analyzer Output after connecting Filter 01 (64 MHz-174 MHz)

The notch filter, strategically placed at 310 MHz, excels in creating a profound attenuation at this specific frequency while preserving a consistently flat signal spectrum elsewhere. At the exact notch center of 310.25 MHz, the output signal maintains a robust power level of 46.26 dBm, ensuring a clean, noise-free signal characteristic of a high-quality TV amplifier. The filter's effectiveness is highlighted by its remarkable ability to reduce signal power significantly, achieving attenuation levels ranging from -36.54 dBm to -70 dBm. This substantial reduction in power demonstrates the notch filter's prowess in suppressing interference specifically at 310.25 MHz without introducing detrimental effects to the broader signal spectrum. The results affirm the notch filter's suitability for targeted interference suppression, showcasing its potential as a valuable tool in optimizing TV signal quality.

3.3 Spectrum Analyzer Observations before and after connecting filter circuit 02 (230 MHz – 470 MHz Frequency Range): Filter 02

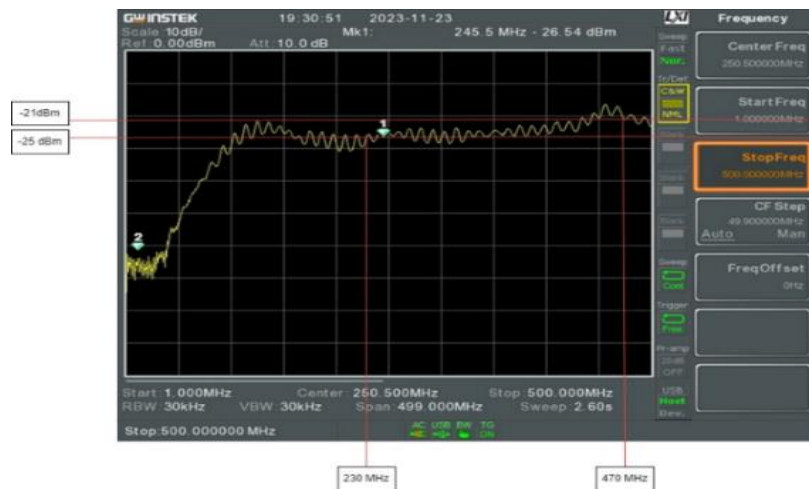


Figure 3.5: Spectrum Analyzer Observations before connecting Filter circuit (230 MHz-470 MHz frequency Range)

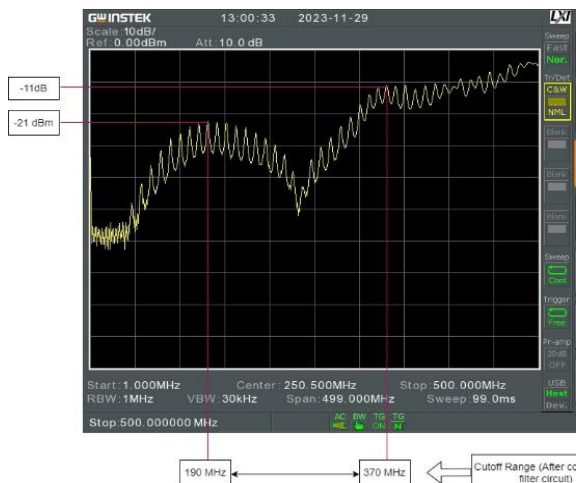


Figure 3.6: Spectrum Analyzer Observations after connecting Filter circuit 02 (230 MHz – 470 MHz frequency Range)

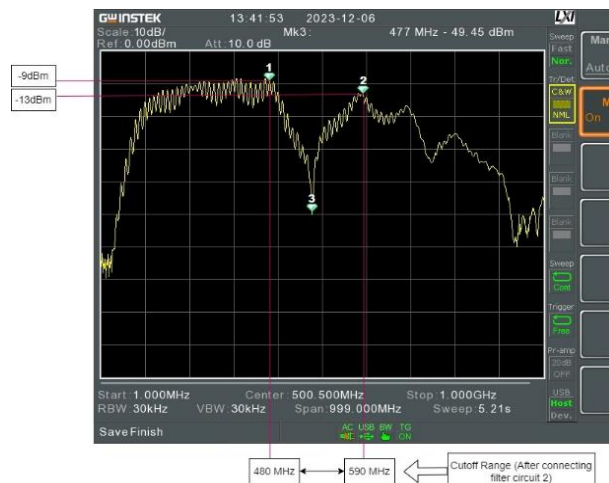


Figure 3.7: Spectrum Analyzer Observations after connecting Filter circuit 03 (230 MHz-470 MHz frequency Range)

3.4 Spectrum Analyzer Observations after connecting filter circuit 03 (230 MHz - 470 MHz Frequency Range):

Placing the notch filter strategically at 480 MHz showcases its exceptional attenuation capabilities, forming a deep notch while maintaining a flat signal spectrum in neighboring frequencies. At the notch center (480 MHz), the output signal remains robust at 58.02 dBm, signifying a clean and noise-free signal typical of a high-quality TV amplifier. With a substantial power reduction of over 10.07 dBm, reaching -68.02 dBm, the notch filter effectively suppresses interference at 480 MHz without adverse effects on the broader signal spectrum. These outcomes underscore the notch filter's suitability for precise interference suppression, affirming its potential as a valuable tool for optimizing TV signal quality.

The results show that precise tuning of notch filters effectively eliminates unwanted signal ranges, ensuring appropriate TV signal ranges and improved signal quality for television broadcasts.

4.0 CONCLUSION

The research is centered on examining TV signal amplifiers operating in the 50 MHz to 900 MHz range. Following the identification of undesirable signal ranges (less than 54 MHz, 68 MHz - 174 MHz, 230 MHz - 470 MHz, over 806 MHz) from the national spectrum allocation [10], A notch filter was designed to eliminate these bands. Upon circuit evaluation, there was a slight drift in the intended elimination range. However, adequate elimination was achieved after tuning the filter circuit and successfully mitigated the unwanted signal ranges. This highlights the efficacy of fine-tuning in addressing interference issues. In conclusion, this study not only highlights the importance of attenuating unwanted signals but also emphasizes the importance of refining filter circuits for optimal performance, promising advancements in TV signal quality and an enhanced viewer experience.

ACKNOWLEDGEMENT

Authors wish to extend their gratitude to staff of the Department of Electronics and Department of Electrotechnology, Wayamba University of Sri Lanka for their assistance given in implementing circuits and taking measurements.

REFERENCES

- [1] Hazlett, Thomas W., et al. "The Social Value of TV Band Spectrum in European Countries." *Info*, vol. 8, no. 2, 1 Mar. 2006, pp. 62–73, <https://doi.org/10.1108/14636690610653590>.
- [2] Adroaldo Raizer, and Mikael Fonseca. "Digital TV Signal Reception and Amplification System." *SET International Journal of Broadcast Engineering*, vol. 2017, 1 Nov. 2017, <https://doi.org/10.18580/setijbe.2017.3>.
- [3] Chen, X., Wang, W., Hong, W., & Zhang, Q. (2021). Design and simulation of a compact filtenna for 5G mid-band applications. *IEEE Transactions on Antennas and Propagation*, 69(6), 3706-3711.
- [4] Beigizadeh, M., Dehghani, R., & Nabavi, A. R. (2018). A low power tunable inductor based on active capacitor with negative resistance. *AEUE - International Journal of Electronics and Communications*, 95, 118-125.
- [5] Wu, Y., Wang, S., & Zhu, Y. (2018). Design and implementation of fully integrated CMOS on-chip bandpass filter with wideband high-gain low noise amplifier. *Microsystem Technologies*, 24(5), 2371-2377.
- [6] Q. Xu, X. Zhang, and L. Zhu, "Design and analysis of a novel compact tunable bandpass filter using coupled resonators," *IEEE Trans. Circuits Syst. II, Express Briefs*, vol. 69, no. 12, pp. 4804-4808, Dec. 2022.
- [7] Y. Zhu, Y. Wu, and S. Wang, "Design and implementation of a reconfigurable bandpass filter for 5G applications," *IEEE Access*, vol. 8, pp. 21668-21674, 2020.
- [8] T. Chen, Z. Zhang, and Y. Wang, "A novel compact bandpass filter with extended stopband bandwidth," *IEEE Microw. Wirel. Compon. Lett.*, vol. 31, no. 10, pp. 760-762, Oct. 2021.

- [9] Y. Li, W. Hong, and X. Zhang, "Design of a compact high-Q bandpass filter using metamaterial structures," *IEEE Access*, vol. 9, pp. 54248-54256, 2021.
- [10] "Frequency Licence - Telecommunications Regulatory Commission of Sri Lanka." *Trc.gov.lk*, 2014, trc.gov.lk/2014-05-12-12-36-13/frequency-licence.html. Accessed Dec. 2023

INVESTIGATION OF ENERGY EFFICIENT LIGHTING SOLUTION FOR DC POWERED SYSTEM

P.F.D.C. Fonseka*, K.K.C.S.Kiriella

Department of Electronics, Wayamba University of Sri Lanka, Kuliypitiya, Sri Lanka

*chathurangafonseka25@gmail.com

ABSTRACT

This research study discusses a new DC-DC buck converter that has been developed specifically for energy efficiency. The converter combines an astable 555 timer IC with an LC filter to reduce DC voltage effectively and minimize power loss, resulting in significant energy savings and cost reductions. It's an ideal choice for environmentally conscious individuals and businesses. The converter has been designed for the lighting sector and provides a reliable and efficient power solution for energy-efficient LED lighting systems. Encouraging sustainable practices is crucial in building a better, more sustainable future. Energy efficiency not only benefits individual devices but also households and businesses. It allows them to reduce their costs, increase competitiveness, and contribute to a greener future.

Keywords: DC-DC buck converter, energy efficiency, LED lighting

1.0 INTRODUCTION

The rising costs of electricity and growing concern for the environment have made energy efficiency a top priority in scientific and technological advancements. Lighting is a crucial area of focus due to its high use of global energy. Although LED technology has the potential to address this issue, it requires reliable and efficient power conversion. This paper presents a groundbreaking DC-DC buck converter that is specifically designed for LED lighting systems. This innovative technology has the potential to revolutionize the way LED lighting is powered and contribute to a more energy-efficient future.

Currently, there are several challenges facing LED power sources. Traditional linear regulators consume a lot of power while existing buck converters often lack the level of precision and effectiveness required to improve LED function. This disparity highlights the urgent need for a DC-DC buck converter that offers exceptional power conversion efficiency, accurately tailors its output to meet LED lighting needs, and reduces both energy waste and operational costs.

The aim of this article is to demonstrate that the designed DC-DC step-down converter, can efficiently lower the cost of LED lighting, conserve energy, minimize energy wastage, and achieve optimal lighting by using less input electrical energy. It presents an overview of existing literature on DC-DC converters, LED drivers, and energy efficiency to provide relevant context. The study also critically evaluates the limitations of current solutions and highlights the advantages of specific circuit components, such as the astable 555 timer IC and LC filter. Furthermore, it explores the theoretical benefits of this approach in terms of efficiency, cost reduction, and environmental impact. The primary objective of this paper is to showcase the significant progress made in developing sustainable and efficient LED lighting through the innovative DC-DC buck converter, which offers a compelling solution for those who prioritize environmental sustainability and cost-effectiveness.

2.0 EXPERIMENTAL

2.1 Literature review

Electrical energy efficiency is the ability to use less electrical energy to achieve the same desired outcome [01]. It refers to the amount of light produced for a specific quantity of electrical energy consumed in the context of lighting. LEDs are considered highly efficient light sources since they convert more than 80% of the input electricity into light, as opposed to traditional incandescent and fluorescent bulbs, which only convert 10%-25%.

Electrical energy efficiency is important for causes other than energy conservation and environmental benefits. By consuming less energy, LED lighting systems translate into lower electricity bills for individuals and businesses, [02] which contributes to financial savings. In addition, illuminated spaces enable improved awareness and a more comfortable and productive work environment, which improves overall quality of life.

Electrical energy efficiency can have an important effect on electricity costs. Replacing incandescent or fluorescent bulbs with LEDs may reduce energy consumption by up to 80%, [02] resulting in significant savings on utility bills.

DC-DC converters are critical in optimizing the electrical efficiency of LED lighting systems. By converting the available DC voltage to the specific voltage required by LEDs, DC-DC converters ensure that LEDs operate at their peak efficiency, maximizing light output while minimizing energy consumption. Efficient DC-DC converters reduce energy losses during the voltage conversion process, enhancing the overall efficiency of the lighting system.

2.2 System implementation

The experiment aimed to test the efficiency of four DC-DC converters. These converters were named an XL6009 boost, an LM2596 buck, an LM317 linear, and a customized buck with a 555 timer and LC filter. The testing process involved connecting the converters to a calibrated power source and an LED array. To measure the emitted light accurately, a custom-made five-sided cubic box with five LDRs attached to each side was utilized. An Arduino Uno was used to convert the readings to lux values. The input power was monitored carefully by measuring the input current and input voltage at specific connection points of each converter using a multimeter. A controlled LED current or PWM adjustments was used to maintain a constant light output. This meticulous setup was designed to identify the most efficient converter and ultimately reveal the top performer in terms of power optimization.

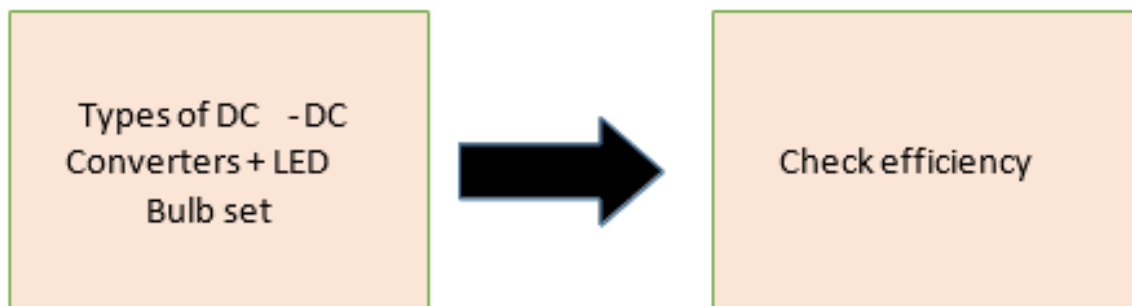


Figure 2.1: Block Diagram of the System

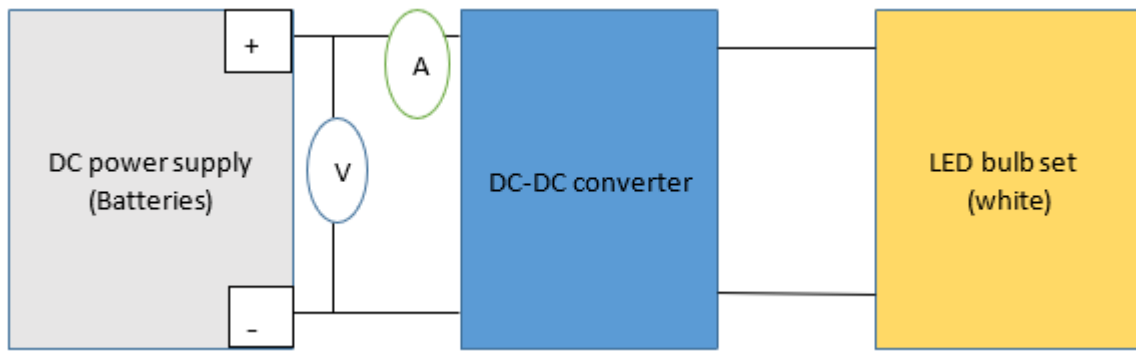


Figure 2.2: Block circuit diagram for investigation efficiency of DC-DC converters

2.3 Input power measuring method

In this study, a digital multimeter was used to precisely measure the input power (P_{in}) of each DC-DC converter by identifying and measuring specific voltage points for each converter. Then, by inserting the multimeter in series with the input line, able to determine the current flow with great accuracy. By applying the formula $P_{in} = V_{in} \times I_{in}$, where V_{in} is the measured input voltage and I_{in} is the measured input current, able to determine the energy consumption of each converter. This quantitative data allowed for a thorough comparison of their efficiency.

2.4 Output power measuring method

To accurately measure the effectiveness of each converter's light emission, a five-sided cubic box fitted with five LDRs in parallel. These LDRs capture the intensity of the emitted light in lux units. By taking the voltage readings from the LDRs and inputting them into an Arduino Uno, able to use custom code to convert the readings into real-time lux values. This gives us a comprehensive quantification of the light output from each converter. To ensure fair comparisons, employ a method of maintaining a consistent light level for each converter. This could involve adjusting the LED current or PWM duty cycle. By implementing this method, achieved a clear and accurate understanding of the output power of each converter.

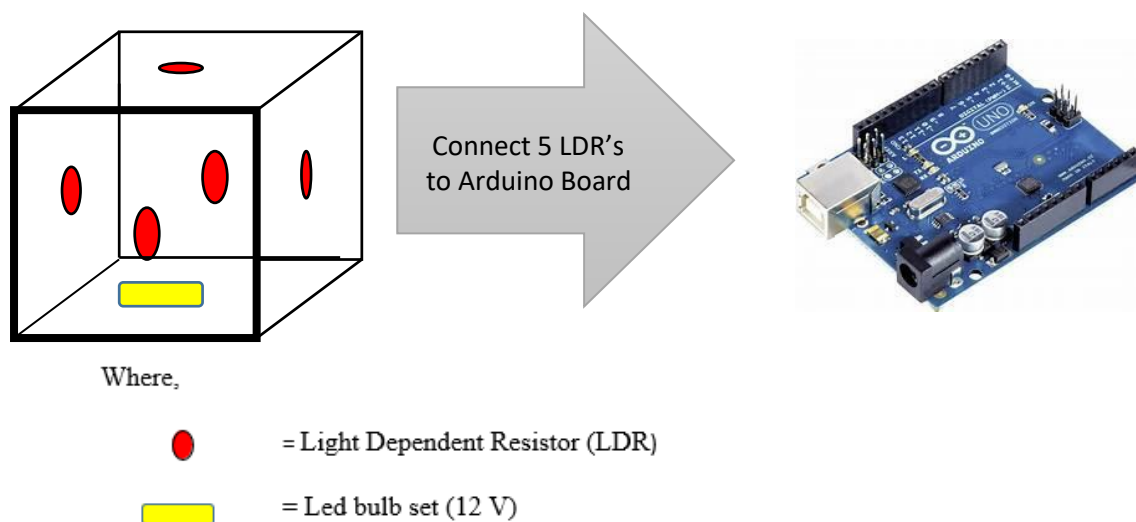


Figure 2.3: Block diagram of Light level measuring system using Arduino and LDR

3.0 RESULTS AND DISCUSSION

3.1 Parameters of designed dc-dc converter

3.1.1 Switching frequency

Table 4.1 Designed converter selected components values

Components	Value
Resistor(R1)	1KΩ
Resistor(R2)	10KΩ
Capacitor(C1)	0.01uF

$$f = \frac{1.4}{(R1 + 2(R2)) * C1}$$

$$f = \frac{1.4}{(1 * 10^3 + 2(10 * 10^3)) * 0.01 * 10^{-6}}$$

$$f = 6.8\text{KHz} \quad [03]$$

3.1.2 Cut-off frequency

The system interaction between the inductor and capacitor is the core of the LC filter. The inductor charges when the MOSFET conducts, storing energy much like the tiny electromagnet. The diode acts when the switch switches, directing the current from the inductor via the capacitor. The pulsing current is slowed down and smoothed down into a constant flow for the load by this shared movement. In between, the desired step-down conversion is accomplished because of the inductor's resistance to the input voltage during its charge period, which effectively decreases the total voltage seen by the load. The LC filter executes the enchanted operation of the buck converter, converting a pulse input into a smooth, regulated DC output in a perfect sequence of energy storage, filtering, and voltage shaping.

Table 4.2 Designed converter selected components values of LC filter

Component	Values
Capacitor 1	100 μF
Capacitor 2	22 μF
Capacitor 3	4.7 μF
Inductor	203.5 μH

$$fc = \frac{1}{2\pi\sqrt{LC}}$$

$$fc = \frac{1}{2\pi\sqrt{(203.5 * 10^{-6} * 126.7 * 10^{-6})}}$$

$$fc \approx 1\text{KHz} \quad [04]$$

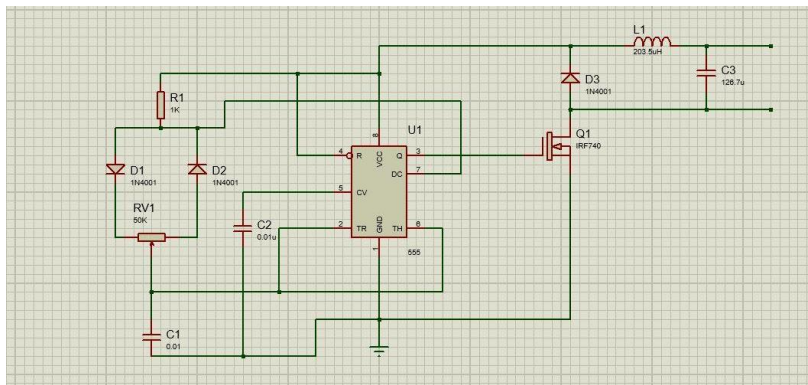


Figure 3.1: Schematic diagram of designed DC-DC buck converter

The 555-timer integrated circuit (IC) powers the designed buck converter in astable mode, producing a pulse width modulation (PWM) signal. A high-speed switch, an N-channel MOSFET, is driven by the timer's output. The MOSFET charges the inductor by connecting it to the input voltage when it conducts. The diode, however, prevents current from returning to the source. The inductor delivers its stored energy through an LC filter made up of a capacitor and itself while the MOSFET is not in use. This filter provides a step-down DC output to the load while eliminating voltage ripple. The PWM signal's duty cycle controls the inductor's charging period as well as the output voltage applied to the load. This design shown in figure 3.1 effectively leverages the switching action of the MOSFET and the energy storage capabilities of the inductor to achieve efficient step-down voltage conversion.

3.2 Measurements of market available dc-dc converters

3.2.1 XL6009 dc-dc boost converter module

Table 4.3 Measurements of XL6009 converter

Input voltage(V)	Input current(*10 ⁻³ A)	Input power(*10 ⁻⁴ W)	Light level in Lux unit
4	20	800	226
4.5	18	810	226
5	17	850	227
5.5	17	935	227
6	16	960	227
6.5	15	975	227
7	14	980	227
7.5	13	975	227

3.2.2 LM2596 dc-dc buck converter module

Table 4.4 Measurements of LM2596 converter

Input voltage(V)	Input current(*10 ⁻³ A)	Input power(*10 ⁻³ W)	Light level in Lux unit
20	13	260	227
19	13	247	227
18	13	234	227
17	14	238	226
16	14	224	226
15	15	225	226
14	15	210	225
13	16	208	225

3.2.3 LM317 voltage regulator circuit

Table 4.5 Measurements of LM317 voltage regulator

Input voltage(V)	Input current(*10 ⁻³ A)	Input power(*10 ⁻³ W)	Light level in Lux unit
20	10	200	226
19	10	190	226
18	10	180	226
17	9	153	226
16	9	144	225
15	9	135	225
14	9	126	224
13	9	117	224

3.2.4 Measurements of designed dc-dc converter

Table 4.6 Measurements of designed dc-dc buck converter

Input voltage of Timer IC (V)	Input current of Timer IC(*10 ⁻³ A)	Input voltage of LC filter (V)	Input current of LC filter(*10 ⁻³ A)	Input power(*10 ⁻⁵ W)	Light level in Lux unit
8	1.04	9	1.13	1849	236
8	1.04	10	1.16	1992	256
8	1.02	11	1.20	2136	271
8	1.02	12	1.28	2352	280
8	1.02	13	1.36	2584	293
8	1.02	14	1.47	2874	295
8	1.02	15	1.78	3486	311

3.3 Comparison of efficiency of dc-dc converter

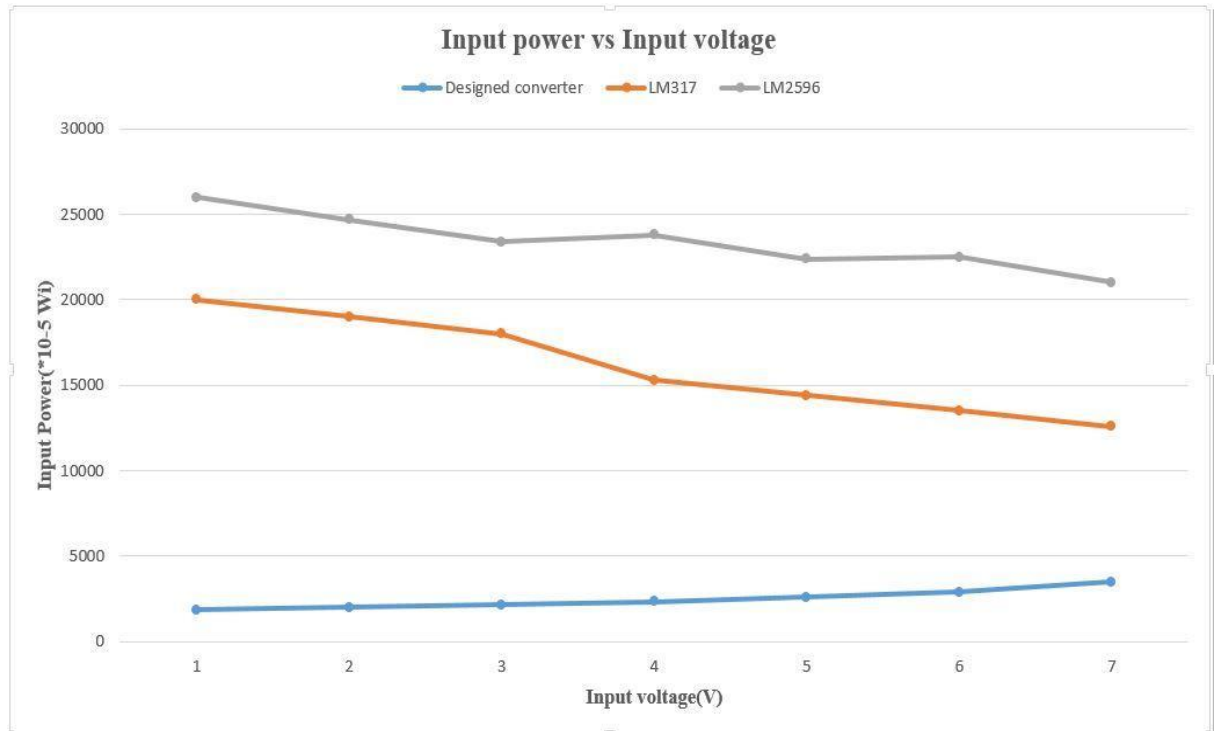


Figure 3.2: Input power VS Input voltage graphs of converters

When compared to the designed dc-dc buck converter and XL6009 dc-dc boost converter, the designed dc-dc buck converter consumes an input power of 0.03486 W for an input voltage 15 V, input current 1.78 mA, and XL6009 dc-dc boost converter consumes input power of 0.0975 W for input voltage 7.5 V, input current 13mA. Therefore, designed DC-DC buck converter is more efficient.

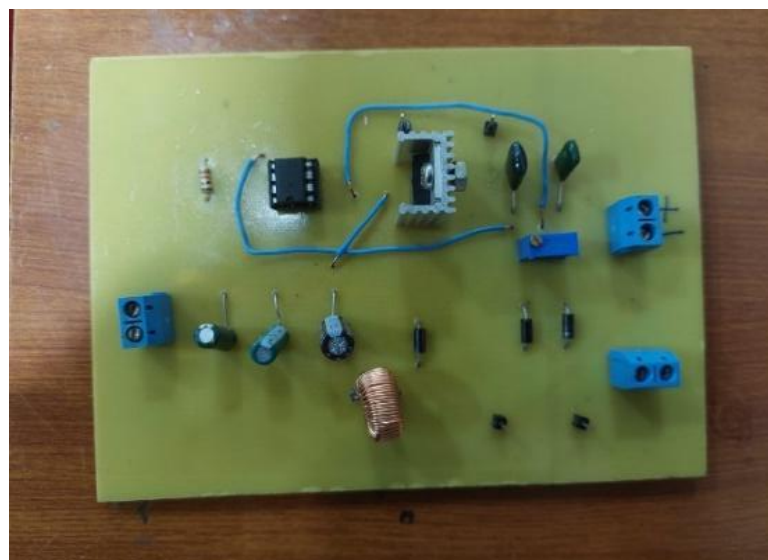


Figure 3.3: Designed dc-dc buck converter

4.0 CONCLUSION

In a highly competitive efficiency investigation, a designed DC-DC converter is the highest efficiency converter than commercial options of LM2596, XL6009, and LM317. This designed converter demonstrated high efficiency by using carefully selected components, precise circuit layout, and meticulous loss reduction techniques. As a result, it consumed less input power and delivered consistently stable light. Compared to other converters, the developed buck converter turned out to be the most effective in managing heat. The LM317 converter encountered difficulties because of linear conversion inefficiency, while the XL6009 boost converter overcame because of heat produced by its high switching frequencies and the LM2596 buck converter had difficulty because of internal resistance. However, because of the 555 timer's effective astable mode and precise component selection that reduced internal resistance and switching losses, the designed DC-DC buck converter was able to successfully regulate the heat. This resulted in a reduced temperature during operation, which may remove the requirement for large heat sinks and improve component life. This study demonstrates the vital importance of converter design in optimizing efficiency, which lays the foundation for energy conservation, cost-effectiveness, and a sustainable future.

ACKNOWLEDGEMENTS

The authors would like to express their gratitude to the academic and non-academic staff of Department of Electronics, Faculty of Applied Sciences, and Wayamba University of Sri Lanka.

REFERENCES

- [1] International Energy Agency (IEA). (2023). Energy efficiency. Retrieved from <https://www.iea.org/topics/energy-efficiency> (Access Date: 2023-12-14).
- [2] National Renewable Energy Laboratory (NREL). (2023). Benefits of LEDs. Retrieved from <https://www.energy.gov/energysaver/led-lighting> (Access Date: 2023-12-14)
- [3] <https://electronics.stackexchange.com/questions/101530/what-is-the-equation-for-the-555-timer-control-voltage> (Access Date: 2023-12-14)
- [4] <https://forum.allaboutcircuits.com/threads/cutoff-frequency-of-lc-filter.141206/> (Access Date: 2023-12-14)

IMAGE PROCESSING BASED MONKEY REPELLENT SYSTEM

M. K. Gunarathna*, M. A. A. Karunarathna

Department of Electronics, Wayamba University of Sri Lanka, Kuliypitiya, Sri Lanka

*manjulagunarathna500@gmail.com

ABSTRACT

This research project offers a new solution for monkey bites on telephone wires. In urban and rural areas, telephone connections often break down due to the monkey bites of these telephone wires, especially fiber telephone wires. While there are several solutions to prevent these attacks, accurately identifying monkeys approaching the telephone wires has been a challenge. In this project, an image processing method is employed to identify monkeys. It trained using a large number of data set. The data set should contain different images of monkeys from different sides for best accuracy.

The image processing model receives images captured by the camera, and it checks for similarity between the received images and those in the dataset. There is a threshold value in the model and it is 50%. This Python code gets 5 captures every 10 minutes and send to the image processing model. It creates a signal according to the result and it sends to output circuit. There is a buzzer and it activates for corresponding signal received from processing unit. The output circuit is very simple and occupies very small space. The buzzer uses only for laboratory demonstration, it should use a speaker to generate specific sound frequency. This project has the capability to identify monkeys and generate a frequency. Due to this technology, it can save energy and avoid unnecessary noise generation.

Key words: Image processing, Repellent system, Wire damage

1.0 INTRODUCTION

In the telecommunication field there are line connections and wireless connections. Lot of consumers use wireless telephone connections, but the most reliable and more speed connection is the wiring line telephone connection. Fiber telephone line is the best telecommunication method among other telephone lines. Wire telephone lines break down due to various reasons. Monkey bites on fiber wires are a common cause of damage to these wires.

There are few solutions to prevent these fiber telephone lines. But all of them are not effective. fiber wires are very sensitive and most efficient media. A light wave is the one of methods to transfer data in Fiber wire. Therefore, it is essential to keep it free from any minor damage. Any damage to the fiber core of the wire can lead to improper functionality, causing signal and power losses. This paper discusses the success of using image processing technology to identify monkeys and prevent Fiber telephone wires from them [01].

2.0 EXPERIMENTAL

2.1 Literature review of research

2.1.1 Monkey repellent frequencies

Monkey repellent frequency is a metric that measures the speed at which monkeys engage in leaps or jumps, offering insights into their mobility patterns, social dynamics, and adaptive strategies in their environment. This metric serves as a key indicator of monkey agility and evolutionary adaptations, crucial for understanding how they navigate complex ecosystems. Researchers analyze repellent frequency to infer behavioral traits and responses to environmental challenges, contributing to wildlife conservation efforts by informing habitat preservation strategies.[01]

2.1.2 Identifying an animal correctly by using image processing

Visual animal identification through image processing uses computational techniques to recognize and categorize species by extracting unique visual features from images or videos. Algorithms, like pattern recognition and feature extraction, automate the process, translating characteristics such as fur patterns into data for classification. Cutting-edge computer vision and machine learning technologies contribute to robust algorithms for efficiently processing wildlife image datasets, enhancing accuracy and enabling rapid analysis. Visual identification through image processing is advantageous for non-intrusive observation, facilitating the study of animals in their natural habitats. Integrating image processing in animal identification advances ecological studies, biodiversity conservation, and sustainable ecosystem management [02].

2.2 Block diagram of the design

Figure 2.1 Shows the block diagram of the developed system.

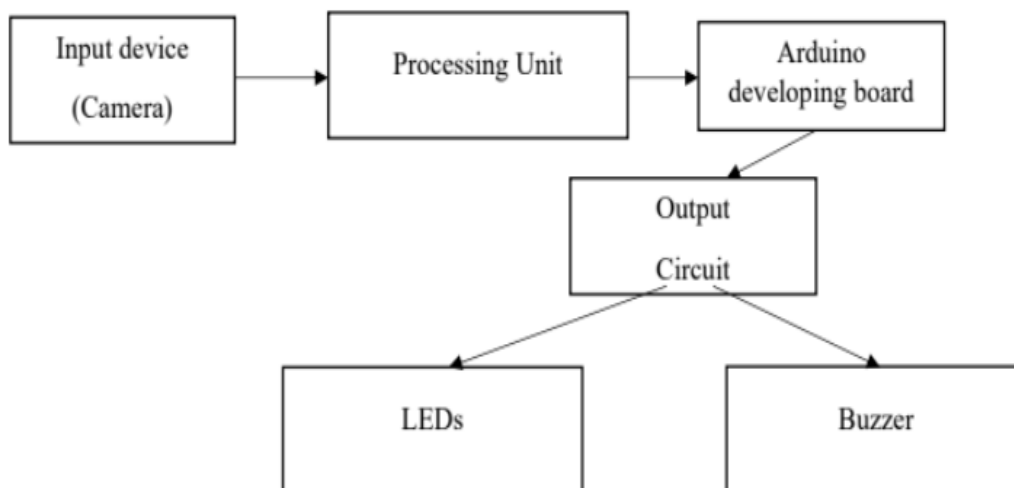


Figure 2.1 Block diagram of system

A camera works as an input device and it sends captured images to the processing unit. The processing unit checks similarities of captured image and images in data set. There is a 50% threshold value and it helps to identify a monkey near the device. This processing unit generates two signal each to identify a monkey and not identify a monkey. The signals pass from the

processing unit to the output through the Arduino development board and into the output circuit. This output circuit is equipped with LEDs and a buzzer. The signal indicating the identification of a monkey is directed to the buzzer via the output circuit. Conversely, a signal confirming the absence of a monkey is routed solely to the LED through the output circuit.

2.3 Image processing model

The image processing model was developed using python language and it uses TensorFlow to deep learning method. Image processing models should be trained by data set before it applies to the system. If the data set is containing large number of data, the output decision is reliable and it has best accuracy. Googlecolaps is the flatform that uses to train the image processing model using data set. This image processing unit wants a processing device to process its processing part [03].

2.3.1 Data set of trained to Image processing model

The dataset used to train the image processing model should contain a large amount of data. The data exists as images, which I used for the dataset. If this model is applied to the field, it should capture real images of monkeys in different situations to achieve the best accuracy [04].

2.3.2 Task of Arduino development board

The CPU works as a processing unit at the laboratory testing. Therefore, connecting directly to the CPU (computer) is challenging because the image processing model operates in Python, while the output circuit functions using power electronics methods. The Arduino development board is used to overcome this problem. The image processing model connects to the Arduino development board via serial communication. There is no any processing part on the Arduino development board. It works as the only communication component. It sends the corresponding signal to the output circuit according to the received signal from processing unit [05].

3.0 RESULT AND DISCUSSION

3.1 Results

The project has a web camera, processing unit(computer), Arduino developing board and output circuit with LEDs and buzzer. It is shown in figure 3.1. At the testing level, it shows an image that is not of a monkey. It identifies that there is no monkey and generates a signal. This signal is sent to the output circuit via the Arduino development board, and it powers up only an LED [06].

It shows an image of a monkey. It identifies that there is a monkey and generates another signal. This signal is also sent to the output circuit via the same Arduino development board, and it activates the buzzer. This is the overall result of the designed system.

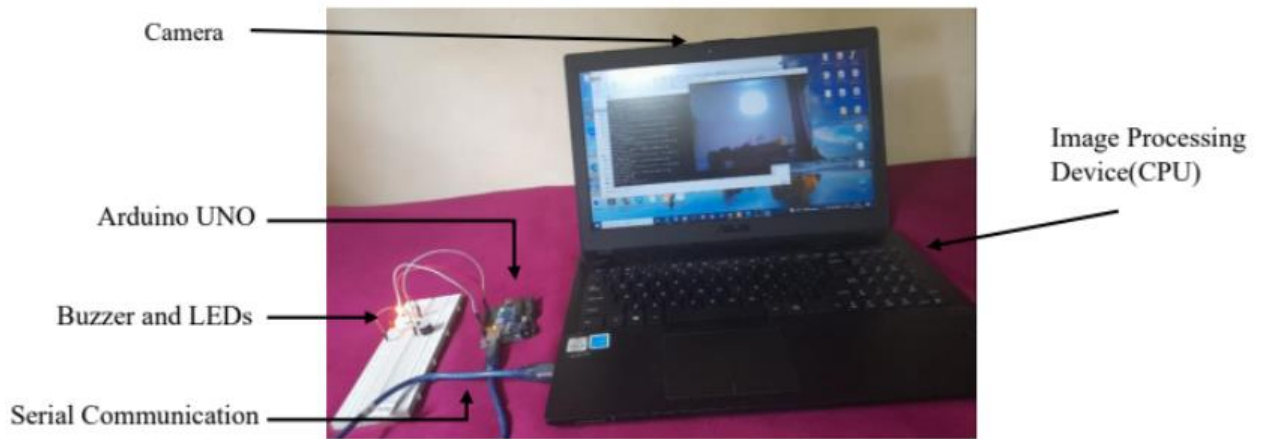


Figure 3.1: Entire system

Figure 3.2 shows state of not monkey detects by camera. This function is not essential for the process of this system; therefore, it can be removed from the system. However, there is a use for the system; we can check whether the system is working properly. If this function is not available in the system, we cannot identify the system's operation when the monkey is not near the camera [07].

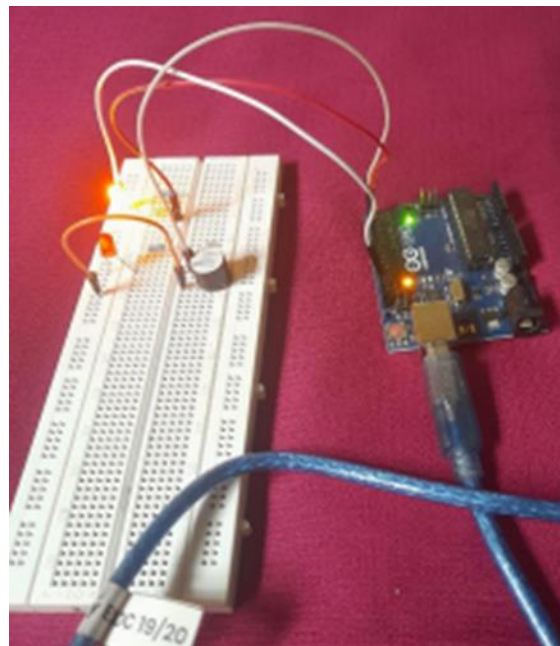


Figure 3.2: State of not monkey detects by camera

3.2 Discussion

Python is the main programming language that is used to implement this system. There is a threshold value for identifying a monkey from captured images. It is initially added as 50%. It can change this threshold value according to users' requirements. If it increases this value, it gives best accuracy from image processing side. However, it may ignore an image of a monkey when the threshold value in high level.

If it decreases this threshold value, the system may identify more images as monkey images. This can help avoid all monkey bites, but it may be an energy-wasting method. Therefore, it should select the best threshold value based on field testing results [08].

The system captures 5 images every 10 minutes using the camera. It can adjust this value to obtain the best results from the image processing side.

4.0 CONCLUSION

This research project aims to reduce the energy waste of current systems and prevent the generation of unnecessary frequencies in the environment. The equipment can be used in the Telecommunication wireline connection maintenance section. This project has been implemented and tested only in the laboratory. If applied in the field, it should be installed on a processing board. This system cannot be applied to a development board.

ACKNOWLEDGEMENTS

The authors would like to express their appreciation to the staff of the Department of Electronics at the Faculty of Applied Sciences, Wayamba University of Sri Lanka.

REFERENCES

- [1] “Deep Learning Innovations for Enhanced Drusen Detection in Retinal Images,” *International journal of performability engineering*, vol. 19, no. 12, pp. 779– 779, Jan. 2023, doi: <https://doi.org/10.23940/ijpe.23.12.p2.779787>.
- [2] T. A. Ortega, H. M. Pask, D. J. Spence, and A. J. Lee, “Stimulated Polariton scattering in an intracavity rbtipo₄ crystal generating frequency-tunable thz output,” *Optics Express*, vol. 24, no. 10, (2016),p. 10254 doi:10.1364/oe.24.010254
- [3] J. L. Kennah *et al.*, “Coat colour mismatch improves survival of a keystone boreal herbivore: Energetic advantages exceed lost camouflage,” *Ecology*, vol. 104, (2022),no. 2 doi:10.1002/ecy.3882
- [4] L. Wen, L. Wang, W. Li, Eirikur Agustsson, and Luc Van Gool, “WebVision Database: Visual Learning and Understanding from Web Data,” *arXiv (Cornell University)*, Aug. 2017,doi: <https://doi.org/10.48550/arxiv.1708.02862>, https://docs.opencv.org/4.x/d2/d96/tutorial_py_table_of_contents_imgproc.html (10/11/2023)
- [5] AlMadhoun, A.S.A. (2023). Arduino Serial Monitor. In: Circuit Design and Simulation Quick Start Guide. Maker Innovations Series. Apress, Berkeley, CA.https://doi.org/10.1007/978-1-4842-9582-3_10
- [6] <https://www.simplilearn.com/tutorials/deep-learning-tutorial/what-is-tensorflow#:~:text=TensorFlow%20is%20an%20open%2Dsource,keeping%20deep%20learning%20in%20mind.> (20/10/2023)
- [7] L. Wen, L. Wang, W. Li, Eirikur Agustsson, and Luc Van Gool, “WebVision Database:

Visual Learning and Understanding from Web Data,” *arXiv (Cornell University)*, Aug. 2017, doi: <https://doi.org/10.48550/arxiv.1708.02862>.

- [8] AlMadhoun, A.S.A. (2023). Arduino Serial Monitor. In: *Circuit Design and Simulation Quick Start Guide*. Maker Innovations Series. Apress, Berkeley, CA. https://doi.org/10.1007/978-1-4842-9582-3_10

A BATTERY ANALYZER FOR A VEHICLE ELECTRICAL SYSTEM DIAGNOSTIC TOOL

J.K.A.T.R. Jayasuriya*, L.D.R.D. Perera

Department of Electronics, Wayamba University of Sri Lanka, Kuliypitiya, Sri Lanka

*thrishul.jayasuriya20@gmail.com

ABSTRACT

This research project introduces a smart Lead-Acid Battery Analyzer to be integrated into a comprehensive Vehicle Electrical System Diagnostic Tool, presenting an overall solution for evaluating the performance of automotive electrical systems. Focused on the wide use of lead-acid batteries in vehicles, the system employs a PIC microcontroller to analyze key battery parameters, including voltage and state of charge (SOC). The functionalities of the designed analyzer can be extended to identify and troubleshoot broader electrical issues within the vehicle, covering critical components. The real-time data monitoring and the user-friendly interface will provide automotive technicians with valuable information for efficient and accurate diagnosis while minimizing disruptions to the vehicle's electrical system. Key features of the designed system include measurement of open terminal voltage of a battery and the voltage under load, cranking voltage and SOC, and testing vehicle electrical charging system. The user-friendly interface presents diagnostic results in an easily interpretable manner. The designed battery analyzer with its extended functions will be a comprehensive tool for vehicle electrical systems diagnosis.

Keywords: Lead-acid battery, Battery analyzer, Vehicle electrical system

1.0 INTRODUCTION

The vehicle's battery is pivotal, providing initial power for engine cranking, acting as an essential power source for the electrical system, and ensuring voltage stability. It serves as a backup during alternator failure, crucial for the Electronic Control Module (ECM), emergency lighting, and cold weather starts. Regular maintenance, including voltage checks and corrosion inspections, is vital for longevity [1, 2]. The electrical battery charging system, centered around the battery, is crucial for continuous power supply. The alternator, voltage regulator, and a network of components ensure reliable electricity generation, distribution, and safety. Regular maintenance and inspection of these elements are imperative for sustained, efficient operation, with any issues requiring prompt attention by qualified mechanics.

Low vehicle battery health can lead to performance issues, impacting reliability and functionality. Warning signs include difficulties starting the engine, frequent jump-starts, diminished cranking power in cold weather, and reduced power for electrical systems. Dashboard lights, like the check engine light, may signal deteriorating health. Unreliable accessory performance and corroded terminals are additional indicators. Persistent low health shortens the battery lifespan and affects the charging system, potentially increasing fuel consumption. Addressing these issues promptly is crucial for optimal vehicle performance and preventing disruptions from a deteriorating battery.

The literature on lead-acid battery analyzers and vehicle electrical system diagnostic tools underscores the critical role these technologies play in automotive maintenance [3]. Lead-acid batteries are pervasive in vehicles, demanding precise analysis for optimal performance [4]. Studies emphasize the importance of accurate battery diagnostics, citing the pivotal role of batteries in initiating engine start, stabilizing voltage, and serving as a power source during non-operational periods. Existing literature underscores the impact of battery health on the broader vehicle electrical system, including alternators, starters, and electronic control modules (ECMs), highlighting the need for comprehensive diagnostic tools [3].

Furthermore, researchers stress the significance of non-intrusive testing methods, minimizing disruption during analysis [5]. The integration of advanced algorithms for real-time monitoring and user-friendly interfaces is a common theme, acknowledging their crucial role in facilitating efficient diagnostics [6]. The literature emphasizes the interconnectedness of the lead-acid battery with the vehicle's charging system, emphasizing the role of alternators, voltage regulators, and associated components. Overall, the existing literature underscores the need for sophisticated lead-acid battery analyzers integrated with comprehensive diagnostics tools to ensure the reliability and longevity of automotive electrical systems [4].

Features of the designed system include testing of lead-acid battery health, state of charge and checking vehicle electrical charging system. This system offers quick and accurate assessments aiding in preventive maintenance. It will enhance vehicle battery life, reduce breakdowns, and ensures optimal vehicle performance.

2.0 EXPERIMENTAL

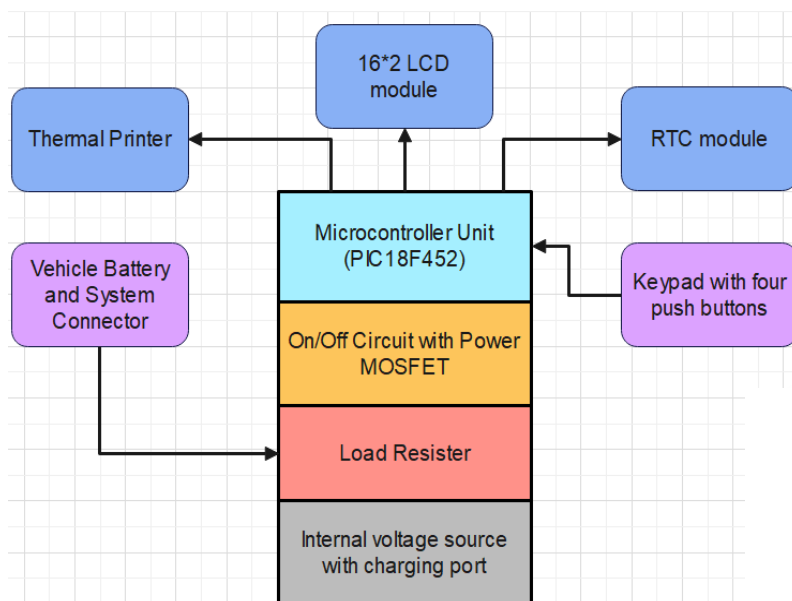


Figure 2.1 Block diagram of the system

The microcontroller unit, on/off circuit, load resistor and internal voltage source are included in main circuit board. The LCD, keypad, RTC module, and thermal printer connected to microcontroller. Battery and system connector is connected to load resistor.

2.1 System Components and Tools

The **PIC18F452 microcontroller** is an 8-bit, CMPS, FLASH-based device with 10 MIPS and 34 I/O pins out of a 40-pin package [7]. With one 8-bit, three 16-bit, an 8-channel, 10-bit analog-digital converter, and I2C, SPI, and USBART peripherals, it's a potent microcontroller. This PIC microcontroller is low power, using less than 0.2 μA for standby and 1.6 mA for regular operation at 5 V and 4 Mhz. This microcontroller was used for main controlling unit of the system.

LCD, or liquid crystal display, is an electronic module widely employed in devices such as phones and computers. Cost-effective and programmable, it supports diverse applications, offering flexibility for custom characters and animations. This display is used for displaying outputs of the system.

A **thermal printer**, commonly known as a receipt printer, finds extensive use in locations like restaurants, ATMs, and shops for generating receipts or bills. Cost-effective and user-friendly, it employs a unique thermochromic printing process on thermal paper, where the printer head's heat causes the paper coating to turn black. The TTL connector facilitates Rx/ Tx communication with the microcontroller, and RS232 can also be employed for printer communication. The power connector powers the printer, and a self-test button enables easy testing. Communication is straightforward through UART, allowing printing of ASCII characters with ease. This system generates a battery and system test report using the thermal printer.

The **DS1302 real-time clock module** is an affordable and accurate solution for various projects, offering information on seconds, minutes, hours, day, date, month, and year. It automatically adjusts the date considering month length and leap years. This module is used to get the real time and date to include in the test reports.

The IRF1010E is an n-channel **power MOSFET** designed for rapid switching applications [8]. It features three terminals - drain, source, and gate. Unlike bipolar junction transistors, it's voltage-controlled, with the gate terminal regulating channel width. The MOSFET manages voltage and current between source and drain, offering high efficiency in low drop switching applications due to its low turn ON resistance This MOSFET is used for switching the load resistor.

MPLAB® X IDE is a cross-platform software for developing applications for Microchip PIC® microcontrollers and dsPIC® digital signal controllers. With a range of features, it facilitates application development and debugging, aiming to simplify and enhance the user's development activities. The CCS C compiler is used as a compiler with MPLAB X IDE. The PIC18F452 microcontroller was programmed using the MPLAB X IDE.

Proteus8 is a versatile software tool for electronic circuit design and simulation. It includes ISIS for schematic capture and simulation, and ARES for PCB layout. With a rich component library, real-time simulation, and user-friendly interface, Proteus supports circuit design and education. The schematic diagram is designed using the Proteus8 software.

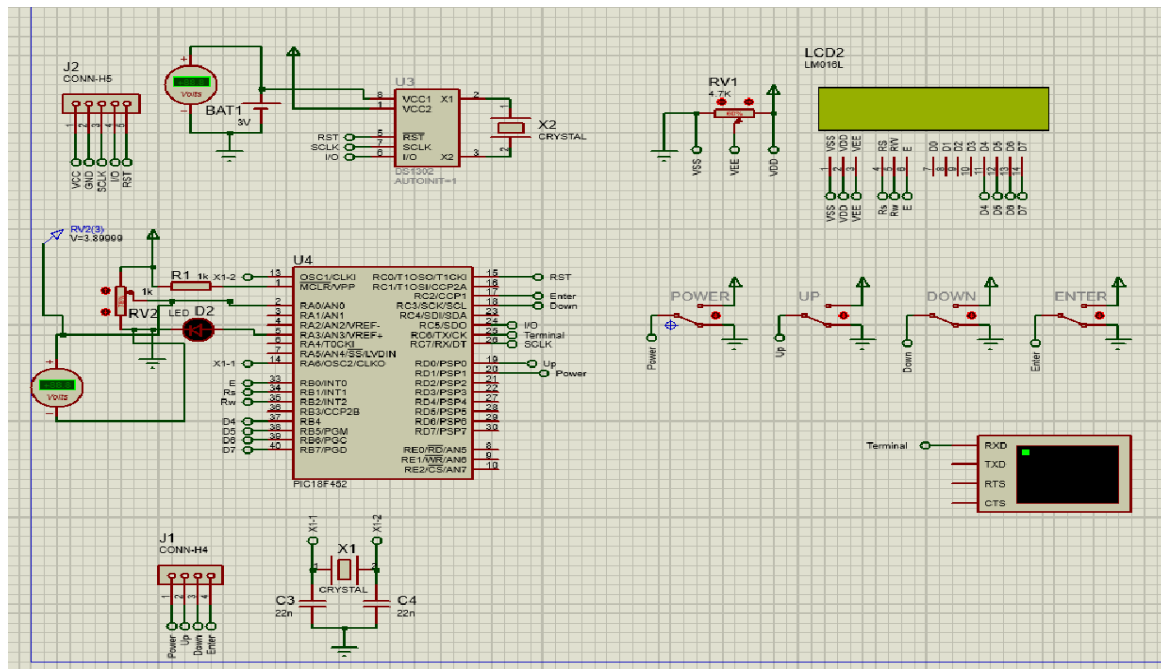


Figure 2.2 Schematic diagram of the designed system

Figure 2.2 illustrates the schematic diagram of the system designed with a PIC18F452 microcontroller, a 16*2 LCD for battery parameters, real-time clock for date/time, and a thermal printer for test reports. Four input switches (Up, Down, Enter, Power) manage the system, while an internal battery powers it during dead battery testing.

The open-circuit voltage (OCV) of a battery, also known as electromotive force (EMF), is its voltage without a load resistor, representing its maximum theoretical output. To measure OCV, a high-impedance voltmeter is used, ensuring negligible current draw. However, in practical scenarios with load resistors, the actual voltage may decrease due to internal resistance and other factors. The open-circuit voltage serves as a theoretical reference for understanding a battery's potential, though the actual voltage under load conditions may be lower, subject to dynamic factors like chemical reactions, temperature variations, and the state of charge.

When a load resistor is introduced, the voltage across the battery depends on factors like internal resistance and current flow. Ohm's Law, expressing $V = I \times R$, is employed. For a battery with internal resistance (r) and load resistor (R_L), total resistance (R_{total}) is the sum of internal resistance and load resistor ($R_{total} = r + R_L$). Current (I) flowing through the circuit is calculated using $I = V_{battery} / R_{total}$, where $V_{battery}$ is the battery's electromotive force (EMF). The voltage across the load resistor (V_{load}) is determined by $V_{load} = I \cdot R_L$. It's crucial to note that as current increases, the voltage drop across the internal resistance rises, impacting the overall voltage delivered to the load. Accuracy requires specific battery details, including EMF, internal resistance, and load resistor value.

2.3 Selection of Battery Type and Ampere Hour

In the battery analysis system, two primary battery types exist: maintenance-free, which is sealed and cannot be refilled, and conventional, which allows acid refilling. The user can select the suitable ampere hour (Ah) rating for the battery, ranging from 2.5Ah to 35Ah, using the

battery analyzer's up and down keys. The ampere hour, indicated on the battery label, helps in assessing battery health before the actual testing process.

2.3 Displaying Battery Health Status and State of Charge (SOC) Value

The system categorizes battery health into five statuses: GOOD & PASS, GOOD & RECHARGE, RECHARGE & RETEST, BAD & REPLACE, and BAD CELL & REPLACE. The 5W 0.33 ohm resistor was used for the load. Each status was determined based on voltage readings with and without load resistance. The State of Charge (SOC) value is then calculated, with percentages reflecting battery charge levels. The system considers voltage thresholds to determine SOC, ranging from 100% for a voltage greater than or equal to 12.76 V for 12 V battery to 0% for a voltage between 0 V and 10.52 V (Table 3.1). The battery health status and SOC values are subsequently transmitted to a thermal printer via RS232 protocol, enabling report generation for comprehensive analysis. The user can decide to print or skip generating a report for each battery, allowing efficient processing of multiple batteries. Additionally, the system tests vehicle electrical systems, distinguishing between self-start and kick-start engines, evaluating cranking volts during engine start, and assessing charging system performance both at idle and under load. Report generation concludes the analysis, providing a detailed record of each battery's health and electrical system performance.

3.0 RESULTS AND DISCUSSION

Figure 3.1 shows the designed prototype of the battery analyzer and Table 3.1 presents the open-circuit voltages and the load test voltages for a 9 Ah and 5 Ah lead-acid batteries.

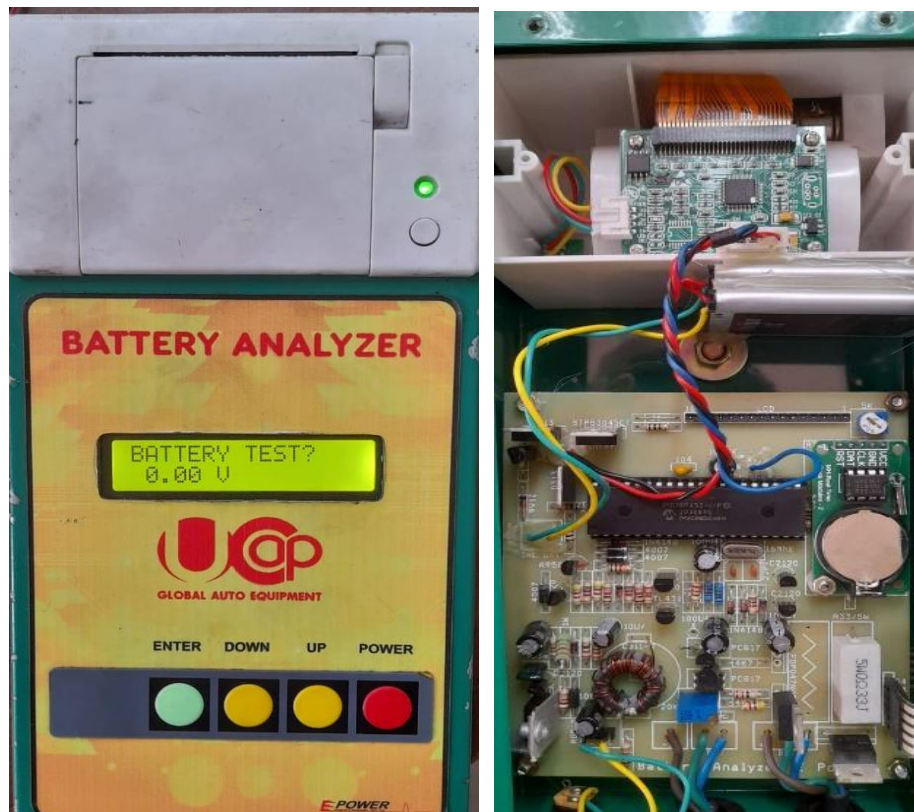


Figure 3.1 Prototype of the system

Table 3.1 Tested values for 9Ah and 5Ah batteries

Open Terminal Voltage	12ms Load test voltage	State of Charge	Open Terminal Voltage	12ms Load test voltage	State of Charge
9Ah	9Ah		5Ah	5Ah	
13.00V	12.49V	100%	12.79V	12.05V	100%
12.74V	12.19V	100%	12.76V	12.04V	100%
12.67V	12.10V	100-75%	12.66V	11.90V	100-75%
12.60V	12.04V	100-75%	12.55V	11.79V	100-75%
12.56V	11.94V	100-75%	12.38V	11.57V	50-75%
12.53V	11.84V	100-75%	12.26V	11.38V	50-75%
12.42V	11.76V	50-75%	12.10V	11.13V	50-75%
12.35V	11.65V	50-75%	11.88V	10.80V	50-25%
12.28V	11.55V	50-75%	11.69V	10.32V	50-25%
12.18V	11.40V	50-75%	11.50V	9.66V	50-25%
12.10V	11.26V	50-75%	10.59V	7.71V	0%-25%
12.03V	11.13V	50-75%			
11.95V	10.94V	50-25%			
11.86V	10.72V	50-25%			
11.75V	10.44V	50-25%			
11.64V	10.11V	50-25%			
11.52V	9.74V	50-25%			
10.76V	8.44V	0%-25%			

Results provide information for determining charging system status and potential issues, so that required maintenance or replacements could be carried out for dependable vehicle operation and preventing unexpected breakdowns.

0.4 CONCLUSION

In conclusion, the research on "Lead-Acid Battery Analyzer to be integrated in to a Vehicle Electrical Diagnostics Tool" underscores the significance of efficient battery analysis and electrical system diagnostics in the automotive context. The developed tool integrates features such as open-circuit voltage measurement, ampere-hour selection, and battery health assessment. This system can also measure the state of charge of the battery and cranking voltage of the battery. The functions of the system can be readily extended to analyze vehicle electrical system, including charging voltage and system performance under load. The generated analysis report on battery health would help identify issues in the battery, vehicle charging system and in the vehicle electrical system.

The system's ability to categorize battery health status and generate comprehensive reports facilitates decision-making by users, allowing them to take measures to maintain or replace batteries as required. The inclusion of a thermal printer for report generation enhances the tool's practicality and utility. The designed analyzer is low-cost, portable and user-friendly. This battery analyzer can be integrate into a vehicle diagnostics system to make it a valuable tool

for automotive technicians, offering a comprehensive solution for optimizing battery performance and ensuring reliable operation of vehicle electrical systems.

ACKNOWLEDGEMENTS

The authors would like to express their sincere gratitude to everyone who helped carry out this project successfully.

REFERENCES

- [1] D. Linden, Handbook of Batteries. (1995) *New York: McGraw-Hill*.
- [2] A history of the Battery, The BatteryGuy.com Knowledge Base,[online]. (2020).Available at: <https://batteryguy.com/kb/knowledge-base/a-history-of-the-battery>.
- [3] Jitendra B. Zalke, Zulqarnain J. Sabir and Amol B. Chavan, Design and Development of a Low-cost Battery Analyzer, *Int. J. for Research and Development in Technology*, ISSN(O) 2349-3585, pp. 345-350.
- [4] J. Bil'anský, Overview of the Battery Types and their Testing. (2020), *SCYR - Nonconference Proceedings of Young Researchers*. Košice, pp. 143-146.
- [5] A. Kawamura and T. Yanagihara, State of charge Estimation of sealed lead-acid batteries used for electric vehicle, *IEEE PESC* (1998), pp. 583-587.
- [6] M. A. Casacca and Z. M. Salameh, Determination of lead-acid battery capacity via mathematical modeling techniques,(1992), *IEEE Trans. Energy Convers.*, vol. 7(3), pp. 442–446.
- [7] PIC18F452 8-bit PIC Microcontroller, components101, 2020, <https://components101.com/microcontrollers/pic18f452-8-bit-pic-microcontroller>.
- [8] IRF1010E– n-Channel Power MOSFET, 2018, <https://components101.com/mosfets/irf1010e-mosfet>.

IOT BASED HEAT DETECTOR FOR DISTRIBUTION TRANSFORMER

U.T. Nanayakkarawasam *, Y.A.A. Kumarayapa

Department of Electronics, Wayamba University of Sri Lanka, Kuliyapitiya, Sri Lanka

*nanayakkarawasam@gmail.com

ABSTRACT

The objective of this research was to develop and implement an internet of things (IoT)-based system designed to monitor and record the temperature of distribution transformers, issuing warnings when temperatures exceed predefined limits. Distribution transformers, integral to power distribution systems, undergo temperature-related challenges such as overloading, insufficient cooling, high ambient temperatures, short circuits in winding coils, lack of transformer oil, and faulty tap changer operations. These issues can lead to elevated temperatures, risking transformer damage and failure. The proposed online monitoring system integrated a global system for mobile communications (GSM) module, an Arduino board and a temperature sensor. This sensor was designed to measure ambient and object temperatures, with the data recorded on the Thingspeak server. In emergencies, the system sends short message service (SMS) messages to designated mobile phones, conveying information based on predefined instructions and policies stored in the Arduino code. Furthermore, the system transmits data to a central control room in the ceylon electricity board (CEB) via the general packet radio service (GPRS) module for comprehensive analysis. With their substantial iron cores and copper windings, transformers constitute one of the heaviest and most expensive components in an electrical distribution system, playing a pivotal role in voltage transformation and isolation. The IoT-based heat detector system presented in this research offers a reliable means to measure and manage transformer temperatures, mitigating the risks of destruction and failure. This mobile monitoring system significantly enhances utility operations by facilitating optimal transformer utilization and enabling the proactive identification of potential issues, ultimately preventing catastrophic failures in power distribution systems.

Keywords: Distribution transformer; Temperature monitoring, IoT, GRPS

1.0 INTRODUCTION

Transformers are widely used in electric power systems to perform primary functions, such as voltage transformation and isolation. Because of the bulky iron cores and heavy copper windings in the composition, transformers are one of the heaviest and most expensive parts of an electrical distribution system [1]. The main problems identified were transformer overheating and destruction pose a significant issue for the ceylon electricity board (CEB), resulting from transformers exceeding their design specifications. Overheating leads to insulation degradation, reduced transformer lifespan, efficiency loss, and potential safety hazards, necessitating effective monitoring and intervention strategies. The research question of this experiment was how can an IoT-based temperature detection system improve safety, prevent overheating, and optimize distribution transformer performance.

A 2018 study has used IOT for thermal monitoring and protection of distribution transformers. In case of abnormal temperature rise, the system triggers alerts and protective measures (use thermal and humidity sensing unit) [2]. Two scholars in a 2019 study introduced an IoT-based

monitoring system specifically designed for oil-immersed transformers [3]. The authors employed IoT technology to remotely monitor parameters such as oil temperature, pressure, and gas concentration.

2.0 EXPERIMENTAL

2.1 Methodology

This Integrated MLX90614 temperature sensor, GSM module, and an Arduino Mega, enable wireless data transmission and real-time monitoring.

Implemented temperature measurement using the MLX90614 non-contact infrared temperature sensor, establishing I2C communication with the Arduino Uno board.

Temperature collected using the non-contact sensor is transferred via IoT to a central control unit (CEB), and the data is displayed on a dashboard. Continuous monitoring with timestamps and transformer location is enabled.

In case of temperature exceeding safe limits, triggered alarms and sent alerts to designated personnel.

In critical situations, automatically sent notifications to the fire brigade including the exact time and location information.

The following figure depicts the block diagram of the designed IoT-based heat detection system.

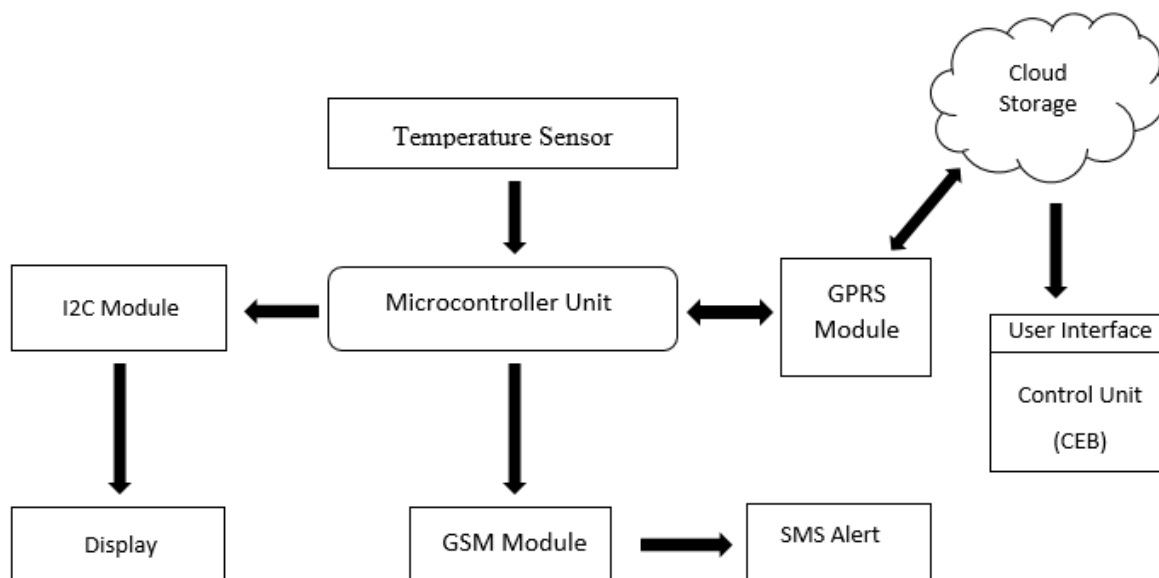


Figure 2.1: Block diagram of the IoT based heat detector (Source: Author compile)

The following figure depicts the hardware implementation of the device proposed in this study.

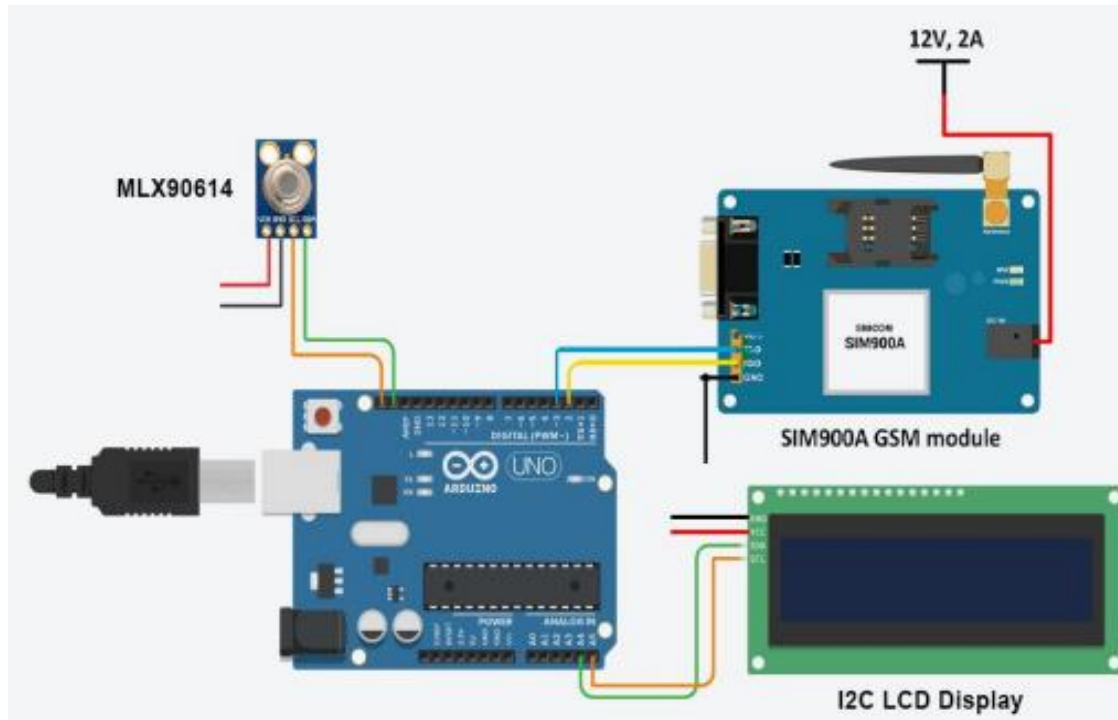


Figure 2.2: Hardware design of the system (Source: Author compile)

2.2. Software Functionality

Figure 2.3 depicts how our device connects with the web server. Read API and Write API enable the data transfer.

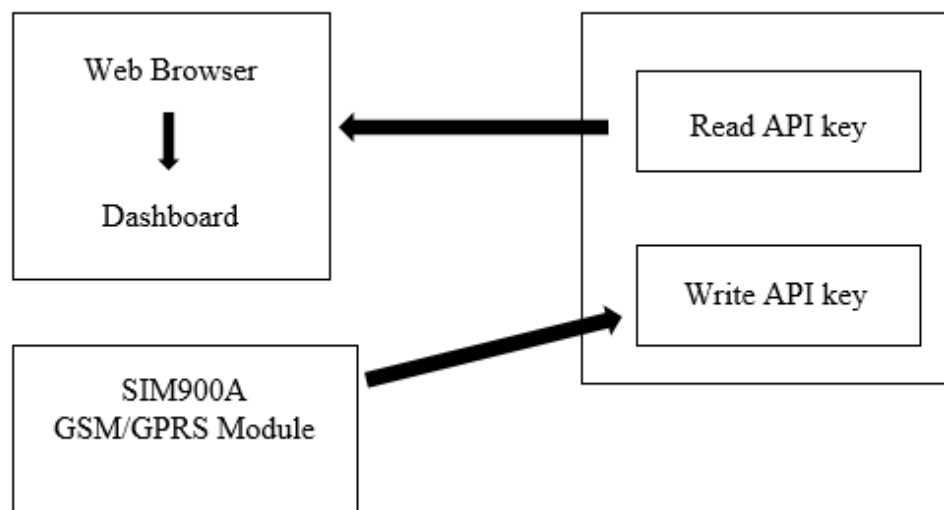


Figure 2.3: Software and network architecture (Source: Author compile)

2.2.1. Client

The client is the electricity board. Dashboards of the systems were viewed through web browsers on the client side. Also, Sim900A GPRS/GSM module acted as a client and it sent data to the server. Client-side web-based dashboards were implemented using HTML and CSS.

Three interfaces were designed and they are as follows.

- Main interface
- Distribution transformer table interface
- Transformer details dashboard

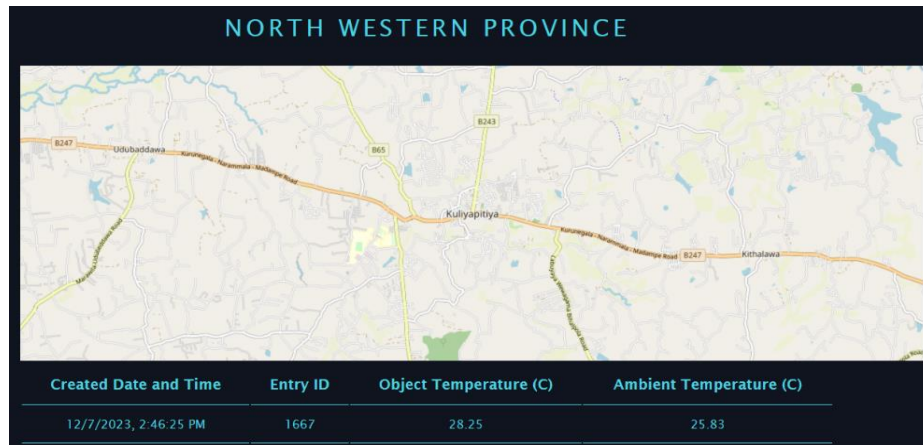


Figure 2.4: Transformer details dashboard (Source: Author compile)

3.0 RESULTS AND DISCUSSION

3.1 Design Overview

The primary objective of this system was to monitor the temperature of the distribution transformer and transmit real-time updates of ambient temperature and transformer temperature via GPRS. This system functions as a real-time monitoring solution.

Figure 3.1. shows the developed system in this research. This system contained two parts. One is the controlling part and the other one is the sensor part. The controlling part takes data from the sensor and displays temperatures on the LCD.



Figure 3.1: Final design of the system (Source: Author compile)

This system measured the temperature of the distribution transformer. The system was capable of performing two things. It displayed the temperature of the distribution transformer and the ambient temperature. The ambient temperature was displayed as it directly affects the temperature transformer. High ambient temperature leads to elevated temperatures within the transformer. Monitoring the ambient transformer helps to anticipate conditions that may lead to overheating and take necessary actions to mitigate those. Transformers need cooling to maintain operational efficiency.



Figure 3.2: Ambient temperature value displayed by the system



Figure 3.3: Object Temperature value displayed by the system

The MLX90614 sensor was a non-contact infrared temperature sensor. It uses IR rays to measure the temperature of the object without physical contact. Hence, it can be installed externally. It can be installed by adding a bracket to the side of the distribution transformer box. The proper placement of a heat detector on a transformer is usually near critical components such as winding or co-areas. The values were taken from the sensor and then transferred to the controlling system via a CAT6 cable. The CAT6 cable was connected to the sensor and the Arduino board.

The CAT6 cable was utilized in the system due to the higher bandwidth and faster data rates. The controlling unit must be placed in a way that there is some distance between the controlling unit and the transformer. Arduino boards and other electronic components may face issues when operating near transformers. This is due to electromagnetic interference (EMI) and electrical noise.

3.2 ThingSpeak Server

The graphs of ambient temperature and object temperature are updated on the IOT-based platform by using the Wi-Fi network-based ThingSpeak server. Two charts shown in Figure 3.4 illustrate how object temperature and ambient temperature change over time.

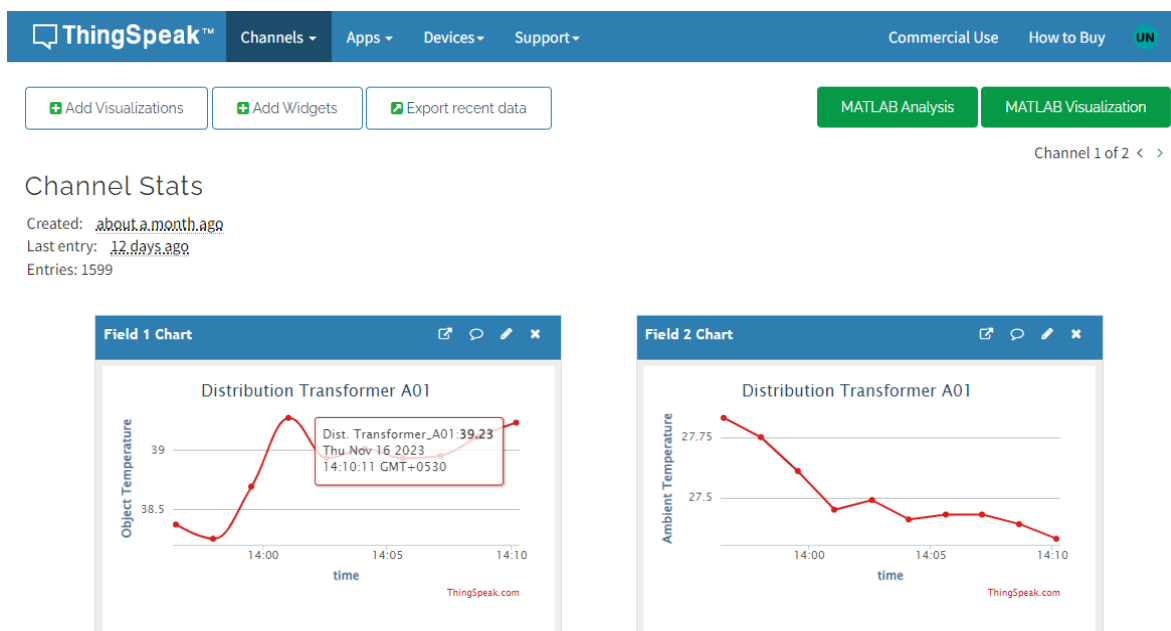


Figure 3.4: Real time updated data on the ThingSpeak server (Source: Author compile)

3.3 SMS Alert

When the temperature exceeds the threshold value system passes a message to the mentioned mobile number via the GSM module. The threshold value refers to the highest temperature that a transformer can reach. The threshold value of a transformer is determined by several factors such as transformer load conditions and transformer design. This value was manually set to the Arduino code. When the threshold value exceeds, a call and an SMS alert are sent to a phone number. The phone numbers were coded.

4.0 CONCLUSION

The Ceylon Electricity Board faces the problem of transformer overheating which leads to the destruction of transformers. The objective of this research was to identify temperature variations in the distribution transformer over 24 hours and develop a program for detecting instances of overheating status. This experiment developed an IoT-based heat detector for the distribution transformer. The device contains two main parts: a controlling unit and a sensor. The device was able to measure the temperature of the distribution transformer and pass that data to the cloud server. When the temperature of the transformer exceeded pre-set limits, SMS alerts and calls were sent to designated personnel. This helped to improve the safety of distribution transformers and take necessary measures to prevent harmful results of distribution transformer overheating. This research has successfully developed an IoT-based heat detector for a distribution transformer and the system provides real-time data on transformer

overheating. The developed system through this project was helpful to CEB to reduce their maintenance cost of transformers and they can prevent transformer explosions and burns.

ACKNOWLEDGEMENTS

Authors would like to thank all the staff of Department of Electronics, Faculty of Applied science, Wayamba University of Sri Lanka.

REFERENCES

- [1] Wang, D., Mao, C., Lu, J., Fan, S., & Peng, F. (2007). Theory and application of distribution electronic power transformer. *Electric power systems research*, 77(3-4), 219-226.
- [2] Jamal, H., Khan, M. F. N., Anjum, A., & Janjua, M. K. (2018). Thermal monitoring and protection for distribution transformer under residential loading using the internet of things. In *2018 IEEE global conference on the internet of things (GCIoT)* (pp. 1-6). IEEE.
- [3] YAMAN, O., & BİÇEN, Y. (2019). An Internet of Things (IoT) based monitoring system for oil-immersed transformers. *Balkan Journal of Electrical and Computer Engineering*, 7(3), 226-234.

IOT BASED BATTERY MANAGEMENT SYSTEM

A.A.P.P. Navoda^{1*}, W.A.S. Wijesinghe¹, and M.P.T.R. Wijebandara²

¹*Department of Electronics, Wayamba University of Sri Lanka, Kuliypitiya, Sri Lanka*

²*Communication Division of Arthur C Clarke Institute for Modern Technologies, Katubedda, Moratuwa, Sri Lanka.*

*pasindupavan617@gmail.com

ABSTRACT

The extensive use of battery-powered applications necessitates advanced Battery Management Systems (BMS) to address challenges like state of charge estimation inaccuracies, cell balancing difficulties, and thermal management complexities. This paper describes an Internet of Things (IoT)-based BMS tailored for the efficient management of a 3-cell battery configuration, with a focus on the intermediate charging stage. The project aims to transform battery management in charging circuits, particularly targeting the intermediate charging phase critical for portable electronic devices and renewable energy applications. By incorporating real-time monitoring of key parameters such as voltage, current, and sensor data, this proposed solution integrates sensors directly within the circuit, enabling a more informed and controlled charging process.

Keywords: Battery Management System, IoT, Cutoff system

1.0 INTRODUCTION

Batteries have become essential in the landscape of modern technology, powering an extensive array of devices, ranging from wearables to electric vehicles and serving as vital components in renewable energy storage system [1]. The growing reliance on energy storage solutions underscores the critical need for efficient battery management, thereby boosting the prominence of Battery Management Systems (BMS). As society pivots towards an increasingly electrified and sustainable future, the importance of optimizing the performance and longevity of batteries becomes paramount [1].

The integration of Internet of Things (IOT) technologies with BMS emerges as a promising avenue, offering advanced monitoring and control capabilities to meet the evolving demands of diverse applications [1]. While traditional BMS have played a crucial role in mitigating risks associated with battery usage, it struggles to keep pace amidst the complex chemistries, higher energy density demands, and rapid technological evolution characteristic of contemporary energy storage systems [2]. Persistent issues such as overcharging and thermal management underscore the need for innovative solutions that align with the evolving landscape of battery technologies.

This study endeavors to address the existing challenges in BMS, with a focus on enhancing their efficiency and agility. By using IoT technologies, this study aims to provide a comprehensive solution that not only mitigates the current issues but also anticipates and addresses the emerging needs of any advanced energy storage systems. The subsequent sections will delve into the specific challenges faced by conventional BMS, the proposed methodology, and the anticipated contributions of this study to the field of battery management [2].

1.1 Literature review

The literature on BMS underscores a dynamic landscape with a focus on optimizing battery performance and safety [1]. Research in state of charge estimation has explored advanced algorithms, including artificial intelligence, to improve accuracy. Cell balancing strategies, ranging from passive to intelligent methods, aim to address energy distribution disparities within battery packs [2]. Robust protection mechanisms against over-current, over-voltage, and over-temperature conditions have been a focal point for enhanced safety [3]. The integration of the Internet of Things into BMS is recognized for its potential in real-time monitoring, remote management, and predictive maintenance. Additionally, a growing emphasis on scalability considers adaptable BMS designs suitable for diverse applications, from small residential setups to large industrial installations. Collectively, these research trends contribute to the continual evolution of BMS, vital for advancing energy storage solutions [4].

It is noteworthy that previous studies have not fully addressed some critical challenges persisting in this domain. Despite advancements in state of charge estimation through the exploration of advanced algorithms, and the implementation of various cell balancing strategies to rectify energy distribution disparities within battery packs, there remains a gap in effectively mitigating the issues of inaccuracies in state of charge estimation, achieving perfect cell balancing, and managing thermal complexities [4]. Furthermore, while robust protection mechanisms against over-current, over-voltage, and over-temperature conditions have been a focal point for enhanced safety, the integration of the IOT into BMS has not been comprehensively harnessed to address these challenges [4]. This study seeks to build upon these insights by proposing a comprehensive solution that addresses the existing gaps and advances the state-of-the-art in BMS.

2.0 METHODOLOGY

The primary objectives of this project are to establish a robust BMS equipped with essential features like cell balancing, auto cutoff system and IoT based monitoring. The implementation of a State of Charging mechanism aims to prevent power shortages and optimize energy utilization, ensuring a consistent and efficient power supply. The development of an intelligent Cell Balancing mechanism is crucial for promoting even energy distribution among cells, thereby extending the overall lifespan of the battery. To fortify battery safety, the project includes the incorporation of protection mechanisms that automatically respond to over-current, over-voltage, and over-temperature conditions. Additionally, the integration of Mobile App functionality enhances user control by enabling remote monitoring and timely alerts, ensuring swift responses to potential issues [2]. Lastly, the project focuses on Scalability, designing the system to be adaptable for various applications, from small residential systems to large industrial setups, to meet the diverse needs of users in different contexts. The block diagram of the system designed using a 3-cell battery system is shown in Figure 2.1.

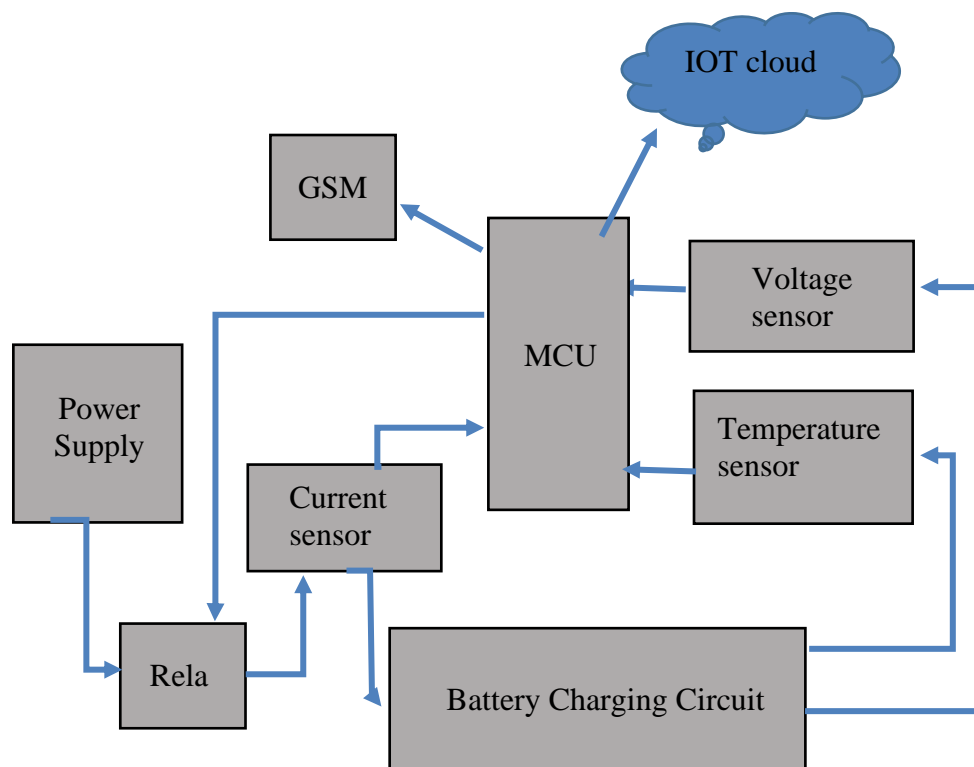


Figure 2.1 : Block diagram of the system

The BMS control circuit plays a crucial role in monitoring battery cells during both charging and discharging phases. BMS control circuit equipped with sensors collects data such as voltage, current, and temperature from individual cells within the battery pack. This control circuit is intricately designed with both charging/discharging circuits and a sensor module. Once the data is acquired, an ESP32 Node MCU processes the sensor-emitted values. The Node MCU then calculates the data from each sensor and transmits it to an IoT cloud for monitoring and control purposes. Subsequently, the ESP32 Node MCU enables users to access and monitor key parameters such as voltage, current, temperature, and state of charge via a dedicated website or mobile application, offering a user-friendly interface for real-time insights into the battery's performance. When the system gets from sensors to the stage of over-voltage, a LED bulb is indicated and the website is updated about all the data including over-voltage, over-current and over-temperature.

2.1 Circuit design of the system

Here, the circuit was powered from 16 V / 2 A bench power supply. Then the input voltage of the circuit was set up as 9 V. When charging the Li-ion battery in 4.2 V / 630 mA, the battery health can increased [5]. Therefore a regulator part of charging current and voltage in own circuit as 630 mA from LM317 was prepared and then the charging was done successfully.

Also there is an auto cutoff system in own circuit. In hear after the voltage of battery become 4.2 V, the system will auto cutoff. That cutoff point can be changed by varying the preset which is shown in Figure: 2.2.

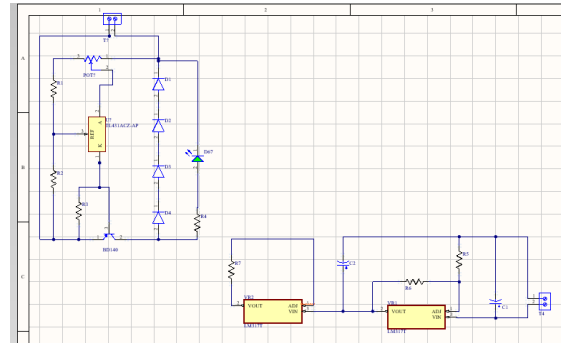
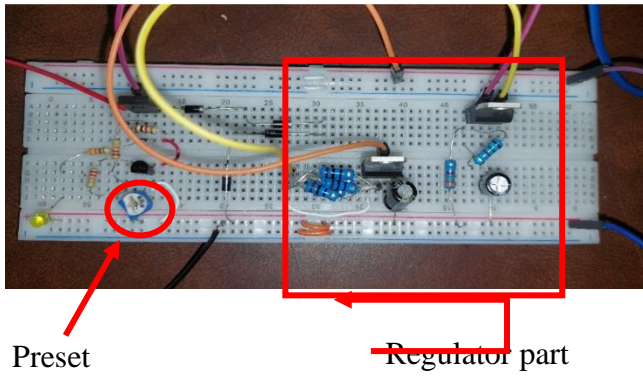


Figure 2.2: Circuit of one cell battery charger

Figure 2.3: Schematic design for one cell

(FIGURES ?)

2.2 Schematic design and PCB design

After that, full circuit (For 3 cell) was drawn according to the schematic diagram of the system which is shown in Figure 2.3. PCB designing techniques and rules were used for low-noises circuit design which is shown in Figure 2.4 and 2.5.

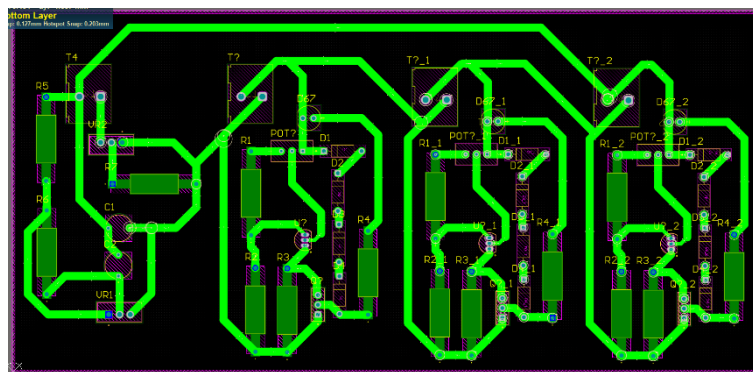


Figure 2.4: PCB layout for the circuit - bottom view

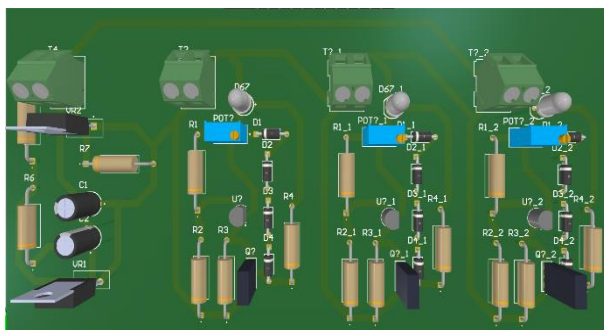


Figure 2.5: PCB layout for the circuit - top 3D view



Figure 2.6: Final charging /discharging circuit

After the full prepared battery charging and discharging which is shown in Figure 2.6 then moved to setup sensors (Voltage, Current and Temperature) and Node MCU and Modules

(Relay, GSM). Temperature sensors were setup on each battery holder and voltage sensors were setup parallel with batteries [5].

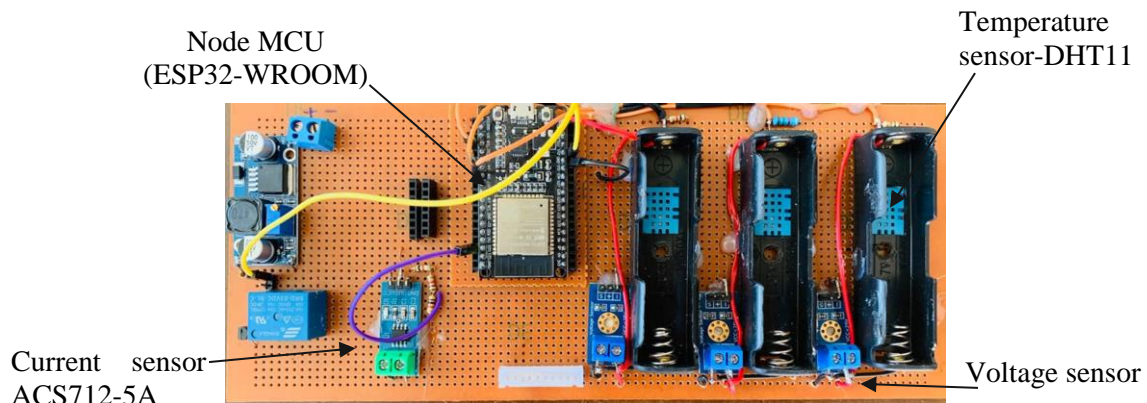


Figure 2.7: Finalized modules and sensors circuit

3.0 RESULTS AND DISCUSSION

3.1 Results

In the 1-cell battery charging circuit, the bench power supply was set to provide 9 V with a current capacity of 1 A. The regulators generated an output of 4.2 V at 630 mA. During the experiment, the current across the battery was measured as 620 mA.

In the 3-cell battery charging circuit, specifically during an intermediate charging stage, sensors were actively connected to monitor key parameters. The bench power supply was configured to provide 14.7 V at 1 A. The regulators produced an output of 4.2 V with a current capacity of 630 mA. At this phase, the current across each battery was measured at 200 mA. Notably, voltage levels across individual batteries were recorded, revealing readings of 3.46 V for Battery 1, 3.40 V for Battery 2, and 3.65 V for Battery 3. These historical data points, captured during the intermediate charging stage, offer valuable insights into the charging dynamics, providing a past passive reference for the circuit's performance under specific voltage, current, and sensor-monitored conditions [3].

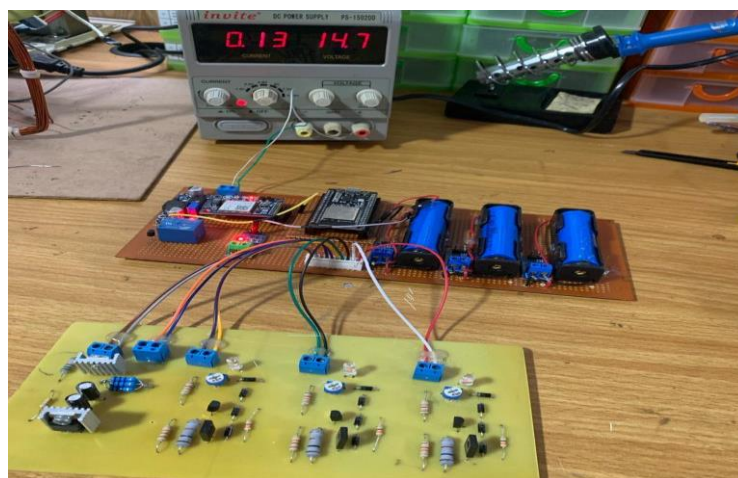
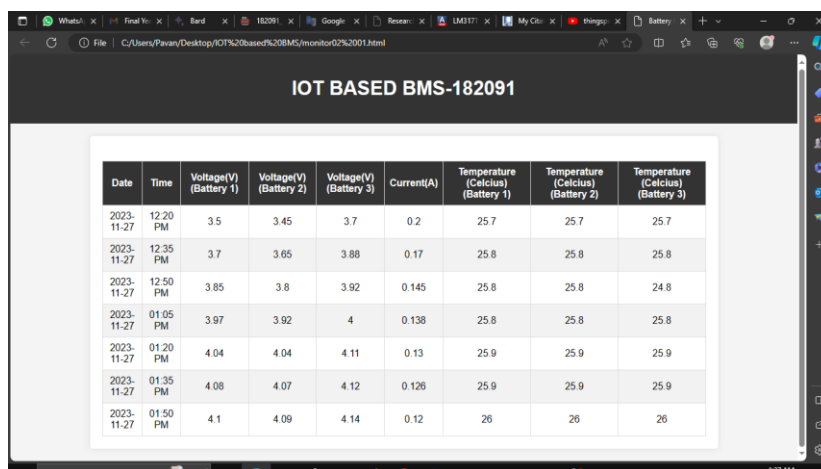


Figure 3.1: Getting readings with sensors and modules

After website was created successfully, Node MCU was connected to the website and monitored the voltage, current and temperature in each batteries Node MCU sent the data by every 15 min to the website [6]. The data extracted by the system when it is in the intermediate charging stage, is shown in the figure 3.2.



Date	Time	Voltage(V) (Battery 1)	Voltage(V) (Battery 2)	Voltage(V) (Battery 3)	Current(A)	Temperature (Celsius) (Battery 1)	Temperature (Celsius) (Battery 2)	Temperature (Celsius) (Battery 3)
2023-11-27	12:20 PM	3.5	3.45	3.7	0.2	25.7	25.7	25.7
2023-11-27	12:35 PM	3.7	3.65	3.88	0.17	25.8	25.8	25.8
2023-11-27	12:50 PM	3.85	3.8	3.92	0.145	25.8	25.8	24.8
2023-11-27	01:05 PM	3.97	3.92	4	0.138	25.8	25.8	25.8
2023-11-27	01:20 PM	4.04	4.04	4.11	0.13	25.9	25.9	25.9
2023-11-27	01:35 PM	4.08	4.07	4.12	0.126	25.9	25.9	25.9
2023-11-27	01:50 PM	4.1	4.09	4.14	0.12	26	26	26

Figure 3.2: Interface of IOT website

4.0 CONCLUSION

This study addresses the critical problems of existing battery management systems in charging circuits, particularly focusing on the intermediate charging stage in a 3-cell battery configuration. The significance of this investigation lies in its potential to improve the performance and longevity of batteries, crucial in the context of portable electronic devices and renewable energy applications. By actively monitoring key parameters like voltage, current, and sensor data during charging, the proposed solution provides real-time insights and enables a more informed and controlled charging process using the presets in regulator circuit. The system's importance is underscored by its ability to offer a comprehensive and adaptable battery management solution, ensuring balanced charging, consistent output, and overall safety with the designed features such as auto cutoff system, IOT based monitoring using web application and cell balancing. The incorporation of an intermediate charging stage contributes to a more nuanced and controlled approach and promotes extended battery lifespan.

ACKNOWLEDGEMENT

Authors would like to thank all the staff of the Department of Electronics, Faculty of Applied science, Wayamba University of Sri Lanka.

REFERENCES

- [1] Battery monitoring system using microcontroller ESP32 ... - research gate. Available at: https://www.researchgate.net/publication/356743232_Battery_Monitoring_System_using_Microcontroller_ESP32_and_Internet_of_Things (Accessed: 12 August 2023).
- [2] Author links open overlay panel Isaias González, Highlights•Lithium-ion Batteries (LiBs) are gaining market presence and R&D efforts. Internet of Things (IoT) is applied to deploy real time monitoring system for a LiB. •The LiB acts as backbone of micro grid with photovoltaic energy and hydrogen. Novelty and Abstract Energy storage through Lithium-ion Batteries (LiBs) is acquiring growing presence both in commercially available equipment and research activities. Smart power grids (2022) IOT real time system for monitoring lithium-ion battery long-term operation in micro

grids, *Journal of Energy Storage*. Available at: <https://www.sciencedirect.com/science/article/pii/S2352152X22006120> (Accessed: 20 September 2024).

- [3] Smart *Battery Management System for electric vehicles using IOT ... - IJCRT*. Available at: <https://ijert.org/papers/IJCRT2304122.pdf> (Accessed: 12 January 2024).
- [4] Ashok, B. et al. (2022), Towards safer and smarter design for lithium-ion-battery-powered electric vehicles: A Comprehensive Review on Control Strategy Architecture of Battery Management System, MDPI. Available at: <https://www.mdpi.com/1996-1073/15/12/4227>, (Accessed: 12 January 2024).
- [5] *Lithium-ion battery data sheet - Ineltro*. Available at: <https://www.ineltro.ch/media/downloads/SAItem/45/45958/36e3e7f3-2049-4adb-a2a7-79c654d92915.pdf>, (Accessed date: 30 November 2023).
- [6] Carlson, L.L. (no date) *Web design references, Web Design References: Books*. Available at: <https://www.d.umn.edu/itss/training/online/webdesign/books.html> (Accessed: 20 January 2024).

SMART MANHOLE MONITORING SYSTEM

K.B.M.N. Neranjan^{1*}, K.P. Vidanapathirana¹, T. Herath²

¹*Department of Electronics, Wayamba University of Sri Lanka, Kuliyaipitiya, Sri Lanka*

²*Digital Lab, Sri Lanka Telecom, Colombo, Sri Lanka*

*maheshanirmal@gmail.com

ABSTRACT

The Smart Manhole Monitoring System is a solution provided to addresses important issues related to managing manhole of Sri Lanka Telecom in a smart manner. The main goals are reducing the overflow of drainage water, keeping an eye on harmful levels, automating inefficient manual monitoring, and improving alert systems. This is accomplished by precisely integrating an array of sensors, such as the MQ-2 smoke sensor, MQ-7 Carbon Monoxide sensor, HC SR-04 ultra-sonic sensor, SEN18 water level sensor, and DHT-22 Temperature and Humidity, into an ESP32 development board. This system's strength lies in its ability to communicate. An 800L SIM module leads primary communication, while a LED-LDR pair facilitates secondary communication. Together, these components create a robust and trustworthy networking infrastructure. The development process involves a methodical approach, including sensor integration, system design, and programming of the ESP32 MCU using the Arduino IDE. The LCD 20 x 4 screen displays real-time data generated and displayed. The MCU plays a critical role in the system, reading data from various sensors, processing it, and triggering the alert system when needed. The channels of communication, which are carefully set up to allow for smooth remote data transfer, provide even more efficiency to the system. A robust alarm with an LCD screen and buzzer is implemented to provide timely and efficient notifications. Thorough testing and calibration processes conducted guaranteeing the accuracy and dependability of the system, with sensor calibration to yield the highest-quality readings. The device is deployed within a manhole for real-time monitoring. This approach not only solves current problems but also sets a notable standard for increased effectiveness and responsiveness in monitoring and managing manholes of Sri Lanka Telecom.

Keywords: Smart manhole monitoring system, Monitoring sensor integration system, Real-time manhole management

1.0 INTRODUCTION

The Smart Manhole Monitoring System, developed at Sri Lanka Telecom Digital Lab, is a viable solution to maintenance and inspection of manholes. It uses advanced sensor technology and smart connectivity to provide real-time data on manhole conditions, reducing risks and enhancing operational efficiency [1]. The system monitors critical factors like gas levels, temperature, oxygen concentration, and water level, ensuring worker safety and improving efficiency [2]. It uses sensors and communication technologies to track the status of manhole covers, monitor environmental conditions, and transmit the data in real-time [3]. This approach prevents accidents and allows for timely intervention when anomalies are detected. This smart manhole monitoring systems underscore the critical importance of sensor integration for real-time data acquisition, seamlessly incorporating diverse sensor types such as proximity, gas, and temperature sensors. The infusion of IoT principles and advanced detection methodologies has driven transformative advancements in the domain of manhole inspection and maintenance [4]. These findings offer valuable guidance for the design and implementation of future smart manhole monitoring systems, promising enhanced safety, operational efficiency, and environmental monitoring [5].

2.0 EXPERIMENTAL

2.1 System design

The system features an ESP 32 Microcontroller, five sensors, an LCD screen, 800L SIM module, buzzer, and VLC communication module as depicted in Figure 2.1.

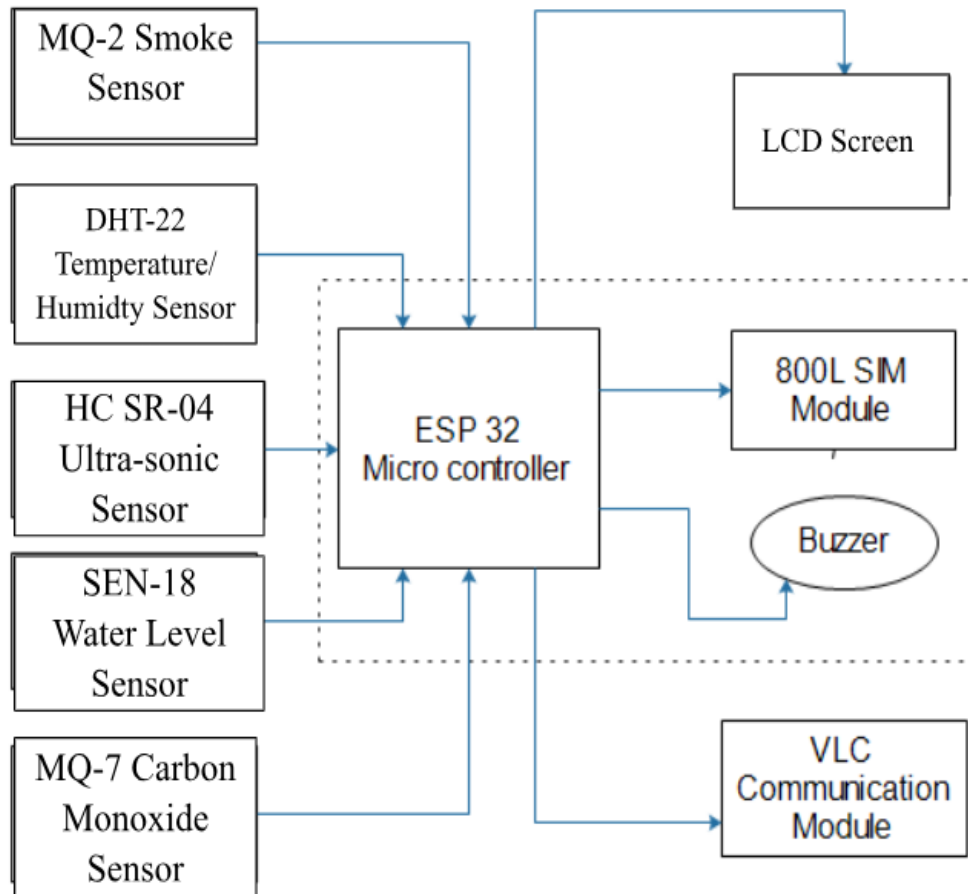


Figure 2.1: Block diagram of the design

Figure 2.1 provides a block diagram of the system based on an ESP32 microcontroller that outlines the components and their connections. The microcontroller controls all other components, with five sensors connected: MQ2 for detecting gases and smoke, DHT22 for temperature and humidity, Ultra Sonic sensor for distance measurement, Water level sensor for water level measurement, and MQ7 for carbon monoxide detection. Four modules: LCD Screen, 800L SM Module, Buzzer for audio signaling, and VLC communication module for visible light communication are connected to the system.

The ESP32 microcontroller was equipped with various sensors to detect and manage environmental conditions. Smoke was detected by the MQ-2 Smoke Sensor, which sent a signal to the microcontroller. This triggered an audio alert via the buzzer, displayed readings on an LCD screen, sent alerts through the SIM 800L GSM module, and communicated this information using visible light communication (VLC) through an LED. Temperature and humidity levels were measured by the DHT-22 Temperature/Humidity Sensor, and if certain

thresholds were exceeded, alerts were triggered. Distance was measured by the HC SR-04 Ultrasonic Sensor using ultrasonic waves, and water levels were monitored by the SEN-18 Water Level Sensor. Carbon monoxide in the air was detected by the MQ-7 Carbon Monoxide Sensor, which alerted when CO levels exceeded safe limits. The ESP32 interacted with several modules, including the Buzzer, LCD Screen, SIM 800L GSM Module, and VLC Module. These modules used LED lights to communicate information visually, which could be interpreted by another device equipped with an LDR (Light Dependent Resistor).

2.2 Design procedure

The process involves hardware assembly including sensors, SIM800L GSM module, LCD display, and buzzer, setup of the Arduino IDE, library installation, code writing, uploading, testing, and deployment of a smart manhole monitoring system in the desired location.

2.3 Challenges

The integration of multiple sensors and components with the ESP32 MCU was complex due to their unique operating voltage and communication protocols. The software development process was complex, with different libraries and functions for each component. Power management was crucial for the system's reliability. Efficient data management was essential for the system's generation. Environmental factors were considered for reliability. Testing and debugging were necessary for correct functionality. System deployment faced challenges, emphasizing the importance of correct sensor positioning.

3.0 RESULTS AND DISCUSSION

3.1 Results

The system consists of an LCD Screen, 800L SIM module, buzzer, and VLC communication module as outputs of the system. The LCD Screen displays information processed by the microcontroller, including sensor readings and status messages. The 800L SIM module connects to the mobile network for remote communication, sending sensor data via SMS or GPRS. The buzzer alerts users to specific conditions detected by sensors. The VLC communication module transmits wireless data using visible light, including sensor readings and status information. The outputs depend on the program running on the ESP32 microcontroller. Figure 3.1 shows developed prototype version of the projec

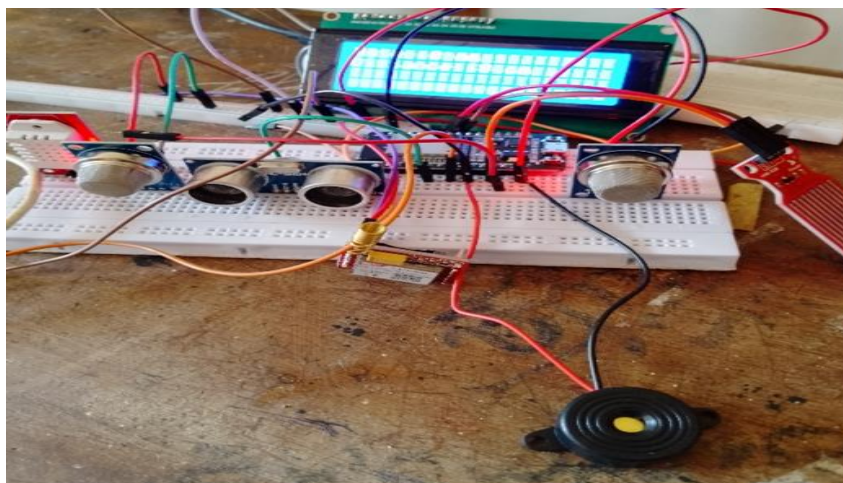


Figure 3.1: Developed prototype version

Figure 3.2 is provided LCD screen readings. The LCD screen offers real-time environmental readings, providing a clear picture of critical parameters like smoke detection, CO levels, and temperature. It also displays depth of water and humidity levels, ensuring awareness of sub-surface conditions. The screen also dynamically communicates alerts triggered by sensor data, providing immediate and actionable information for effective monitoring and management. This integration of real-time data and alert visualization enhances the screen's utility.

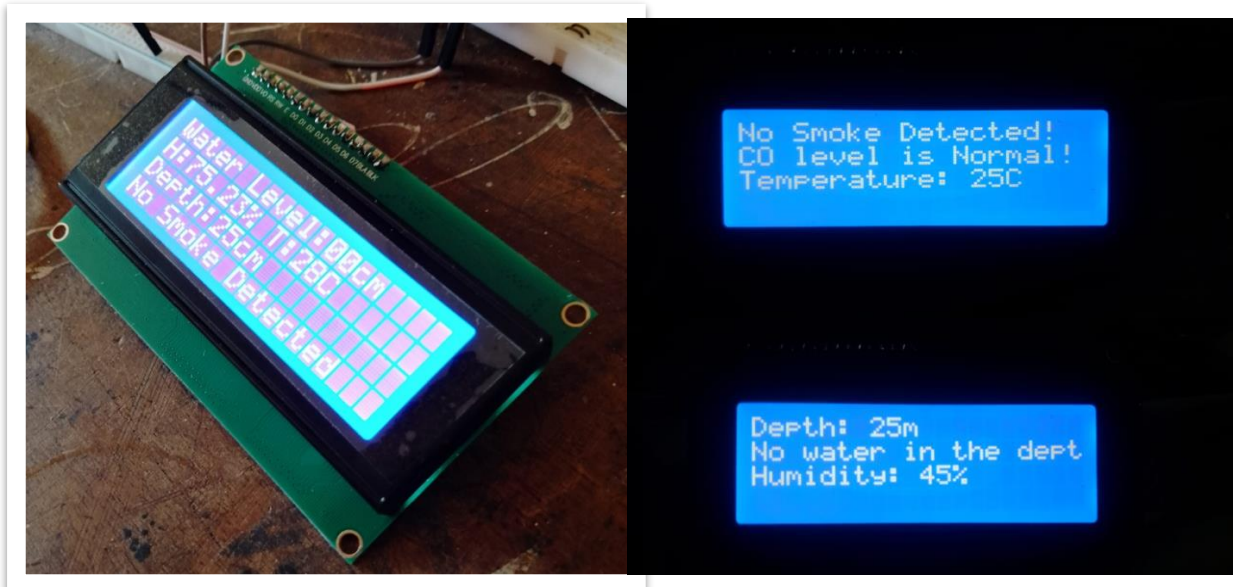


Figure 3.2 : LCD readings

Figure 3.3 shows serial monitor outputs of VLC receiver end. The display uses VLC-based communication to display real-time environmental readings, indicating hazard-free conditions and safe CO concentrations. It also shows depth of water and humidity levels. It also sends alerts if abnormal conditions arise, enhancing its functionality for effective environmental monitoring and management. This integration of real-time data and alert visualization enhances the display's functionality and providing immediate actionable information.

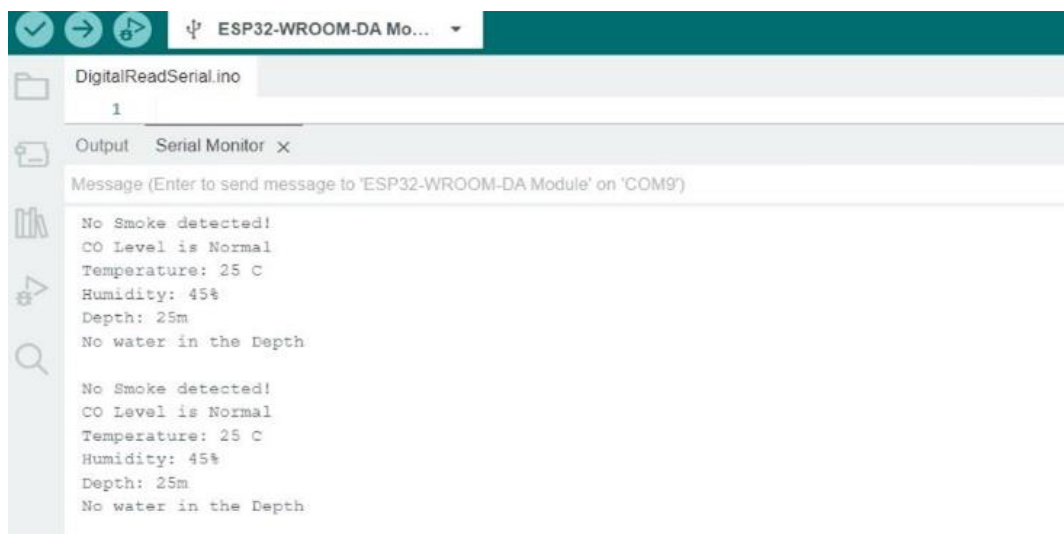


Figure 3.3: VLC receiver end serial monitor outputs

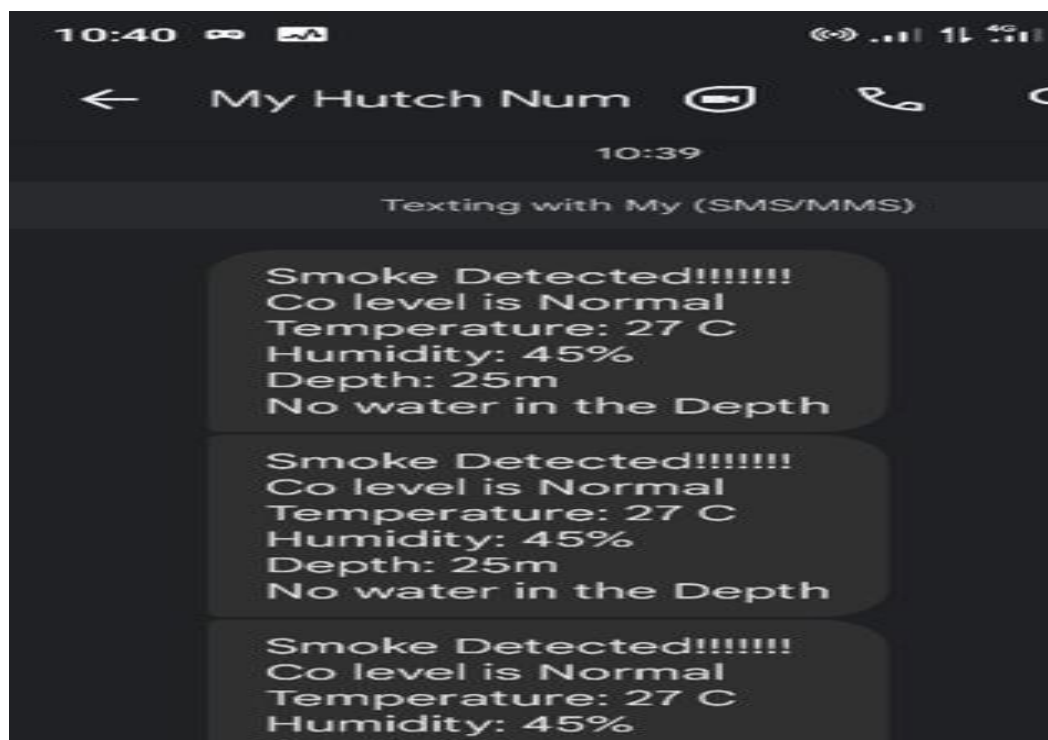


Figure 3.4: SMS data sent by GSM module

Figure 3.4 provide image of SMS sent using GSM module. GSM network interacted with electronic devices through the utilization of a GSM module. To incorporate a GSM module, an appropriate module is selected, interfaced with the system, configured, software is adapted, and the system is thoroughly tested.

3.2 Discussion

The system uses multiple sensors for comprehensive monitoring of parameters like gas levels, temperature, humidity, and water level. It sends real-time alerts via GSM network and visible light communication, logs data for trend analysis, and offers an easy-to-use interface. It can be integrated with existing infrastructure management systems for easier maintenance. However, it has weaknesses like power consumption, environmental factors, complexity, security, and scalability. It must be robust, secure, and easy to maintain, requiring frequent battery replacements or reliable external power sources.

As recommendation and further work, the proposed system includes advanced data analysis algorithms for predictive maintenance, real-time alerts, integration with existing infrastructure, power optimization, robustness and durability, user interface improvements, and scalability. Advanced machine learning algorithms could be used to identify patterns in sensor data, while real-time alerts could be developed to notify authorities or maintenance teams. The system could also be integrated with existing infrastructure management systems for easier maintenance. Extensive testing and user interface improvements could ensure the system's long-term durability and efficiency.

4.0 CONCLUSION

The smart manhole monitoring system project uses an ESP32 microcontroller unit, sensors, a GSM module, an LCD display, and a buzzer to monitor various manhole parameters. The system is programmed using Arduino IDE and designed using Fritzing. The project showcases the potential of modern electronics and software tools to improve infrastructure management and safety. However, challenges such as hardware integration, software complexity, power management, data management, environmental factors, and PCB design were addressed through careful design, testing, and iterative improvement. Future work should include advanced data analysis algorithms, real-time alert systems, integration with existing systems, optimizing power consumption, improving user interface, planning for scalability, and ensuring data security.

ACKNOWLEDGEMENT

Authors would like to acknowledge the support provided by the staff of Department of Electronics, Faculty of Applied Sciences and staff, of SLT Digital Lab for the successful completion of the project.

REFERENCES

- [1] K Ravi Kumar, K Vijaya Lakshmi, G Rohin Kumar, G Jagan Mohan, *Smart Manhole Monitoring System*, (2023), <https://www.researchgate.net/publication/369249229-Smart-Manhole-Monitoring-System>, (2023.07.15)
- [2] Varun Krishna Nallamothe; Saahith Medidi; Swetha Priyanka Jannu, *IoT based Manhole Detection and Monitoring system*, (2022), DOI-10.1109/ICDCECE53908.2022.9793287
- [3] Guruprasath V.A, Sowmya H.D, *Manhole detection and monitoring system*, (2022), DOI-10.26562/irjcs.2022.v0909.08
- [4] Prof. Swati Khawate, Prof., Dr.Sharan Inamdar, Nitin Battula, Naveen Cheerla, *IOT based Manhole Detection and Monitoring System*, (2023), DOI-10.22214/ijraset.2023.52786
- [5] Snehal K. Jagtap, Shradha S.Khalate, Pratiksha Y. Madane, Kshitija k. Shirke, *Smart Manhole Managing and Monitoring System using IoT*, (2022), DOI-10.4108/eai.16-4-2022.2318149
- [6] S. K. Hussain, Vishnu Vishnu Battu, Dr.Thimmaiah, *Development of an IoT Based Real Time Embedded System for Monitoring Temperature and Humidity by using ESP WROOM 32 MCU*, (2023), <https://www.ijrti.org/papers/IJRTI2306162.pdf>, (2023.07.23)
- [7] Roberto Pasic, Ivo Kuzmanov, Kokan Atanasovski, *Espressif esp32 development board in Wi-Fi station communication mode*, (2020), https://www.researchgate.net/publication/370048437_ESPRESSIF_ESP32_DEVELOPMENT_BOARD_IN_WIFI_STATION_COMMUNICATION_MODE, (2023.07.27)
- [8] A. T. Ajiboye, J. F. Opadiji, Adebimpe Ruth Ajayi, *Graphical method for determination of mq-series gas sensor circuit parameters for a stand-alone gas alarm system*, (2021), DOI- 10.48141/sbjchem.21scon.20_abstract_ajiboye.pdf

- [9] Manpreet Kaur, Jai Pal, *Distance Measurement of Object by Ultrasonic Sensor HC-SR 04*, (2015), <https://www.semanticscholar.org/paper/Distance-Measurement-of-Object-by-Ultrasonic-Sensor-Pal>, (2023.08.21)
- [10] Whisnumurti Adhiwibowo, April Firman Daru, Alauddin Maulana Hirzan, *Temperature and Humidity Monitoring Using DHT22 Sensor and Cayenne API*, (2020), DOI:10.26623/transformatika.v17i2.1820

